

University of Southern Queensland
Faculty of Engineering and Surveying

Measurement of Mechanical, Electrical and Thermal
Properties of Glass Powder Reinforced Epoxy Composites
and Modelling

A dissertation submitted by

Kwok Yeung Peter Wong

0050092612

in fulfilment of the requirements of

the degree of

Master of Engineering

March 2012

Abstract

Organic- inorganic hybrid material has received much attention in recent time. Due to the smaller size and longer specific surface area, glass powder filled epoxy resin becomes important research target. Epoxies are widely used in commercial applications but comparatively more expensive than other polymer resins. This project is to develop a material having a combination of lower cost and improved mechanical properties, using epoxy resin as matrix and glass powder as filler. The composites were post-cured in a conventional oven as well as in microwaves.

Main objectives of the project are

- To make specimens with different percentages by weight of glass powder starting from 0% to 35%, at 5% interval in epoxy resin.
- To post- cure the specimens in microwaves and in an oven with standard procedures.
- To conduct tensile and flexural tests, permittivity tests and DMA tests to measure mechanical, electrical and thermal properties of epoxy composites.
- To analyze the results and compare them with the results of other researchers and draw up a conclusion.
- To propose models for the mechanical properties of the composites
- To recommend the best composition by weight of glass powder and epoxy resin on the basis of cost and physical properties for different industrial applications.

The project concluded that microwave post-curing method is more effective than its counterpart. Samples having higher percentage of glass powder irrespective whether they are post-cured conventionally or in microwave exhibit similar results.

Limitation of use

University of Southern Queensland

Faculty of Engineering and Surveying

ENG8002 *Project and Dissertation***Limitations of Use**

The Council of the University of Southern Queensland, its Faculty of Engineering and Surveying, and the staff of the University of Southern Queensland, do not accept any responsibility for the truth, accuracy or completeness of material contained within or associated with this dissertation.

Persons using all or any part of this material do so at their own risk, and not at the risk of the Council of the University of Southern Queensland, its Faculty of Engineering and Surveying or the staff of the University of Southern Queensland.

This dissertation reports an educational exercise and has no purpose or validity beyond this exercise. The sole purpose of the course 'Project and Dissertation' is to contribute to the overall education within the student's chosen degree program. This document, the associated hardware, software, drawings, and other material set out in the associated appendices should not be used for any other purpose: if they are so used, it is entirely at the risk of the user.

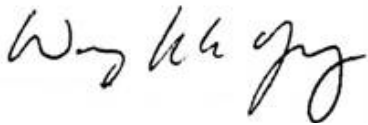
Prof. F Bullen

Dean

Faculty of Engineering and Surveying

Certification

I certify that the ideas, design and experimental work, results, analysis and conclusions set out in this dissertation are entirely my own effort, except where otherwise indicated and acknowledged. I further certify that the work is original and has not been previously submitted for assessment in any other course or institution, except where specifically stated.



Kwok Yeung Peter Wong

Student Number: 0050092612

29-Jan-2012

Date

Endorsement

Dr. Harry Ku

Date

Dr. Jayantha Ananda Epaarachchi

Date

Acknowledgements

It is with pleasure I would like to thank all the people who made this project possible. First of all I thank my supervisors Dr. Harry Ku and Dr. Jayantha Ananda Epaarachchi for guiding me throughout the project. I would also like to thank Mr Mohan Trada to provide his expert instructions for the safe use of different equipments and machines during the construction and testing of specimens. I would like to thank the University of Southern Queensland for providing the equipments to prepare specimens and conduct required tests. Last but not the least; I deeply appreciate the support, motivation, patience and perseverance of my family during the project.

Table of Contents

Abstract	i
Limitation of use	ii
Certification	iii
Acknowledgements	iv
Table of Contents	v
List of Tables	xi
1. INTRODUCTION	1
1.1 Project Topic	1
1.2 Project Background	1
1.3 Aims of the Project.....	2
1.4 Objectives of the Project	2
1.5 Publications	2
1.6 Concluding Remarks	3
2 LITERATURE REVIEW	4
2.1 Introduction	4
2.2 Introduction to Composites	4
2.3 History of Composites.....	5
2.4 Epoxy Resin	8
2.4.1 Manufacturing Process of Epoxy Resin	8
2.4.2 Properties of Epoxy Resins	12
2.5 Fillers.....	12
2.5.1 Glass Powder	13
2.6 Dielectric Fundamentals.....	14
2.6.1. Dielectric constant.....	14

2.6.2 Loss Tangent	16
2.6.3 Microwaves	18
2.6.4 Dielectric Mechanism.....	18
2.6.5 Penetration Depth.....	20
2.6.6 Thermal Runway	21
2.7 Post Curing.....	21
2.8 Permittivity Test.....	22
2.9 Dynamic Mechanical Analysis (DMA).....	23
2.9.1. Viscoelasticity of material.....	23
2.9.2. Glass Transition Temperature	23
2.9.3 Storage Modulus and Loss Modulus	23
2.10 Tensile Properties of Material	25
2.10.1 Yield Strength.....	26
2.10.2 Tensile Strength.....	26
2.11 Modelling	27
2.12 Work of Others	27
3 METHODOLOGY.....	28
3.1 Introduction	28
3.2 Resin and Catalyst Used.....	28
3.3 Glass Powder.....	30
3.4 Mixing	30
3.5 Initial Curing Of The Specimens.....	33
3.6 Methodology	34
3.7 Post Curing.....	35
3.7.1 Post Curing in Microwave.....	36

3.7.2 Post Curing In Oven.....	38
3.7.3 Comparison Of Conventional Oven And Microwave Curing.....	39
3.8 Dielectric Constant And Loss Tangent Measurement.....	40
3.8.1 Calculation Of Dielectric Constant And Loss Tangent.....	40
3.9 Dynamic Mechanical Analysis (DMA) Test.....	41
3.10 Tensile Tests.....	43
3.11 Optical Microscopy	45
4 RESULTS AND DISCUSSIONS	45
4.1 Introduction	45
4.2 Permittivity Test Results	46
4.2.4 Measured Loss Tangent.....	46
4.3 Dynamic Mechanical Analysis (DMA) Test Results	49
4.3.1 Relationship Between Glass Transition Temperature And Percentage Of Glass Powder.....	53
4.3.2 Relationship Between Storage Modulus (E') And Percentage Of Glass Powder ..	53
4.3.3 Relationship Between Loss Modulus (E'') And Percentage Of Glass Powder	53
4.4 Tensile Test Results.....	53
4.4.1 Yield strength	53
4.4.2 Tensile Strength.....	54
4.4.3 Young's Modulus	55
4.5 Scanning Electron Microscope (SEM) Results	57
4.6 Modelling	58
4.6.1 Yield Strengths	59
4.6.2 Tensile Strengths	63
4.6.3 Young's Modulus	66
4.6.4 Other Models.....	69

4.6.5 New Models	71
5 CONCLUSIONS.....	73
5.1 Introduction	73
5.2 Discussion Of Results	73
5.2.1 Permittivity Test.....	73
5.2.2 DMA Tests	74
5.2.3 Tensile Tests.....	74
5.2.4 Microscopic Inspection	75
5.2.5 Modelling	75
5.3 Recommendation And Future Research Scope	77
LIST OF REFERENCES	78
Reference.....	78
Appendix A	82
A.1. Permittivity Test Results	82
A.2. DMA Test Graphs	85
A.3. Tensile Test (Microwave cured sample)	87
A.4. Tensile Test (Sample Cured Conventionally)	103
 LIST OF FIGURES	
Figure 2.1: Classifications of composites.....	4
Figure 2.2: Applications of composite in different industries	6
Figure 2.3: Structure of epoxide (oxirane) group (a) and glycidyl group (b)	8
Figure 2.4: Reaction of NAOH with BPA	9
Figure 2.5: Further reactions amongst ECH, BPA and NAOH.....	9
Figure 2.6: Final end product DGEbPA	10

Figure 2.7: Propagation of linear chain	10
Figure 2.8: Formation of branched structure	11
Figure 2.9: Final Cross linked epoxy resin structure	11
Figure 2.10: Hollow glass microsphere	13
Figure 2.11: Arrangement of parallel plate capacitor across DC voltage	14
Figure 2.12: Arrangement of parallel plate capacitor across AC voltage	15
Figure 2.13: Vector Diagram of complex permittivity	17
Figure 2.14: Electromagnetic waves	18
Figure 2.15: Polarization mechanisms	19
Figure 2.16: Permittivity of water at different temperature (Bows 1999)	21
Figure 2.17: Summary of permittivity measurement techniques	22
Figure 2.18: Stress-strain curve	25
Figure 2. 19: Tensile strength of epoxy composite reinforced with varying glass powder by weight with varying glass powder by weight	28
Figure 3.1: Resin and catalyst used	29
Figure 3.2: Weighted glass powder	32
Figure 3.3: Mixing	33
Figure 3.4 : Composite mixture poured into the moulds	33
Figure 3.5 : SANYO 800 W microwave with attached air duct	36
Figure 3.6: Handheld Infrared thermometer	37
Figure 3.7: Eurotherm 3200 series controller	38
Figure 3.8: Parallel plated method set up	40
Figure 3.9: DMA test machine (TA instruments Q800)	42
Figure 3.10: Tensile test machine	44
Figure 3.11: Vernier calliper	44

Figure 3.12: Optical Microscope	45
Figure 4. 1: Loss tangent of epoxy-glass powder (5%) post-cured in oven and microwaves	47
Figure 4. 2: Loss tangent of epoxy-glass powder (15%) post-cured in oven and microwaves	47
Figure 4. 3: Comparison of loss tangent of 5 % weight of glass powder filled epoxy resins from different curing method	48
Figure 4. 4: Comparison of loss tangent of 15 % weight of glass powder filled epoxy resins from different curing method	49
Figure 4. 5: DMA test results for samples cured in microwaves with 5 % weight of glass powder	50
Figure 4. 6: DMA test results for samples cured in microwaves with 10 % weight of glass powder	51
Figure 4. 7: DMA test results for samples cured in microwaves with 15 % weight of glass powder	52
Figure 4. 8: Yield strength of epoxy composite reinforced with varying glass powder by weight	54
Figure 4. 9: Tensile strength of epoxy composite reinforced with varying glass powder by weight	55
Figure 4. 10: Young's modulus of epoxy composite reinforced with varying glass powder by weight	56
Figure 4. 11: SEM image of fractured neat epoxy resin, 200X	57
Figure 4. 12: SEM image of fractured 25 % glass powder filled epoxy composite, 200X	58
Figure 4. 13: Values of yield strength of the composites obtained from Nicolais and Narkis' prediction and experiments	61
Figure 4. 14: The yield strengths of glass powder filled epoxy composites post-cured in an oven and from Ku and Wong's model	62
Figure 4. 15: yield strengths of glass powder filled epoxy composites post-cured in microwaves and from Ku and Wong's model	62
Figure 4. 16: Tensile strengths of glass powder filled epoxy composites post-cured in an oven and from Tavman's model	64

Figure 4. 17: Tensile strengths of glass powder filled epoxy composites post-cured in microwaves and from Tavman’s model	64
Figure 4. 18: Tensile strengths of glass powder filled epoxy composites post-cured in an oven and from Ku and Wong’s model.....	65
Figure 4. 19: Tensile strengths of glass powder filled epoxy composites post-cured in microwaves and from Ku and Wong’s model.....	66
Figure 4. 20: Young’s moduli of glass powder filled composites of Neilsen’s model, post-cured in an oven and post-cured in microwaves	67
Figure 4. 21: Young’s moduli of glass powder filled composites of Neilsen’s model, Einstein’s prediction and post-cured in microwaves	68
Figure 4. 22: Young’s moduli of glass powder filled composites of Ku and Wong’s model, Einstein’s prediction and post-cured in microwaves.....	69
Figure 4. 23: The three-part models: (a) Paul model, model 1, (b) Ishai-Cohen model, model 2.....	71
Figure 4. 24: proposed models: (a) Four-part model, model 3, (b) Five-part model, model 4.....	72

List of Tables

Table 2.1: Spherical hollow glass powder properties.....	14
Table 2.2: Dielectric constant and loss tangent of different materials (NCR, 1994).....	20
Table 3.1: Uncured and cured characteristics of R246TX and H160 (ATL Composites, undated).....	29
Table 3. 2: Spherical@60P18 hollow glass powder.....	30
Table 3. 3: Mixing ratio of epoxy resin, hardener and glass powder	31
Table 3. 4: Microwave curing stages	37
Table 4. 1: DMA test results for samples cured in microwaves	52
Table 4. 2: Volume fractions of other W/t % of glass powder and epoxy resin	59
Table 4. 3: Yield strengths from Nicolais and Narkis’ prediction	60

1. INTRODUCTION

This chapter acquaints the reader with the project background, followed by purposes and objectives of the research project.

1.1 Project Topic

Measurement of Mechanical, Electrical and Thermal Properties of Glass Powder Reinforced Epoxy Composites and Modelling.

1.2 Project Background

The drawback of epoxy resin is still ‘low toughness’. Many researchers have reported that the addition of rigid filler particles is useful for toughening cured epoxy resins. The hard particles have been known to contribute to enhancement in fracture toughness mainly by pinning and blunting. If those mechanisms occur in the presence of hollow-glass microspheres (glass powder) in the matrix, it would be more beneficial than solid particles, because in addition to the possible toughening, the composite density can also be lowered. Such composites are used in electrical applications, e.g. high voltage bushings and encapsulating materials for integrated circuits.

Since a lot of work have been done on the fracture toughness of the composites. This study would like to evaluate the tensile, flexural, thermal as well as the dielectric loss tangent of the composites to explore more applications for them. This research project aims to investigate the tensile and flexural properties of glass powder reinforced epoxy composites post-cured conventionally and in microwaves. They are made with varying percentage by weights of glass powder with a view to finding out the optimum percentage by weight of the filler used in the composites.

In this study, the dielectric properties of the prepared composites were measured and were correlated with the thermal properties. The percentage by weight of glass powder studied for mechanical properties was varied from 0 to 35 %, while that for thermal and dielectric loss tangent was form 5 to 15 %. Half of the samples were post-cured conventionally and the other half of them was post-cured in microwaves.

1.3 Aims of the Project

- To reduce the cost of an epoxy resin composites by filling glass powder as much as possible and at the same time maintaining the strength of the composites
- To investigate the tensile and flexural properties of glass powder reinforced epoxy composites post-cured conventionally and in microwaves
- To develop model to predict the mechanical properties of particulate composites

1.4 Objectives of the Project

- i. Research existing information relating to fillers reinforced phenolic composites post-cured in microwaves.
- ii. Study the analysis method and develop tests to mechanical properties (flexural strength and fracture toughness) for fillers reinforced phenolic composites post-cured in microwaves.
- iii. Conduct tests and analyses on fillers reinforced phenolic composites post-cured in microwaves.
- iv. Investigate the optimum percentage by weight of the fillers used in the composites.
- v. Based on the results obtained propose a set of design formulas for determining the optimum percentage by weight of the filler used in the composites.
- vi. Verify the proposed design formulas by comparisons with existing experimental results and those developed by other researchers.
- vii. Modelling the results.

1.5 Publications

- i. Ku H, Wong P, Maxwell A, Huang J, Fung H, & Mohan T. A pilot study on the Relationship between Mechanical and Electrical Loss Tangents of Glass Powder Reinforced Epoxy Composites Post-cured in Microwaves. *Journal of Applied Polymer Science*, 2010; Volume 119, no. 5, pp. 2495–3116.
- ii. Ku H, Wong P, Huang J, Fung H, and Mohan T. Tensile Tests of Glass Powder Reinforced Epoxy Composites: Pilot Study. *Advanced Materials Research*, 2011; Vol. 214 pp 1-5.
- iii. Ku H, Wong P, Maxwell A, Huang J, Fung H and Trada M. A pilot study on the Relationship between Mechanical and Electrical Loss Tangents of Glass Powder

Reinforced Epoxy Composites Post-cured in Microwaves. *Advanced Materials Research*, 2011; Vol. 214, pp. 26-30.

1.6 Concluding Remarks

This chapter has given detailed information on the aims of the project and how the testing and analysis will be conducted. Chapter 2 will be literature review and Chapter 3 will be Methodology and will provide more detailed information on epoxy resin, its hardener and glass powder. It also discusses in depth the tests and curing processes used for composites. Chapter 4 will be results and discussion and Chapter 5 will be conclusions.

2 LITERATURE REVIEW

2.1 Introduction

This chapter explains the technical aspects of the project. It includes the history, chemical properties, advantages and commercial applications of epoxy resin and glass powder. It also covers the process of adding different fillers to composites. Post-curing and testing processes of specimens are discussed in detail in the later part of the chapter. It should be noted that some of the information in this chapter were gathered from non published sources like university study material, previous students reports, material safety data sheet (MSDS) and communication with the project supervisors and professors.

2.2 Introduction to Composites

As per the ASTM D 3878- 95c, the composites can be defined as “the substance consisting of two or more material, insoluble in one another, which are combined to form a useful engineering material, possessing certain properties not possess by the constituents”.

As shown in Figure 2.1, Harper (1992) classified composite materials in five basic types: fiber, particle, flake, laminar or layered and filled composites.

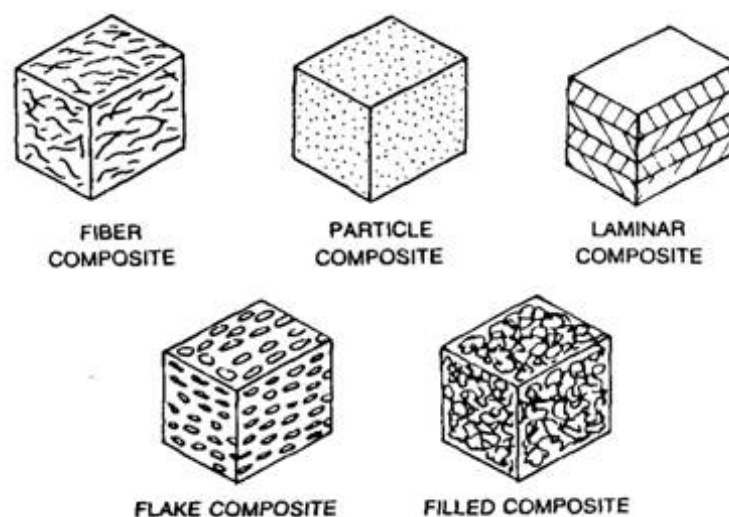


Figure 2.1: Classifications of composites

2.3 History of Composites

Wood is the example of natural composite made up of cellulose in a matrix of lignin (Hon and Shiraishi, 2002). First synthetic composite material was fibreglass developed in 1930. A glass was reinforced with polymers to make it stronger, stiffer and light weight. Fiberglass composites were widely accepted by aircraft industry. They were using fiberglass and phenolic resin composite to make dies for aerospace parts. Afterwards, reinforced plastic dies became preferred material for prototype parts of aircraft. Eventually, it became standard for forming and holding tools like jigs and fixtures. Phenolic resin – fiberglass composites were providing the required strength with high machinability and formability which cannot be achieved in metal or plastic alone. The development of composites was accelerated during the World War II. Sandwich structure using cellular core, fire resistant composites and many more composites were developed to increase ease of manufacturing and strength to weight ratio (Scala, 1996).

When the World War II ended suddenly, the composites manufacturing industries felt sudden decrease in demand. Therefore they began to diversify their business to commercial market. Some companies started manufacturing fiber glass reinforced manufacturing boat, while some companies emerged in to automobile industry. With the introduction of composite materials, the revolution in automobile industry has begun. Some of the products like tubes and shower assembly, trays, furniture, non corrosive pipes, storage container produced after the World War II using composites found major market (Peters 1998).

The first carbon (graphite) fiber was produced in 1961. Afterwards, numbers of new advanced performance fibers were developed which led to enormous development in transportation, sports equipments, aerospace industries, medical devices and many more applications. As per the recent report of Summer Publishing composite institute (SPI), the overall usage of composite material in different industries is as depicted in Figure 2.2 (SPI, 2009).

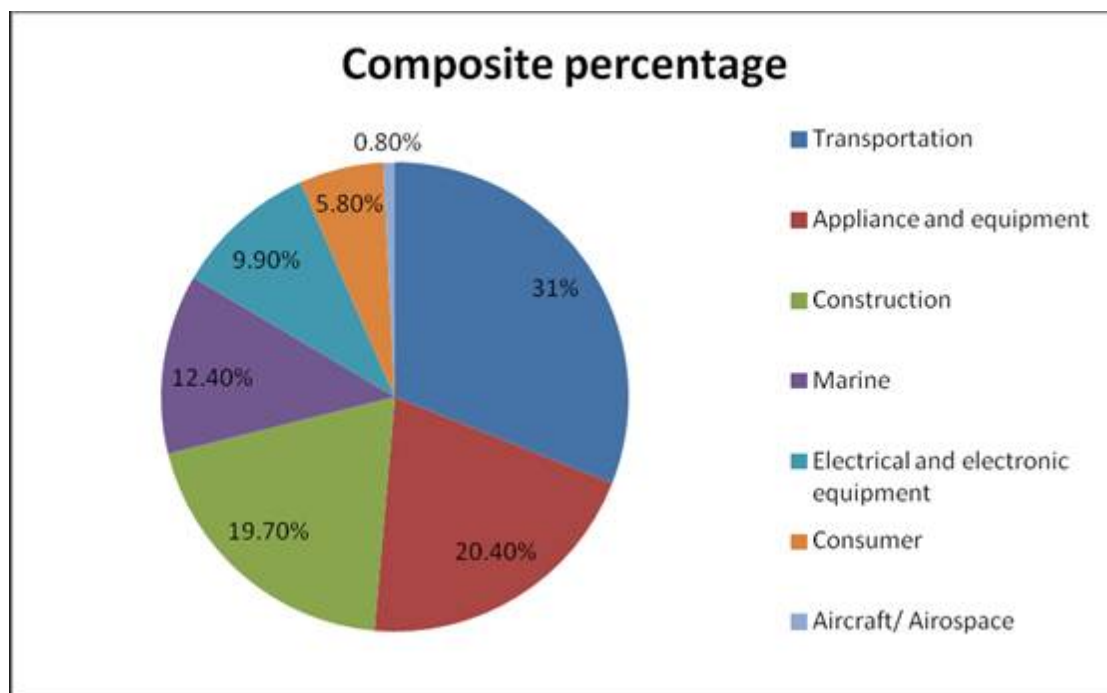


Figure 2.2: Applications of composite in different industries

(Source: SPI composite institute report 2009)

Common Composites Widely Used In Commercial Applications

- Wood -Cellulose Fiber in Lignin
- Plywood- Cross-Laminated Veneer
- Fiberglass- Glass Fiber in Polyester
- Damascus- Laminated Steel & Iron
- Concrete- Steel & Rock in Cement
- MMC- SiC Fiber/Particles in Aluminium
- CRP -Carbon Fiber in Epoxy (Lee, 1990).

In conclusion, there is no universally accepted definition of composite materials. Definitions in literature vary considerably and they consider different structural levels of matter. At the macrostructural level, gross structural forms of constituents, e.g., matrices, particles, and fibres are dealt with. A composite material is, therefore, a combination of two or more chemically different materials with a distinct interface between them. Microscopically, separate identities of the constituent materials are maintained, but the combined materials produce different characteristics and properties from those of the parent materials. One of the

constituents forms a continuous phase, the matrix; the other is present in the form of fibres or particulates which act as reinforcement and this reinforcement forms a discontinuous phase that is uniformly dispersed throughout the matrix. The matrix material in a composite can be a polymer, metal, or ceramic. Depending on the matrix used, composite materials are classified as polymer matrix composites (PMCs), metal matrix composites (MMCs), or ceramic matrix composites (CMCs). Most of the commercially used composites have polymers as their matrix. Various chemical combinations, compositions, and microstructural arrangements are possible in each matrix category. Both MMCs and CMCs which find high temperature applications are attracting more users. The primary effect of the reinforcement relies somewhat on the matrix used. In polymer based composites, the fibre increases the modulus and strength of the composite materials many times because polymers have very low modulus and strength as compared to the reinforcing fibres. On the other hand, the fibre reinforcement in ceramic matrix composites increases the fracture toughness of the matrix and makes the materials less susceptible to brittle failure. Ceramic matrix composites have low fracture toughness but their modulus is more or less the same as that of the reinforcing fibres. The addition of fibres with controlled interfacial properties to the ceramic matrix also increases its crack resistance significantly. Fibres can either be used in continuous or discontinuous lengths but are more effective when used in the former case. For discontinuous fibres, the fibre aspect ratio can be varied but the length is usually less than 6 mm. The most common form in which fibre-reinforced composites are used in structural applications is called a laminate. Laminates are obtained by stacking a number of thin layers of fibres and matrix and consolidating them into the desired thickness. Fibre orientation in each layer, as well as the stacking sequence of various layers can be controlled to generate a wide range of physical and mechanical properties for the composite laminates. Traditionally, fibres have been used in the reinforcement of polymer, metal and ceramic matrices but particulates are now finding wider applications because they can be incorporated into those matrices with more ease. Particulates, however, are generally less effective than fibres in reinforcing the matrix.

The term advanced composites is being used to differentiate composite materials with high-performance characteristics, generally strength and stiffness, from the simpler forms like reinforced plastics. Most advanced composites are used in structural applications. The fibres are long with length-to-diameter ratio of over 100. The strength and stiffness of the fibre is much greater, often a multiple of those of the matrix material.

2.4 Epoxy Resin

The family of polymers gets its name from the epoxy functional group that terminates molecules or that is internal to the structure. Epoxies are really polyethers, because the monomer units have an ether type of structure with oxygen bonds, R—O—R whereas the building blocks and chemical reactions involved in producing and crosslinking of unsaturated polyesters are similar for different polyester types, the situation is rather complex with epoxies. A wide range of building blocks are used in polymerization and numerous different compounds in crosslinking. In the following, only one epoxy configuration is considered and will have to serve as a representative for the entire epoxy family. An epoxide, or oxirane, group consists of one oxygen and two carbon atoms arranged in a ring as shown in Figure 2.3(a). Often the epoxide group contains yet another carbon atom and is then referred to as a glycidyl group as shown in Figure 2.3(b).



Figure 2.3: Structure of epoxide (oxirane) group (a) and glycidyl group (b)

2.4.1 Manufacturing Process of Epoxy Resin

Simplest form of epoxy resins are produced from reaction between epichlorohydrin and bisphenol –A. There are two basic stages for manufacturing epoxy resin

Stage 1: Making diglycidyl ether of bisphenol A (DGEbPA)

Pre-polymer is made by mixing bisphenol A (BPA) and epichlorohydrin (ECH) in the presence of sodium hydroxide (NAOH). Step by step reaction is explained in Figure 2.4. First, hydroxide ion of NAOH reacts with BPA and swap hydrogen from BPA to make water. At the same time Na⁺ Stabilize BPA's negatively charged oxygen atom (Bhatnagar, 1996).

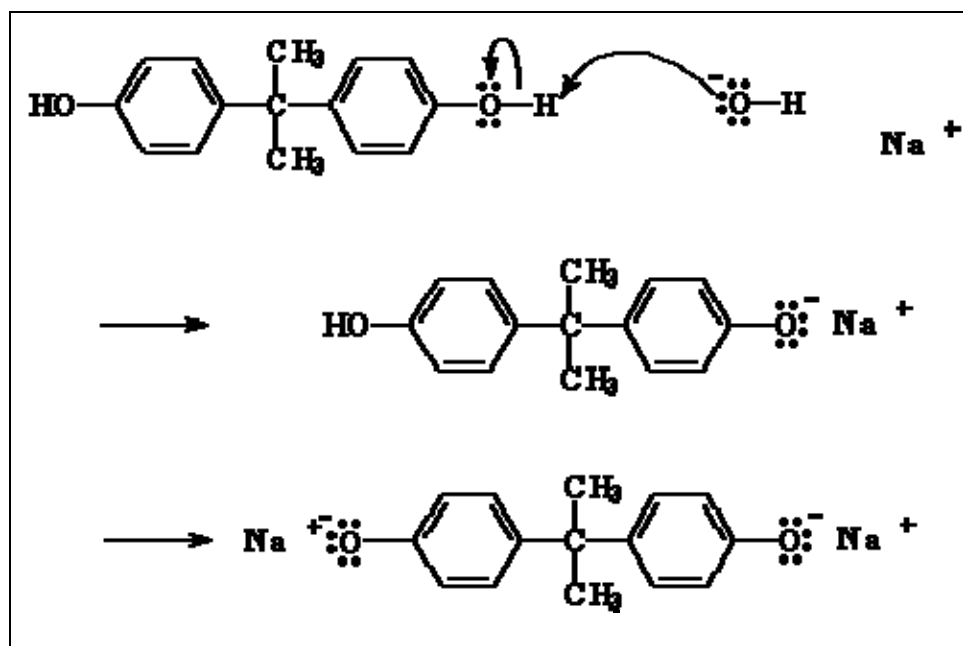


Figure 2.4: Reaction of NaOH with BPA

Next, charged oxygen atoms on BPA bond with ECH molecules and knock away chlorine atoms from ECH. Then, Cl^- neutralised by the sodium (Na^+) atoms as shown in Figure 2.5 (Bhatnagar, 1996).

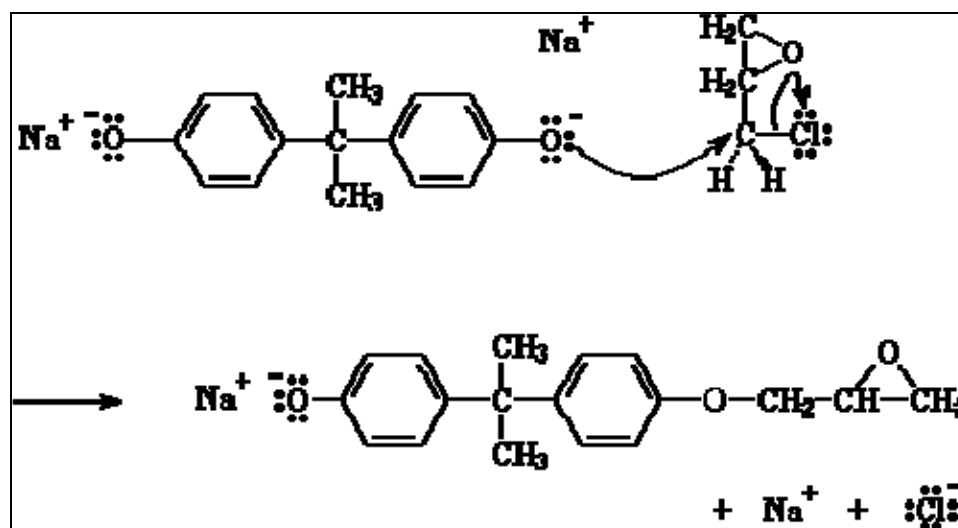


Figure 2.5: Further reactions amongst ECH, BPA and NaOH

At the end of this process, diglycidyl ether of bisphenol A (DGEBA) is produced. In Figure 2.6, n shows degree of polymerization. Depending on the mixing ratio of BPA and ECH, degree of polymerization varies. The value of n varies from 0 to 25 (Lubin, 1982).

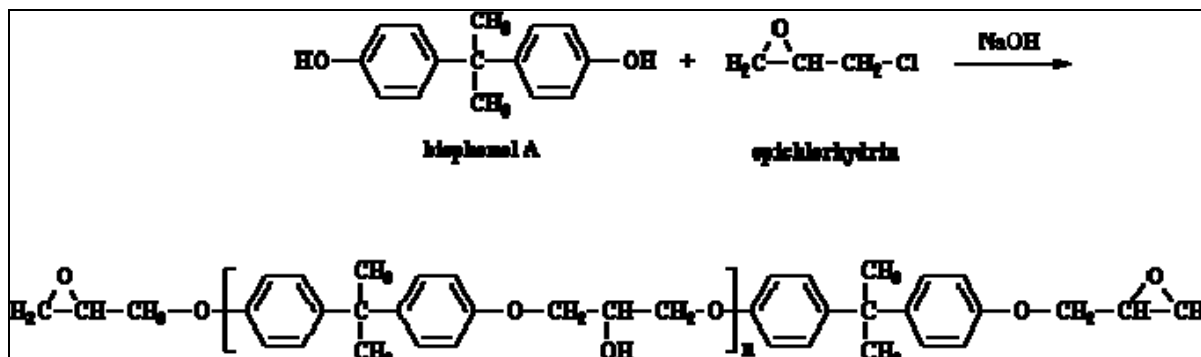


Figure 2.6: Final end product DGEBA

Stage 2: Curing DGEBA with Diamine

As oxygen is electronegative, they took all the electrons away from the nearest carbon. Now as they were sharing electrons unequally, the bond between carbon and oxygen broke down and new bond forms between nitrogen and carbon as illustrated in Figure 2.7 (Bhatnagar, 1996).

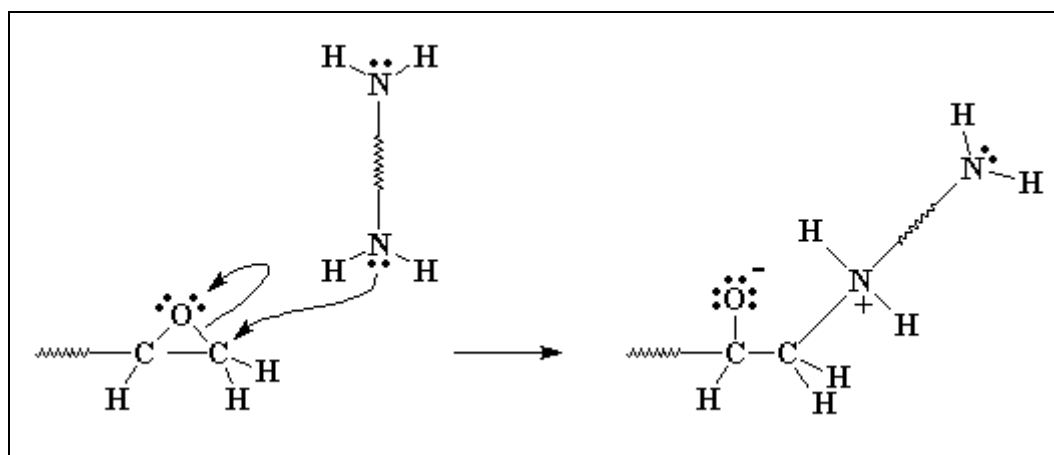


Figure 2.7: Propagation of linear chain

Now, as the oxygen has three pair of electrons that is not shared with any atoms, they attack on the hydrogen of amine group. They bond with them and form alcohol group. As shown in Figure 2.8, one amine group bonds with four epoxy group and form branched structure.

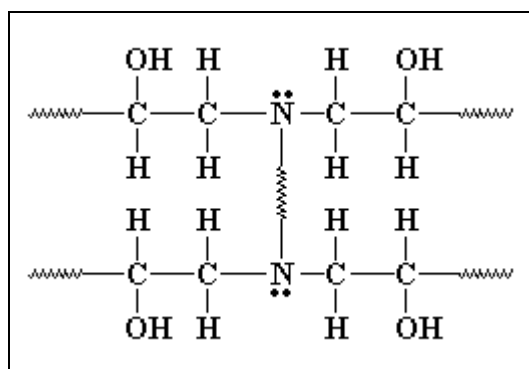


Figure 2.8: Formation of branched structure

In the same way, other amine groups bond with another epoxy group and formed a cross linked structure as shown in Figure 2.9 (Bhatnagar, 1996).

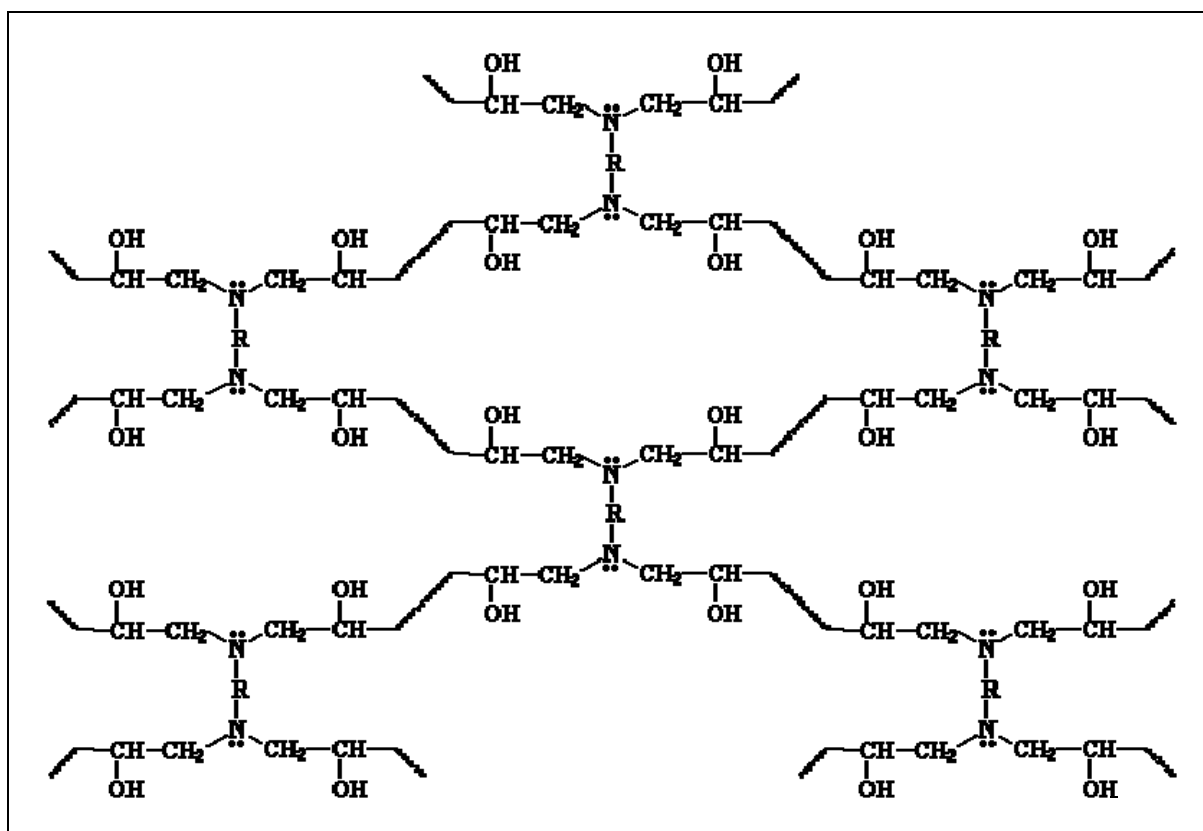


Figure 2.9: Final Cross linked epoxy resin structure

2.4.2 Properties of Epoxy Resins

Epoxy resins are the most versatile amongst all other polymers; it exhibits a number of highly desirable properties like

- Low shrinkage
- Excellent chemical resistance
- Outstanding mechanical strength
- High adhesion to a many substrates
- Good electrical insulating properties (Peters 1998).

A standard epoxy resin after seven days curing possesses following typical properties,

- Tensile Strength - 38,610 KPa
- Compressive Strength - 85,500 KPa
- Flexural Strength - 87,560 KPa
- Elongation at Break - 2.0 % (Bhatnagar, 1996)

Epoxy resins are extensively used in composites, bonding, adhesives, construction materials, laminates, textile finishing, coatings and moulding. Modern epoxy resins have found wide application in air and spacecraft industries.

Although it has good mechanical, electrical, thermal and chemical properties, it also possesses some undesirable properties like poor surface resistance. It tends to get yellow in outdoor exposure (Lubin, 1982).

2.5 Fillers

Fillers are mixed with epoxy resin to improve certain physical properties, increase versatility and reduce cost of material. The selection of filler depends on the application of composites. Silica is added in epoxy resin to increase density and prevent sagging. Silica filled epoxy resin used in filleting material and putties. Graphite powder is mixed to make low friction coating. It is used to make centre boards, rudders and boat bottoms. Wood flour filled epoxy resin can be used as a thickening agent. The colour of the mixture is consistent brown and can be used as a glue joints in naturally finished wood. Carbon fibers are used to increase chemical resistance of epoxy resin (Strong, 2000).

2.5.1 Glass Powder

Hollow Glass Micro spheres (Figure 2.10) are mainly made from soda lime (A-sphere) or borosilicate (E-sphere) (<http://srnl.doe.gov/hilights01.htm>). It has found greater use in recent years due to higher mechanical properties, substantial weight, excellent chemical stability and low heat conductivity. They can be dispersed very easily in organic materials like epoxy resin and reduce cost of material without affecting physical properties. They are widely used in commercial application such as luxurious yacht, aviation, bowling balls, heat insulating dope and space. The general properties of hollow glass microsphere are shown in Table 2.1 taken from Potter's industries website.

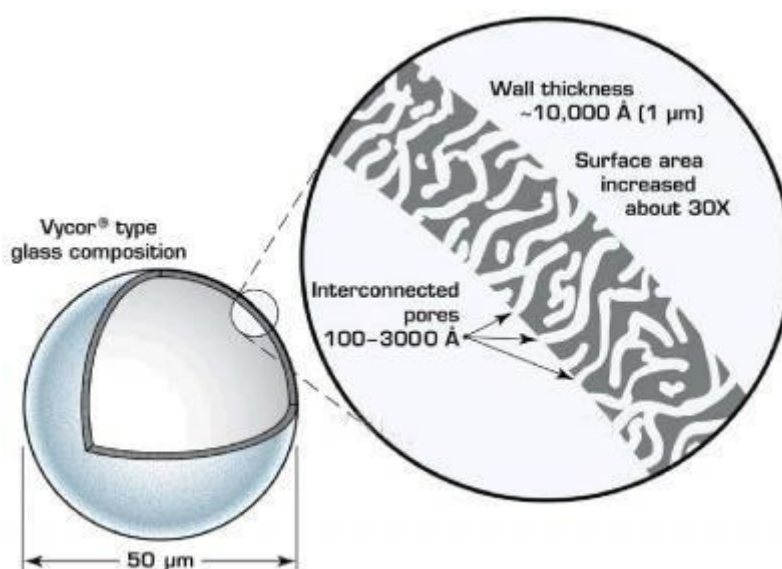


Figure 2.10: Hollow glass microsphere

The glass powder used is SPHERICEL® 60P18 (spherical) hollow glass spheres. They are chemically inert, non-porous, and have very low oil absorption. Typical properties of the spheres are shown in Table 1. SPHERICEL® 60P18 hollow spheres products offer formulators flexibility in polymer composites. The addition of hollow spheres to fibreglass reinforced plastics (FRP), epoxy, compounds, and urethane castings can provide weight reduction cost, savings and improved impact resistance. Insulating features of hollow spheres also work in thermal shock and heat transfer areas. The density of the hollow glass powder used in this research is 600 kg/m³ because the other filler, ceramic hollow spheres or SLG used in similar study is 700 kg/m³; this will give a better basis for comparison of results

obtained. When polymer used in concrete, hollow spheres provide a cost effective alternative without degrading physical properties.

Table 2.1: Spherical hollow glass powder properties

Shape	Spherical
Colour	White
Composition	Proprietary Glass
Density	1100 kg/m ³ and 600 kg/m ³
Particle Size	Mean Diameter 11 and 18 microns
Hardness	6 (Moh's Scale)
Chemical Resistance	Low alkali leach/insoluble in water
Crush Strength	>70 MPa

2.6 Dielectric Fundamentals

Every material has unique electrical characteristics which are dependent on its dielectric properties. Accurate measurement of them can provide information about its possible applications. It is also useful to improve design of product made by particular material.

2.6.1. Dielectric constant

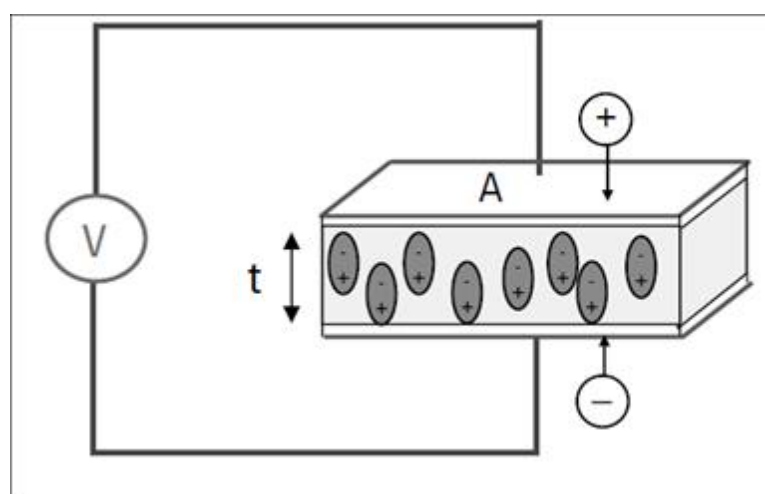


Figure 2.11: Arrangement of parallel plate capacitor across DC voltage

A material is said to dielectric if it has ability to store energy when external field is applied (Meredith, 1998). In simple words, if dielectric material is placed between capacitor plates as shown in Figure 2.11 and a DC voltage is applied, the capacity of capacitor to store energy will increase. Dielectric material has a property to neutralize charges at the electrodes. As shown in the Figure 2.12, if V is voltage of DC source, than capacitance without dielectric material will be

$$C_0 = \frac{A}{t} \quad (2.1)$$

where,

A is the Area of capacitor plate

t is the Distance between capacitor plates

If dielectric material is placed between capacitor plates, capacitance can be found by equation

$$C = C_0 \epsilon_r' \quad (2.2)$$

where, ϵ_r' is the real part of dielectric constant or permittivity

If AC power source is placed (Figure 2.12) instead of a DC source across the capacitor, than total current can be written as

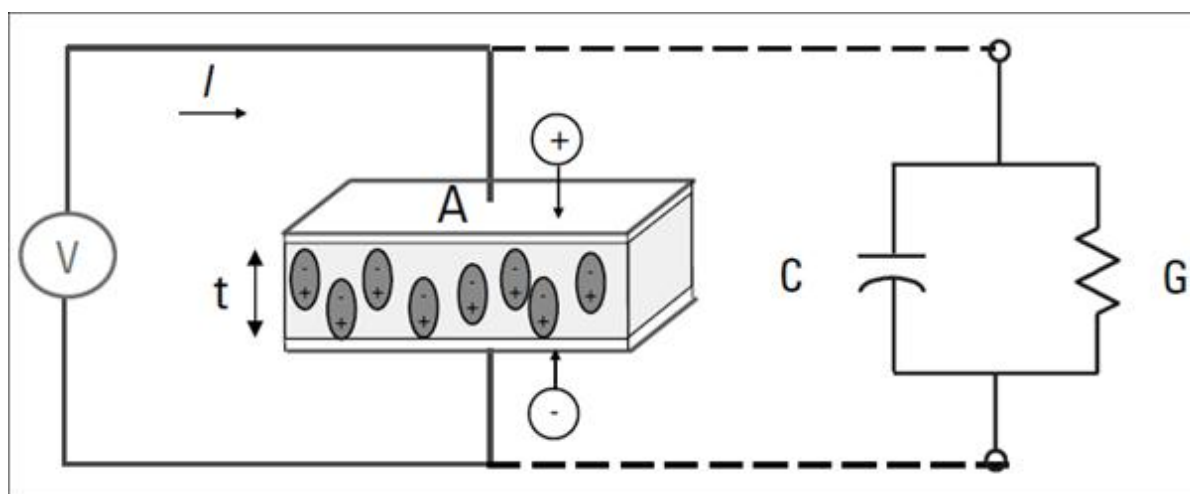


Figure 2.12: Arrangement of parallel plate capacitor across AC voltage

$$\begin{aligned}
I &= I_C + I_g \\
&= V (C_p + G) \\
&= V (j\omega C_0 \epsilon_r' + C_0 \epsilon_r'') \\
&= V j\omega C_0 (\epsilon_r' - j\omega \epsilon_r'') = j\omega V C_0 \epsilon_r' (1 - j \tan\delta)
\end{aligned} \tag{2.3}$$

$$I = V j\omega C_0 \epsilon_r \tag{2.4}$$

where,

I_C – Charging current

I_g – loss current

C_p – Capacitance = $j\omega C_0 \epsilon_r'$

G – Conductance

Now, the complex dielectric constant (ϵ_r) represents the real part ϵ_r' and imaginary part ϵ_r'' . ϵ_r' measures how much energy from an external field is stored in a material. ϵ_r'' measures how lossy a material is to an external field. Loss factor of dielectric shows the lag in polarization upon application of the field. The value of loss factor varies with temperature, frequency, moisture content, composition and physical state of material.

2.6.2 Loss Tangent

Dielectric properties can be used to classify materials as conductors, quasi conductors or insulators. The alternating polarisation of the molecules can consume energy, this is polarisation loss. A complex permittivity is required to characterise these materials. Materials can be good conductors at some frequencies while becoming a dielectric at other frequencies. A dielectric material is a substance that is a poor conductor of electricity, but an efficient supporter of electro static fields. An important property of a dielectric is its ability to support an electrostatic field while dissipating minimal energy in the form of heat. The lower the dielectric loss, the proportion of energy lost as heat, the more effective is a dielectric material.

The dielectric tangent loss of the samples of glass powder filled epoxy composites cured under ambient conditions and ambient conditions plus post-curing in an oven were measured.

The complex relative permittivity of a dielectric is $\epsilon = \epsilon' - j\epsilon''$; ϵ' , the real part is the dielectric constant; ϵ'' , the imaginary part is referred to as the loss factor. The ratio of these two values is the loss tangent, $\tan \delta = \frac{\epsilon''}{\epsilon'}$ (Meredith, 1983). The method used to obtain the dielectric tangent loss will be by measuring the capacitance and conductance with a meter.

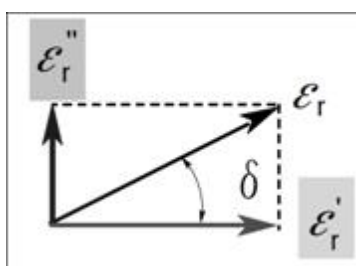


Figure 2.13: Vector Diagram of complex permittivity

As shown in Figure 2.13, if complex permittivity is shown in vector diagram, it forms angle delta (δ) with real part so $\tan \delta$ can be written as follows

$$\tan \delta = \frac{\epsilon''}{\epsilon'} \quad (2.5)$$

$$\tan \delta = \frac{\text{Energy lost per cycle}}{\text{Energy stored per cycle}}$$

$\tan \delta$ is known as the loss tangent. Loss tangent ($\tan \delta$) predicts the ability of the material to convert the incoming energy into heat (Meredith, 1983).

Loss tangent is frequency dependant. This experiment will be made at one hundred, 100, 120, 1k, 10k, 20k, and 100k. This is within the range of the measuring device. If the properties of the dielectric are constant over the frequency range of interest, then C will be constant and G will be proportional to frequency, and the loss tangent can be easily calculated by the formula $G = \omega C \tan \delta$.

2.6.3 Microwaves

As shown in Figure 2.14, microwaves are the electromagnetic waves and depend on the interrelationship between time varying electrical and magnetic fields (Sadiku, 2001).

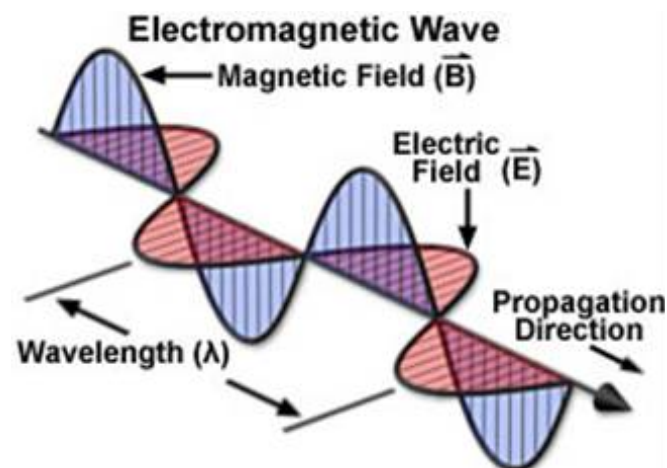


Figure 2.14: Electromagnetic waves

When microwave fields incident on highly conductive material like metal, they will almost be completely reflected from the surface. Microwave partly reflects from dielectric material like ceramic (Harper, 1992).

2.6.4 Dielectric Mechanism

The value of dielectric constant (ϵ') and loss tangent also depend on the magnitude of polarization of material in electromagnetic fields. The interaction of dielectric material with microwaves causes polarization of material. As shown in the Figure 2.15, net Polarization is the summation of four basic polarization mechanisms electronic, molecular, ionic and interfacial (National Research Council, 1994).

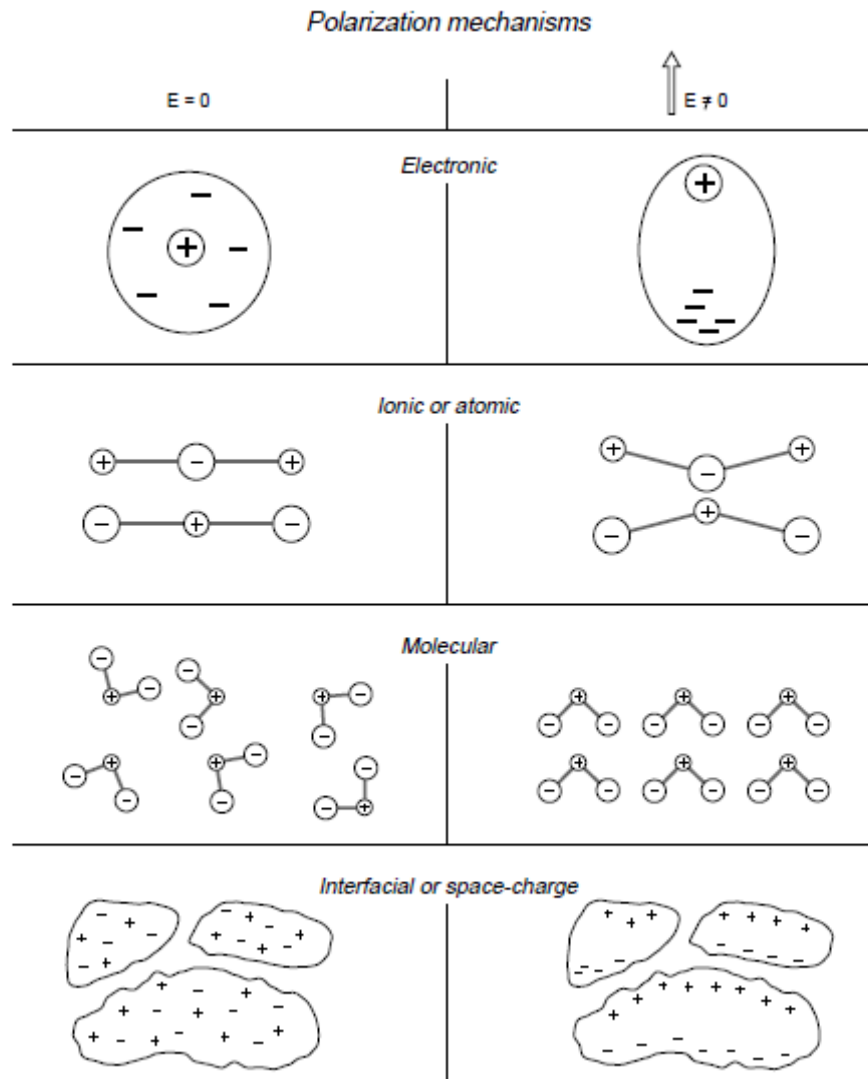


Figure 2.15: Polarization mechanisms

As the dielectric properties of material have been explained in the previous section, it is now time to analyse some of the materials dielectric properties in microwaves. Now, for the optimum conversion of microwave energy into thermal energy, values of ϵ' , ϵ'' and $\tan \delta$ should be high. From Table 2.3, it is found that distilled water has relative dielectric constant of 78 and loss tangent of 0.16 which are comparatively high. It means that distilled water can be efficiently heated using microwaves. However, some types of plastics and glasses have low of dielectric constants and loss tangents. Therefore, it is just wastage of electricity by trying to heat them using microwaves. Epoxies have dielectric constant 3.0 and loss tangent of

0.015. By calculating value of loss factor of dielectric (ϵ'') using loss tangent equation, it is found to be 0.045.

Table 2.2: Dielectric constant and loss tangent of different materials (NCR, 1994)

Material	Relative dielectric constant (ϵ')	Loss tangent ($\tan \delta$)
Distilled water	78	0.16
Raw beef	49	0.33
Mashed potato	65	0.34
cooked ham	45	0.56
Peas	63	0.25
Ceramic (aluminium)	8-11	0.0001 - 0.001
Most plastics	2-4.5	0.001 - 0.02
Some glasses (Pyrex)	Approx. 4.0	0.001 - 0.005
Papers	3 – 4	0.05 - 0.1
Woods	1.2 – 5	0.001 - 0.1
Ice	3.2 - 3.3	0.0007 - 0.001

Epoxies have moderate value for all these parameters. Therefore, it can be heated using microwave.

2.6.5 Penetration Depth

Another important parameter to consider while heating the material is the heat penetration depth in the material. The depth of penetration can be found out by the equation (Bows, 1999)

$$D = \frac{2}{\omega \sqrt{\mu_0 \epsilon_0 \epsilon' \tan \delta}} \quad (2.6)$$

where ω is the radian frequency of the microwave;

μ_0 is the permeability of free space;

ϵ_0 is the permittivity of free space.

From the equation, it is clear that skin depth is inversely proportional to the loss tangent. In simple words, as the value of loss tangent is low, skin depth is high and material heat more thoroughly. Since the value of loss tangent for epoxy is moderate, it can be heated thoroughly using microwaves.

2.6.6 Thermal Runway

Thermal runaway is the phenomenon of thermal instability due to interaction between the electromagnetic waves and materials and inhomogeneous nature of the composite (Meredith, 1998). In some part of the material, temperature rises suddenly while another part remains cool. Therefore hotspots get hotter and hotter uncontrollably and accelerate decomposition of the material. In a worst situation, it can damage the material. To avoid the problem of thermal runaway and keep all the spots at same temperature, a glass filled with little water can be placed in the centre of microwave. As shown Figure 2.16, permittivity of water has nearly linear relationship with temperatures. Therefore, it helps to keep uniform temperature in all the areas inside microwave cavity (Bows, 1999).

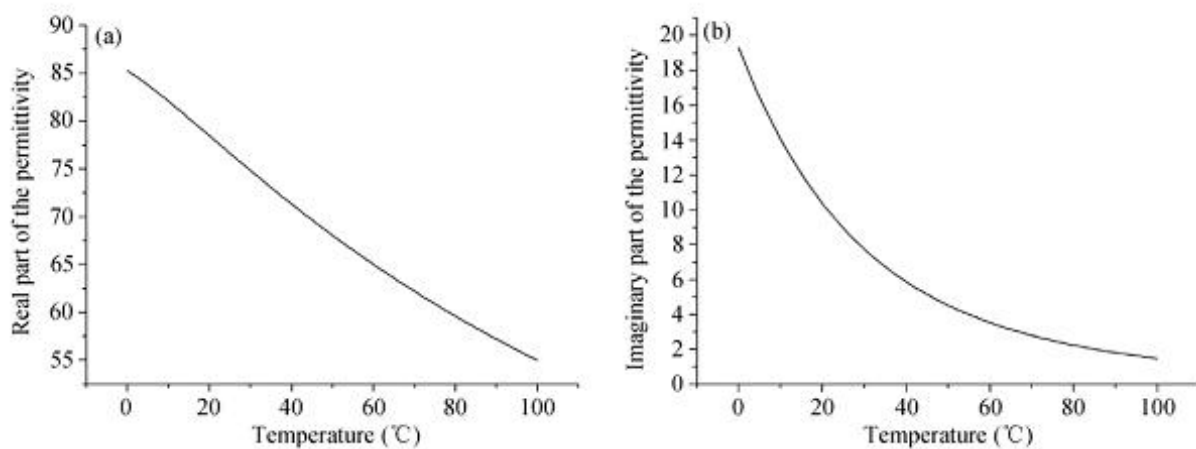


Figure 2.16: Permittivity of water at different temperature (Bows 1999)

2.7 Post Curing

It is the process of hardening or toughening of polymer by cross linking polymer chains using heat, ultraviolet radiation or additives. Study shows that all the thermoset resins have identical curing behaviour. Initially, the viscosity of mixture drops with the application of heat and degree of cross linking between the resin and hardener increases. At the end of this

process, 3-dimensional network of oligomer chain is created. This process is also known as a gelation (Strong, 2000).

2.8 Permittivity Test

Dielectric properties have already been explained in the section of dielectric fundamentals. Many techniques have been developed to measure dielectric constant and loss tangent. The most common techniques are

- Coaxial probe method
- Transmission line method
- Free space method
- Parallel plate method
- Resonant cavity method

Selection of methods depends on the factors like material properties, i.e. isotropic, homogeneous, sample size, material form, i.e. solid, liquid, powder, sheet, required measurement accuracy, frequency of interest, temperature. Figure 2.17 summarizes the suitability of different techniques in different conditions (Tereshchenko et al., 2011).

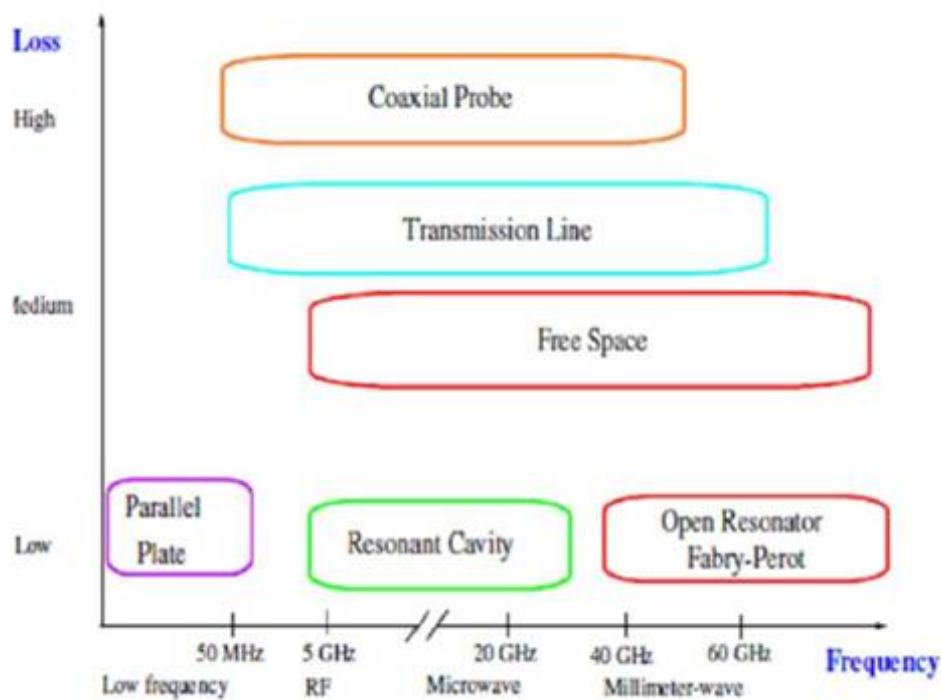


Figure 2.17: Summary of permittivity measurement techniques

2.9 Dynamic Mechanical Analysis (DMA)

2.9.1. Viscoelasticity of material

Recalling the basics, elastic materials regain their original shape after the removal of the stress while viscous fluid have high resistance to deformation under tensile or shear stress. Viscoelasticity is the property of material to exhibit both viscous and elastic behaviour while undergoing deformation. Polymer composed of long molecular chain exhibit deformation characteristics of both elastic solid and Newtonian liquid. Dynamic mechanical analysis (DMA) is the very important tool to study viscoelastic behaviour of the material (Ferry, 1980).

2.9.2. Glass Transition Temperature

Glass transition temperature is a particular phenomenon applicable to polymers only. Harper (1992) explained that glass transition temperature is the temperature at which polymer changes their mechanical properties from rigid and brittle state to tough and rubbery state or vice versa. In simple words, if the polymer glass transition temperature (T_g) is above room temperature, material behaves like a brittle glass material. If the T_g of a polymer is below room temperature, it behaves like an elastomer or rubber. If the glass transition temperature is just around the ambient temperature, it will be strong as well as tough with good impact resistance. At glass transition temperature, there is enough thermal energy in the structure of polymer to create adequate free volume and allow carbon atoms to move together. It makes polymer leathery. To explain it more clearly, take an example of rubber band. Rubber band is elastic in nature at room temperature. Now, if rubber band is cooled to a low temperature of $-40\text{ }^\circ\text{C}$, it will become stiff and brittle in nature. Because it has been take to below its glass transition temperature (Harper, 1992).

2.9.3 Storage Modulus and Loss Modulus

When a sinusoidal force is applied to perfectly elastic material, resulting stress and strain is always in phase. When sinusoidal force is applied to perfectly viscous material, the resulting stress and strain will have 90° phase difference. Viscoelastic material will have phase lag between 0° and 90° . If the phase lag between stress and strain is δ , than stress and strain equation can be written as,

$$\sigma = \sigma_0 \sin (\omega t + \delta) \quad (2.7)$$

$$\varepsilon = \varepsilon_0 \sin (\omega t) \quad (2.8)$$

where,

$$\omega = 2\pi f$$

f is the frequency in Hz

σ_0 is the maximum stress

ε_0 is the maximum strain

Storage modulus (E') is a measure the stored energy during elastic deformation of material. It represents the elastics portion and can be written as

$$E' = \frac{\sigma_0}{\varepsilon_0} \cos \delta \quad (2.9)$$

Loss modulus (E'') is the non reversible heat loss due to temperature rise above the glass transition temperature.

$$E'' = \frac{\sigma_0}{\varepsilon_0} \sin \delta \quad (2.10)$$

E' , the storage modulus is the elastic component of the composite and related to the sample's stiffness. E'' is the loss modulus and is the viscous component of the material and is related to the sample's ability to dissipate mechanical energy through molecular motion. The tangent of phase difference, or $\tan \delta$, is another common parameter that provides information on the relationship between the elastic and inelastic components. All of these parameters can be calculated as a function of time, temperature, frequency, or amplitude (stress or strain) depending on the application. The ratio of the 2 modulus is equal to damping coefficient or the tangent delta or loss tangent, indicating the ability of the material to dissipate energy.

$$\tan \delta = \frac{E''}{E'} \quad (2.11)$$

At the glass transition temperature (T_g), the storage modulus (E') decreases significantly and the loss modulus (E'') reaches a maximum (Ferry, 1980).

2.10 Tensile Properties of Material

When a material is subjected to tensile force, stress and strain in the material can be found out by following equations

$$\text{Stress } (\sigma) = \frac{\text{Load}}{\text{Original cross sectional area}} = \frac{P}{A} \quad (2.12)$$

$$\text{Strain } (\varepsilon) = \frac{\text{Change in length}}{\text{Total length}} = \frac{\Delta L}{L} \quad (2.13)$$

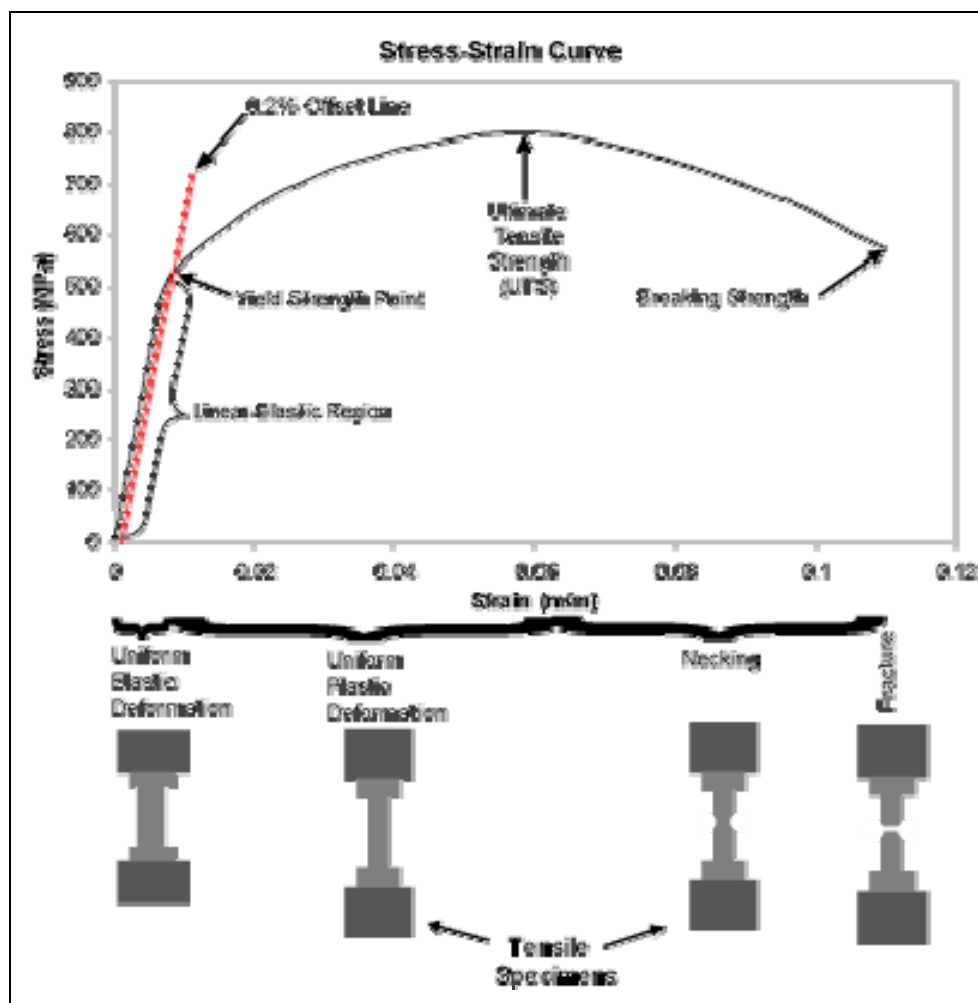


Figure 2.18: Stress-strain curve

Figure 2.18 shows the stress-strain curve for a ductile material. In the initial stage, stress and strain have linear relationship and obey Hooks' law. In this region, if the applied force is removed, the material will regain its original shape. The slope of this elastic region is called Young's modulus. It measures the stiffness of the material within elastic limit and can be determined by following equation (Silva, 2006).

$$\text{Young's modulus (E)} = \frac{\text{Stress}}{\text{Strain}} = \frac{\sigma}{\varepsilon} \quad (2.14)$$

2.10.1 Yield Strength

In stress strain curve, permanent deformation of the material starts at some point. At this point onwards, strain increases faster than stress. This point is known as the yield point of the material and stress at that point is known as the yield strength of the material. It can be written as follows (Silva, 2006).

$$\text{Yield Strength} = \frac{\text{Yield load (P)}}{\text{Original cross sectional area (A)}} \quad (2.15)$$

For most of the material, there is a gradual transition from elastic to plastic region. Therefore it is hard to determine the exact point at which plastic deformation begin. To find out yield point of the material, offset yield strength measurement method is developed. This method is discussed in ASTM E8 (metals) and D638 (plastics). An offset is specified as a % of strain (for metals, usually 0.2% from E8 and sometimes for plastics a value of 2% is used).

2.10.2 Tensile Strength

It is the maximum strength than material can withstand without breaking. It is the highest point in stress-strain curve and can be find out as follows,

$$\text{Tensile Strength} = \frac{\text{Maximum load (P)}}{\text{Original cross sectional area (A)}} \quad (2.16)$$

Material is not necessary broken at tensile strength. It depends on the type of material and service temperature. After this point, cross section area begins to decrease, popularly known as the necking. The load at which material breaks is known as breaking load and it is always

lower than ultimate tensile load as shown in Figure 2.18. Some materials do not break at maximum load during laboratory test but when exposed to extreme cold conditions in service; it may break at maximum load (Silva 2006).

2.11 Modelling

There are many models available to predict the mechanical properties of particulate composites. Models are available to predict yield and tensile strength as well as the elastic modulus and elongation at breakage of composite materials. In general these properties are determined by developing a relationship between the different constituents of the composites, in this case the matrix, epoxy resin, and the filler, glass powder.

The aspect ratio, which is determined by dividing the length of the particle by its diameter, is at unity, the particles can be considered spherical as shown in many studies. The Young's modulus of the composite is governed by a number of factors including the particulate loading and particle size. Fu et al. (2008) conducted this study and in doing so found that adhesion at the interface between the matrix and the filler has negligible effect on the modulus of particulate composites. It must be noted that small differences in particle size tend to have little to no effect on the mechanical properties of the composite and only when the particle size is reduced into the nano scale will there be a major difference.

2.12 Work of Others

There were some similar researches that had been carried out by other people. One of the researches was to analyze the tensile properties of the glass powder reinforced epoxy composites post-cured conventionally and in microwaves. The study found that 5% by weight glass powder filled epoxy resin had the highest value of yield strength, tensile strength and Young's modulus (Ku et al., 2011). Figure 2.19 shows the results of tensile strength of epoxy composite for varying percentage of glass powder taken by Ku et al. (2011).

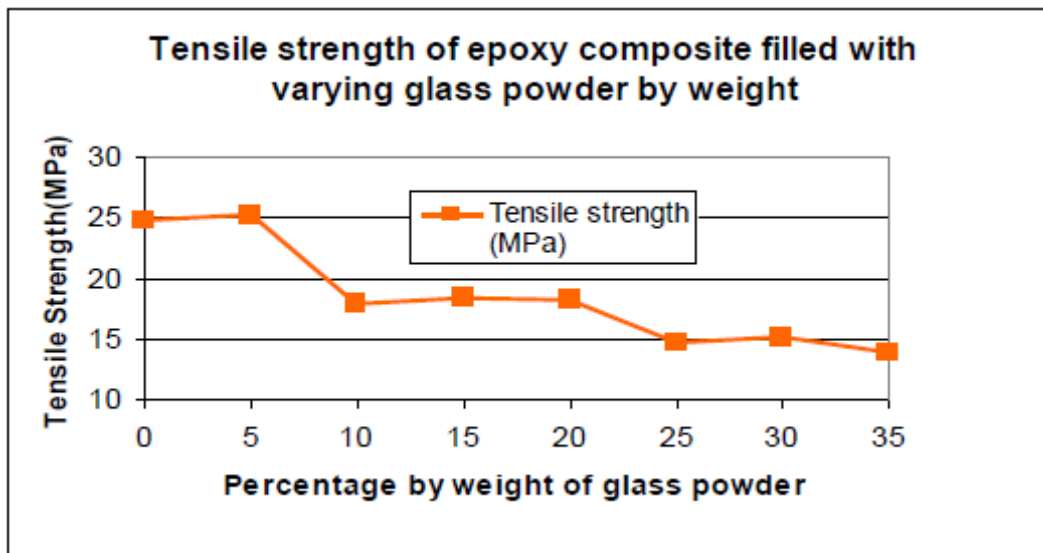


Figure 2. 19: Tensile strength of epoxy composite reinforced with varying glass powder by weight with varying glass powder by weight

Another research was to evaluate the Fracture Toughness of glass powder reinforced vinyl ester resin. This study was also carried out by Ku et al. (2009). The research concluded that glass powder can improve the properties of vinyl ester resin. The best percentage by weight of glass powder to vinyl ester resin was 15 percent (Ku et al., 2009).

3 METHODOLOGY

3.1 Introduction

This chapter will briefly outline the steps taken to retrieve results i.e. preparation, mixing process, post-curing, testing, and microscopic analysis of the samples. The testing method used in this project was kept similar to previous year methods for the purpose of comparing results. However, post curing in microwaves had slight changes compared to previous projects.

3.2 Resin and Catalyst Used



Figure 3.1: Resin and catalyst used

The resin used in this experiment is Kinetix R246TX (Figure 3.1). It is solvent free and thixotropic epoxy resin. It can be specifically cured using H126, H128, H160, H161 and H162 hardener at room temperature or low elevated temperature. In this experiment H160-medium hardener (Figure 3.1) was used because cured mechanical properties of Kinetix R246TX using H160 are excellent. The cured and uncured properties of R246TX and H160 are shown in Table 3.1 (ATL Composites, undated).

Table 3.1: Uncured and cured characteristics of R246TX and H160 (ATL Composites, undated)

UNCURED PROPERTIES		
	R246TX	H160- MEDIUM
Physical State	Opaque liquid	Clear pale brown liquid
Viscosity mPas at 25 °C	900- 1100	30
Specific Gravity g/ml at 25 °C	1.10	0.95
CURED CHARACTERISTICS OF R246TX RESIN & H160 HARDENER		
Pot Life - 100g at 25 °C	120 minutes	
Thin laminate open time at 25 °C	8 hrs 45 minutes	
Demould time at 25 °C	28 hrs	
Mix Viscosity mPas at 25 °C	300	

3.3 Glass Powder

The glass powder used is SPHERICEL® 60P18 (spherical) hollow glass spheres. They are chemically inert, non-porous, and have very low oil absorption. SPHERICEL® 60P18 hollow spheres products offer formulators flexibility in polymer composites. The addition of hollow spheres to fibreglass reinforced plastics (FRP), epoxy, compounds, and urethane castings can provide weight reduction cost, savings and improved impact resistance. Insulating features of hollow spheres also work in thermal shock and heat transfer areas. The density of the hollow glass powder used in this research is 600 kg/m^3 because the other filler, ceramic hollow spheres or SLG used in similar study is 700 kg/m^3 ; this will give a better basis for comparison of results obtained. When polymer used in concrete, hollow spheres provide a cost effective alternative without degrading physical properties.

3.4 Mixing

The weight ratio of resin to hardener used to make composite was 4:1. For 1000 gm mixture of composite with 30% glass powder, the required amount of resin is 560 gm, catalyst 14 gm and glass powder 300 gm as shown in the Table 3.3.

Table 3. 2: Spherical®60P18 hollow glass powder

Shape	Spherical, Non-Porous
Composition	Fused Inorganic Oxides
Appearance	White powder
Particle Size (μm)	6-32
True Density (g/cc)	0.60

Table 3. 3: Mixing ratio of epoxy resin, hardener and glass powder

Percentage of Glass Powder	Resin (g)	Catalyst (g)	R+C	Glass Powder (g)	Composite (g)
0%	800	200	1000	-	1000
5%	760	190	950	50	1000
10%	720	180	900	100	1000
15%	680	170	850	150	1000
20%	640	160	800	200	1000
25%	600	150	750	250	1000
30%	560	140	700	300	1000
35%	520	130	650	350	1000

The epoxy resin used in this study is Kinetix R246TX Thixotropic Laminating Resin, an opaque liquid, and the hardener used is kinetic H160 medium hardener which has a pot life of 120 minutes. Other hardeners like H126, H128, H161 and H162 can also be used. The glass powder was first mixed with epoxy resin, after this the hardener, kinetic H160 medium was added. The by weight ratio of resin to hardener used was 4:1. The composite was then cast to moulds of tensile test pieces and left to cure under ambient conditions for 24 hours. The tensile test specimens were taken out of the moulds and then post-cured in oven at 40 °C for 16 hours, and then at 50 °C for 16 hours and finally at 60 °C for 8 hours. This is to ensure the heat distortion temperature (HDT) is above 63 °C. To bring the ultimate HDT to 68 °C, another 15 hours of post-curing will be required. The dielectric losses of specimens were then measured.

The followings are the detailed steps used for making glass powder-epoxy resin composites.

Step 1: the moulds were cleaned and prepared

Step 2: correct amount of glass powder (60P18) was weighted in small plastic container (Figure 3.2).



Figure 3.2: Weighted glass powder

Step 3: correct amount of epoxy resin (R246TX) were weighted in another small plastic container.

Step 4: the resin and filler were mixed evenly and slowly with spoon and mechanical blender inside fume cabinet (for safety) in order to ensure a more homogeneous mixture.

Step 5: the weighted kinetix medium hardener, H160 was then added.

Step 6: the composite was mixed properly and slowly with spoon and mechanical blender (Figure 3.3).

Step 7: the mixture was poured into the moulds and the moulds with composites then put under the fume cabinet. Before pouring the mixture, plate surface was covered by a glossy paper as shown in Figure 3.4 to facilitate easier removal of composite after solidification. As the composite mixture was too sticky on the mould surface and it was hard to take it out of mould after curing, iron alloy plates were used instead of convention mould for tensile samples.



Figure 3.3: Mixing



Figure 3.4 : Composite mixture poured into the moulds

3.5 Initial Curing Of The Specimens

It can also be called as a solidification process where composite mixture takes on a rigid shape. In this process, exothermic reaction took place and material being cross-linked at room temperature. In initial curing stage, mould was kept on a flat surface at atmospheric temperature for more than 24 hours.

As newly formed composites has a high resistance to forces but brittle in nature due to random cross linking of molecules. Therefore, to improve its mechanical properties, post curing of composite mixture is required. Before the post curing, sample was cut into required standard sizes.

3.6 Methodology

The filler was glass powder and it was made 5 % to 35% by weight in the cured composite, PF/GP (X %), where x is the percentage by weight of the filler. As the raw materials of the composites are liquid and microscopic hollow ceramic spheres, the flexural test specimens were cast to shape. Table 2 shows the mass in grams of resin, catalyst and glass powder required respectively to make 1000 grams of uncured composite of 15 % by weight of glass powder. The uncured composite was then cast into the moulds and cured in ambient conditions. In this project, the x % by weight of PF/GP (X %) was varied from 5 to 35 % in step of 5 % by weight. The number of samples used for each percentage by weight of glass powder will be six.

After initial 24-hour curing when the test pieces were removed from the mould, they were post-cured in an oven or microwaves. For half of the samples, this was achieved by baking the pieces in an oven. Oven temperature and time are as follows:

- 16 hours at 40°C
- 16 hours at 50°C
- 8 hours at 60°C

Table 3.3b: Weight of materials required to make 1000 g of EP/GP (15%)

	Resin (R)	Hardener(H)	R + H	Glass powder	Composite
Ratio by weight	4	1	---	---	---
Percentage by weight	---	---	90	10	---
Weight of materials in 1000 g of EP/GP (15%)	680(g)	170 (g)	850 (g)	150 (g)	1000 (g)

The other half of the samples were post-cured in microwaves for 4 minutes using a power level of 320 W and the temperature reached was 40 °C. The temperature was measured using an Oakton TempTester Infra Red handheld thermometer. Allow the samples to cool in the oven cavity to room temperature. The samples were again heated to 50 °C by exposing them to a power level of 320 W for 6 minutes. Allow the samples to cool in the oven cavity to room temperature. The samples were again heated to 60 °C by exposing them to a power level of 320 W for 8 minutes. Allow the samples to cool in the oven cavity to room temperature. The processes were equivalent to heating the samples in a conventional oven

with the above parameters. In both cases, the intermittent and final temperatures were made the same in post-curing the composite samples.

The dimensions of the specimens of resins were 250mm x 10mm x 4mm and tested at a crosshead speed of 1 mm/min.

For samples used in thermal and dielectric measurements, they were made 5 % to 15% by weight of glass powder in the cured epoxy composite, EP/GP (X %), where X is the percentage by weight of the filler for the Electrical measurements. The glass powder percentages by weight vary in step of 5 %. As the raw materials of the composites are liquid and glass hollow spheres, the specimens of 120 mm x 120 mm x 6 mm (for dielectric loss tangent) and 60 mm x 10 mm x 4 mm (for thermal analysis) were cast to shape. The resin is an opaque liquid and is first mixed with the catalyst. After that the glass powder is added to the mixture, they are then mixed to give the uncured composite. The mixture of glass powder, resin and hardener were blended with mechanical blender to ensure a more homogenous mixture. The uncured composite was then cast into the moulds curing in ambient conditions. After initial 24-hour curing, half of the test pieces were removed from the mould and post-cured conventionally in an oven for 40 hours. The other half was post-cured in microwaves. Their dielectric loss tangent values then were measured. The samples for thermal analysis were then measured by DMTA equipment. The dielectric loss tangent of the specimens was then measured as well.

3.7 Post Curing

Post curing helps resin composites to reach its full physical characteristics. There are two common methods used for post curing of epoxy resin namely conventional oven and microwaves.

3.7.1 Post Curing in Microwave



Figure 3.5 : SANYO 800 W microwave with attached air duct

Figure 3.5 shows the SANYO 800 W microwave used for this project. All the windows were kept open during the experiment to keep good air circulation. The microwave can be set at 10 different power levels starting from 80 W to 800 W at an interval of 80 W. For this project, four different power levels were used i.e. 80 W, 160 W, 240 W, 320 W. To avoid thermal runaway, low power levels had been used.

As shown in the Table 3.4, microwave curing was carried out in stages to avoid thermal runaway problem and ensure all samples achieve specified temperature. One more point to be noted here, unlike the past projects, this time each stage was divided in to two steps to ensure uniform heating of the material. Samples were first heated up to 30 °C at power level of 80W and afterwards power was increased to 160 W, 240 W and 320 W to achieve 40 °C, 50 °C and 60 °C temperature respectively in each stage.

Table 3. 4: Microwave curing stages

	Temp (°C)	Power (W)	Time Taken (min)
Stage 1	30	80	5
	40	160	7
Stage 2	30	80	5
	50	240	8
Stage 3	30	80	5
	60	320	9

The time taken in each stage is mentioned in Table 3.4. The temperatures of the samples were measured by infrared thermocouple as shown in the Figure 3.6. Temperature was measured at different spots inside microwave cavity to ensure that each sample achieved the desired temperature in each stage. In some cases, different temperature at different spots was measured. In that case, the samples which were not at required temperature were placed back in the microwave cavity until the desired temperature was achieved. After completion of each stage, samples were allowed to cool to room temperature. No thermal runaway was observed at the end of curing. In other words, no material decomposition or burn spots were noticed.

**Figure 3.6: Handheld Infrared thermometer**

3.7.2 Post Curing In Oven

In conventional curing, first temperature was set to the required one, then the temperature rose quickly to the required one and was held there for a specified period of time. Heating in conventional oven provided energy to excite the molecule of epoxy composite, causing them to move closer and form bonds.

Post curing in oven was carried out in three stages over a time period of 40 hours. Time and temperature for oven curing were given below:

- Stage 1 : 16 hours at 40 °C
- Stage 2 : 16 hours at 50 °C
- Stage 3 : 8 hours at 60 °C

As shown in Figure 3.7, temperature and time were set using Eurotherm 3200 series controller. Once the temperature and time were set in the controller, it controlled time and temperature without interaction with anything.



Figure 3.7: Eurotherm 3200 series controller

All the specimens were placed together by maintaining same space between them to avoid uneven temperature region. At the completion of curing, specimens were allowed to cool before taking them out of oven.

3.7.3 Comparison Of Conventional Oven And Microwave Curing

There are couple of advantages using microwaves over conventional oven. The most important benefit of microwave heating is volumetric heating which means that material can directly absorb the microwave energy and convert it into thermal energy. It gives rapid, uniform, selective and controlled heating. Other advantages of using microwaves include uniform heating, high heating rates, reduction in cost and cycle time, less space requirement. In this project, microwave curing of all the specimens hardly took 6-7 hours while conventional oven took 40 hours in total. It means 34 more hours were required by conventional oven compared to microwaves for curing same number of samples. In industrial applications, where a large number of samples needs to be cured, this time difference is significant as it increases time and cost of post curing. One of drawback of microwave curing in comparison with the oven one is that it cannot be set at a particular temperature.

As per the Figure 2.17 of chapter 2, the ideal method for inspecting electrical properties of material in microwaves is resonant cavity method (Ku et al. 1999). Due to the limitation of signal generating capability of LCR meter used in this project, parallel plate method was used. The maximum signal that could be generated by LCR meter was 100 KHz. Although experiment was carried out at lower frequency, it can give an approximate idea of electrical properties of material.

Parallel plate method has similar arrangement as shown in Figure 3.8. The experiment was carried out in the specially designed room. The room has metal door, roof and ceiling. The earthed metal wall and roof reduce outside electromagnetic interference in the experiment.

Metal door was closed during the experiment. In this experiment, parallel copper plates (110mm x 110mm) were used as a capacitor and a sample plate (120 mm x 120 mm) was sandwiched between them. Copper plates and sample were clamped between wooden block as shown in Figure 3.12. AGILENT 4263B LCR meter was connected to the specimen to measure electrical properties of the material. The setup was connected to 240 V AC source and the power rating was 45 VA. Basic procedure to perform the experiment is attached in appendix B. The parameter that had been measured using the above shown setup is parallel capacitance (C_p), Loss tangent (D) and Shunt conductance (G). Electrical properties of the material were manually noted in a spreadsheet in frequency ranging from 100 Hz to 100

3.8 Dielectric Constant And Loss Tangent Measurement

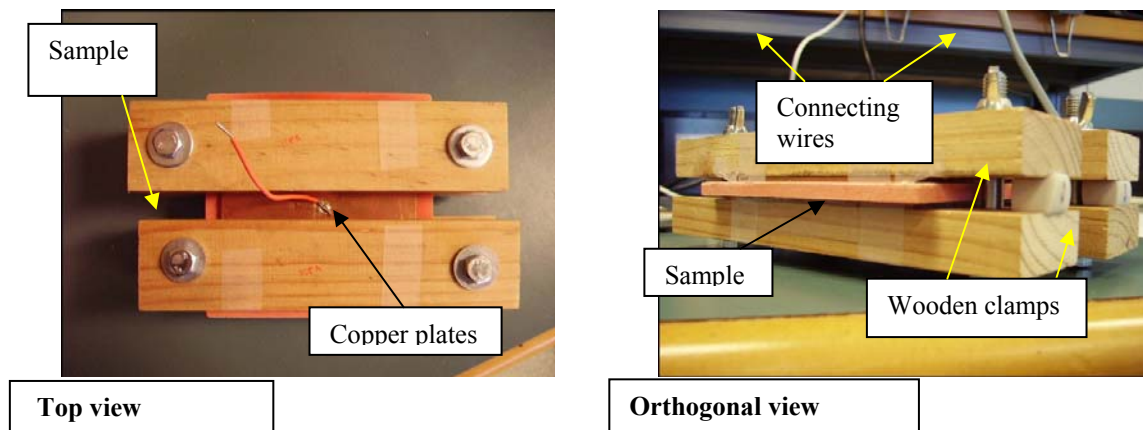


Figure 3.8: Parallel plated method set up

KHz. The accuracy of method is $\pm 1\%$ for parallel capacitance (C_p) and $5\% \pm 0.005$ for loss tangent (ASTM, undated).

3.8.1 Calculation Of Dielectric Constant And Loss Tangent

As in chapter 2, capacitance of capacitor can be calculated by,

$$C_p = \frac{\epsilon_0 \epsilon' A}{t} \quad (3.1)$$

ϵ_0 is the absolute permittivity of the material in free space = 8.854187×10^{-12} F/m

Rearranging the terms, dielectric constant ϵ' can be determined by

$$\epsilon' = \frac{C_p t}{A \epsilon_0} \quad (3.2)$$

Generally, the properties of the dielectric are constant over the used frequency range for this experiment. Therefore, capacitance of material will be constant and shunt conductance will be proportional to frequency, and the loss tangent ($\tan \delta$) can be calculated by the equation,

$$G = \omega C \tan \delta \quad (3.3)$$

3.9 Dynamic Mechanical Analysis (DMA) Test

This method is used to measure storage modulus (E'), loss modulus (E''), phase angle ($\tan \delta$) and glass transition temperature of viscoelastic material (Menard, 1999). In this method, sinusoidal force is applied to material to make it oscillate. The oscillation can be of two types. In first type, the free oscillation in which force is removed, once material begins to oscillate while in other, force is continuously applied to the material throughout the testing period. The former is known as forced oscillation (Schwikart, 1998). For this project, forced oscillation methods is used because forced oscillation can provide more accurate result as frequency of oscillation of material is same as applied force.

There are two test modes to carry out in this experiment. One mode is temperature sweep and other is frequency sweep. In temperature sweep mode, material is being tested under sinusoidal stress at constant low frequency while increasing the temperature. In frequency mode, temperature remains constant and material is tested at various frequencies.

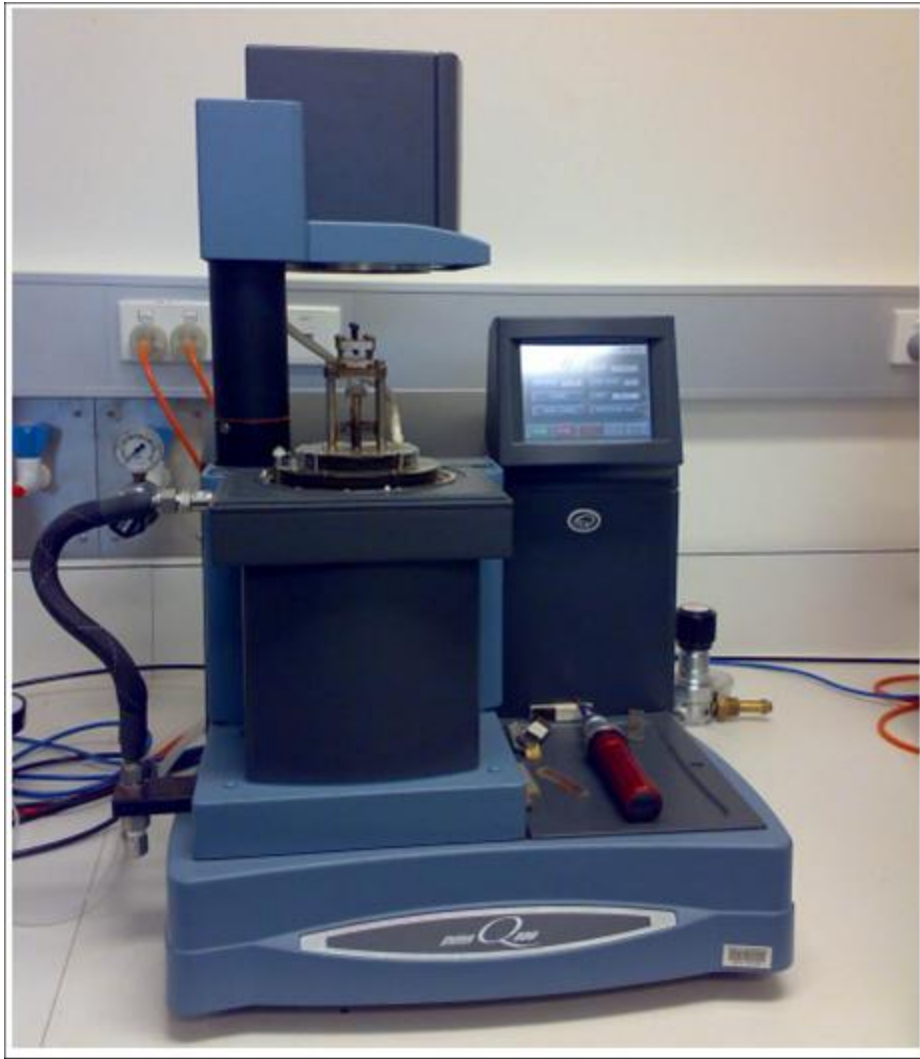


Figure 3.9: DMA test machine (TA instruments Q800)

Figure 3.9 shows the DMA test machine TA instruments Q800 used for project. The sample tested is first held tightly into clamps and secured at both the ends. Top cover was then moved down to close the testing area. Enclosed test chamber provide better control for testing temperature. Computer was connected to the testing machine to analyse stress, resulting strain and other parameters. The test began at room temperature and the maximum temperature was set at 270 °C with temperature ramp rate of 3 °C per minute. The test was carried out at fixed 1 Hz frequency.

Viscoelastic material has two different physical states. Below glass transition temperature (T_g), it is in solid elastic state. While once T_g is reached, material begins to turn in a viscous fluid and strain gradually lags behind the stress with increase in temperature. When material completely turns into viscous fluid, the phase angle (δ) between stress and strain becomes 90°.

Storage modulus, loss modulus and phase angle had been calculated and graph was generated by the software in the connected computer.

Dynamic mechanical thermal analysis (DMTA) is an important technique used to measure the thermal properties of elastomers. It provides information on the ability of materials to store and dissipate mechanical energy upon deformation, which is used to determine which materials can be used in dynamic applications, such as rollers or wheels. Many materials, including polymers, behave both like an elastic solid and a viscous fluid, thus the term viscoelastic. Polymeric materials, which are viscoelastic in nature, are subject to time, frequency and temperature effects on mechanical properties which can be analysed by this method. The machine used is DMA Q800. The dimensions of the samples used for analysis are 60 mm x 10 mm x 4 mm. The mode used here is 'dual cantilever'; the sample is clamped at both ends and flexed in the middle. If the sample is clamped at one end, then it is single cantilever, which is a good general-purpose mode for evaluating thermoplastics and highly damped materials (elastomers). Dual cantilever mode is ideal for studying the cured thermosets. For this study, the temperature change was 5°C per minute and the final temperature was 270-280°C. While heating, the composite is deformed (oscillated) at constant amplitude (strain) over a range of frequencies and the mechanical properties measured.

The basic properties obtained from a DMTA test include elastic modulus (or storage modulus, E'), viscous modulus (or loss modulus, E'') and damping coefficient ($\tan \delta$) as a function of temperature, frequency or time. Results are typically provided as a graphical plot of E' , E'' and $\tan \delta$ versus temperature. DMA identifies transition regions in plastics, such as the glass transition, and may be used for quality control or product development.

3.10 Tensile Tests

The tensile tests were carried out using MTS 810 material test system. Figure 3.10 shows the essential part of the machine. For this experiment, the gauge length was set to 75 mm and test rate was 1 mm/min. As shown in Figure 3.11, electronic vernier caliper was used to measure the width and thickness of the specimens. Computer was connected to the testing machine so that elongation of specimens with increase in the tensile load can be trace. Samples were clamped to the jaw. Care was taken so that samples do not slip from its grips by using the

right size jaws and selecting appropriate clamping pressure. Correct clamping pressure had been applied to the samples. If too much pressure is applied, sample may break and if the clamping pressure is too low, material may slip.

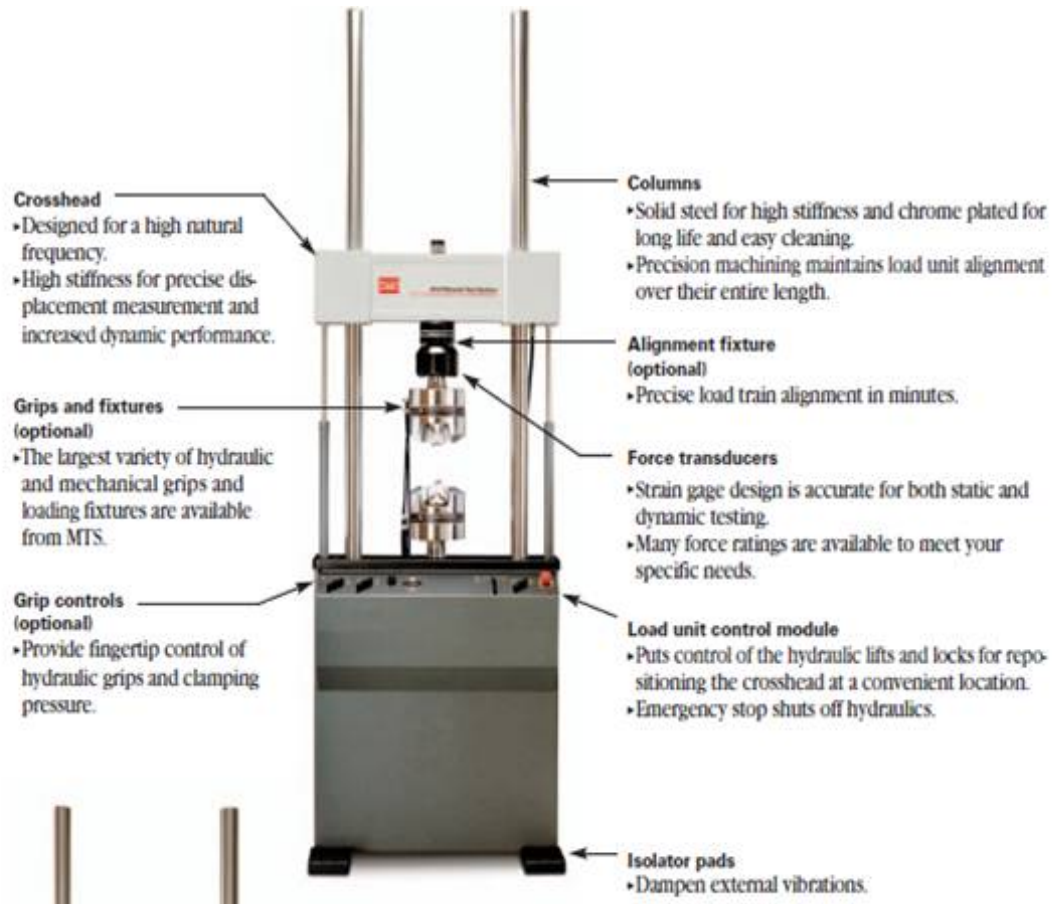


Figure 3.10: Tensile test machine



Figure 3.11: Vernier calliper

3.11 Optical Microscopy

As shown in Figure 3.12, samples were examined with an Olympus BX41M optical microscope. The microscope has a magnification range from 50X to 300X. The epoxy composites were examined to determine whether the samples were well mixed or not.

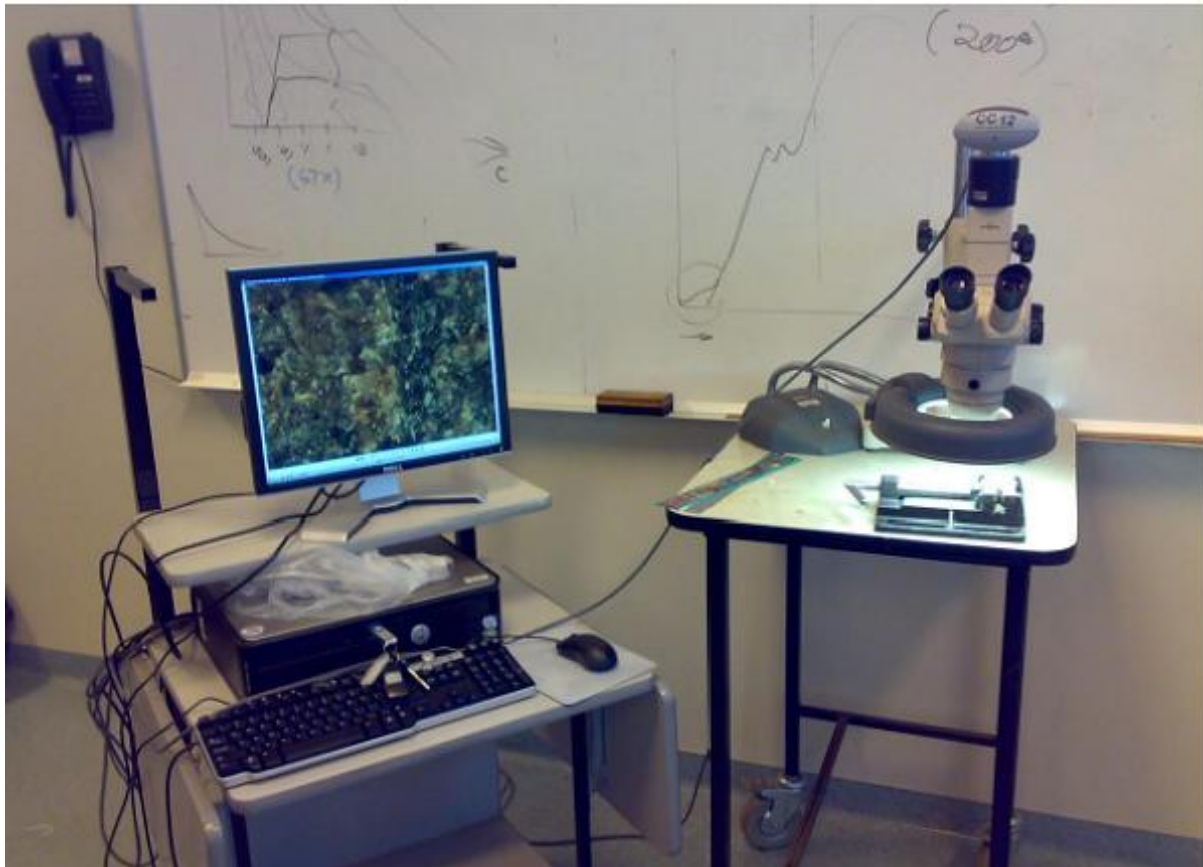


Figure 3.12: Optical Microscope

The samples having highest, medium and lowest value of tensile strength were inspected under optical microscope.

4 RESULTS AND DISCUSSIONS

4.1 Introduction

This chapter analyses and discusses the results obtained from the permittivity, DMA, tensile tests and microscopic examination which were outlined in Chapter 3. The DMA and permittivity tests provide the information about change in thermal and electrical properties of

epoxy composites with varying percentage of glass powder while tensile tests provide the information about mechanical properties of the composites.

4.2 Permittivity Test Results

Ideal dielectric materials store and return energy without any loss. They are poor conductor of electricity but efficient supporter of electrostatic field. Therefore, material said to be dielectric, if loss tangent is less than 0.01; conductor, if $\tan \delta > 100$, semi-conductor, if $0.01 < \tan \delta < 100$ and dielectric, if $\tan \delta < 0.01$. Dielectric properties can then be used to classify materials as conductors, quasi conductors or insulators. The alternating polarisation of the molecules can consume energy, this is polarisation loss. A complex permittivity is required to characterise these materials. Materials can be good conductors at some frequencies while becoming a dielectric at other frequencies. A dielectric material is a substance that is a poor conductor of electricity, but an efficient supporter of electro static fields. An important property of a dielectric is its ability to support an electrostatic field while dissipating minimal energy in the form of heat. The lower the dielectric loss, the proportion of energy lost as heat, the more effective is a dielectric material.

4.2.4 Measured Loss Tangent

The dielectric tangent loss of the samples of glass powder filled epoxy composites cured under ambient conditions and ambient conditions plus post-curing in an oven were measured. Figure 4.1 and 4.2 show the comparison of loss tangent for varying percentage of glass powder. Samples have higher value of loss tangent at lower frequency; however it gradually decreases with increase in the frequency. Samples with 5 % weight of glass powder composites have the low values of loss tangent, while higher values of loss tangent have been noted for higher percentage of glass powder mixture. Samples with 5 % weight glass powder have lowest values of loss tangent at all frequency, while 15 % weight of glass powder microwave cured composite has higher values of loss tangent. Therefore, it can be concluded that (a) at lower frequency (120 Hz), there is higher electrical loss tangent, while at higher frequency, lower electrical loss tangent (it can be noted that there is not gradual decrease of electrical loss tangent with the increase in frequency). (b) When post-curing in microwaves, the values of electrical lost tangent decreases with addition of glass powder at low frequency (120 Hz in Figs. 4.1 and 4.2).

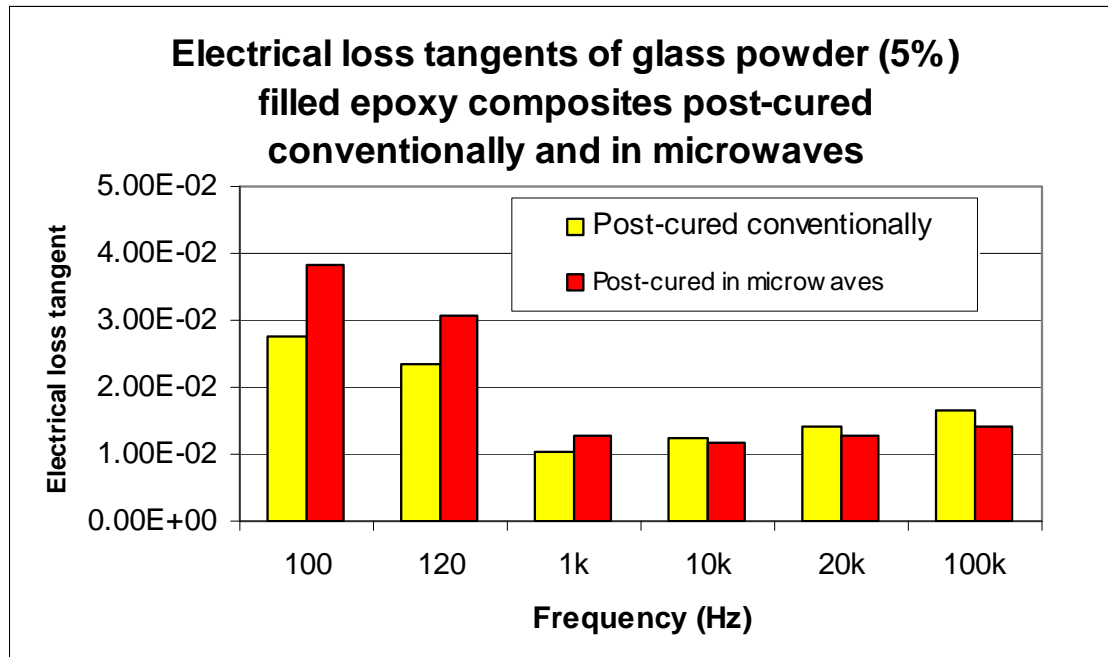


Figure 4. 1: Loss tangent of epoxy-glass powder (5%) post-cured in oven and microwaves

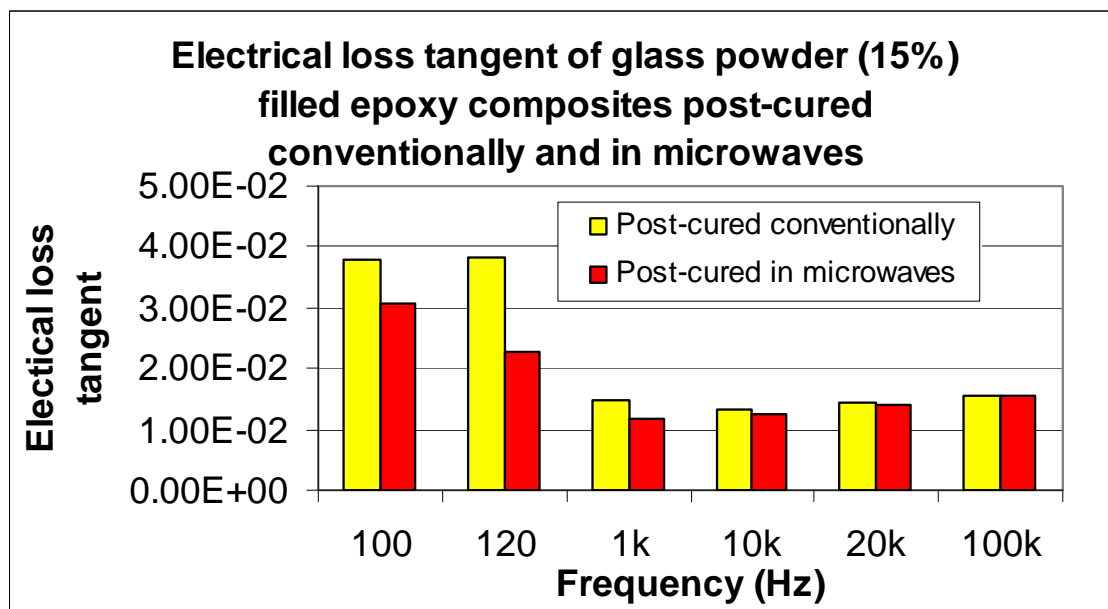


Figure 4. 2: Loss tangent of epoxy-glass powder (15%) post-cured in oven and microwaves

From Figure 4.3, it found that sample post cured in microwave is more effective to convert incoming microwave energy in to heat compare to conventional oven. One more important relationship as explained in 2.6.5 of chapter 2, loss tangent is inversely proportional to skin depth. It means that samples cured in conventional oven can penetrate to more depth compare to samples cured in microwave. Depth of penetration increases with increase in the glass powder percentage and frequency. Samples with 5 % weight and 15 % weight of glass powder have shown similar behaviour. However, values of loss tangent decrease with increase in the percentage of glass powder.

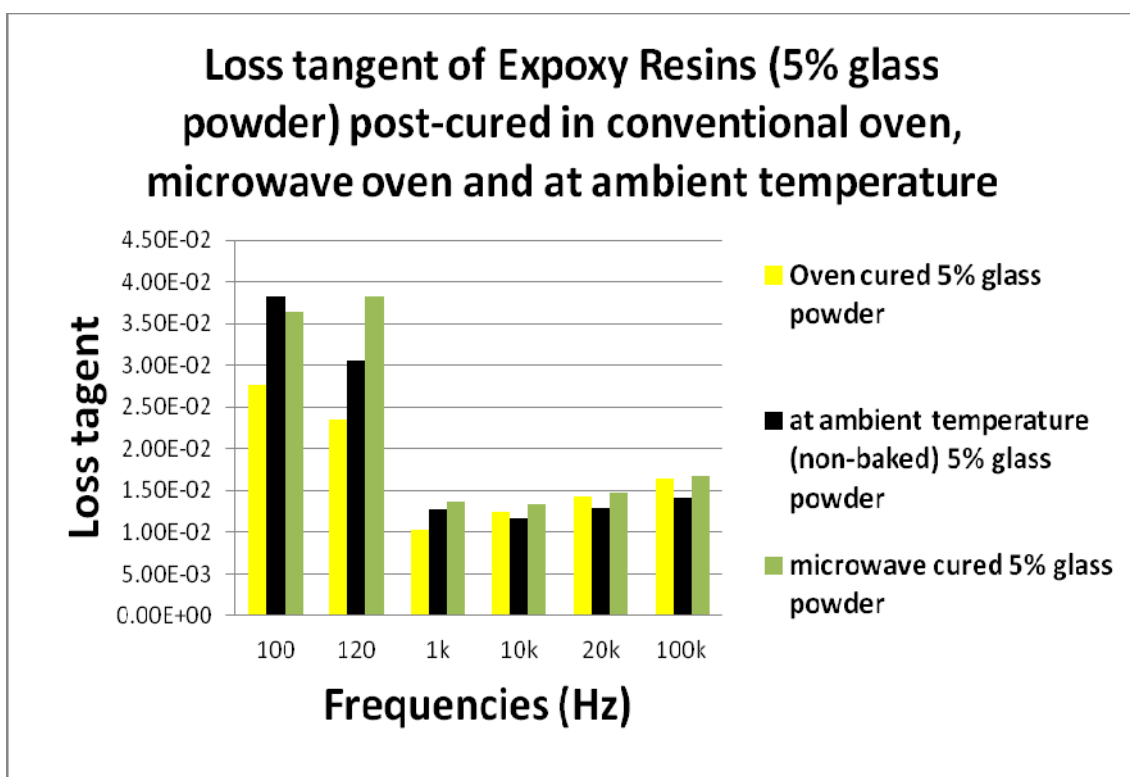


Figure 4. 3: Comparison of loss tangent of 5 % weight of glass powder filled epoxy resins from different curing method

As shown in Figure 4.4, unlike samples with lower percentage of glass powder, samples with 15 % weight of glass powder have higher values of loss tangent cured in conventional oven compare to samples cured in microwave. Therefore, it can be concluded that the values of loss tangent of samples cured in microwave are higher than those cured in conventional oven.

The figures for other samples with varying percentage of glass powder are attached in Appendix B.

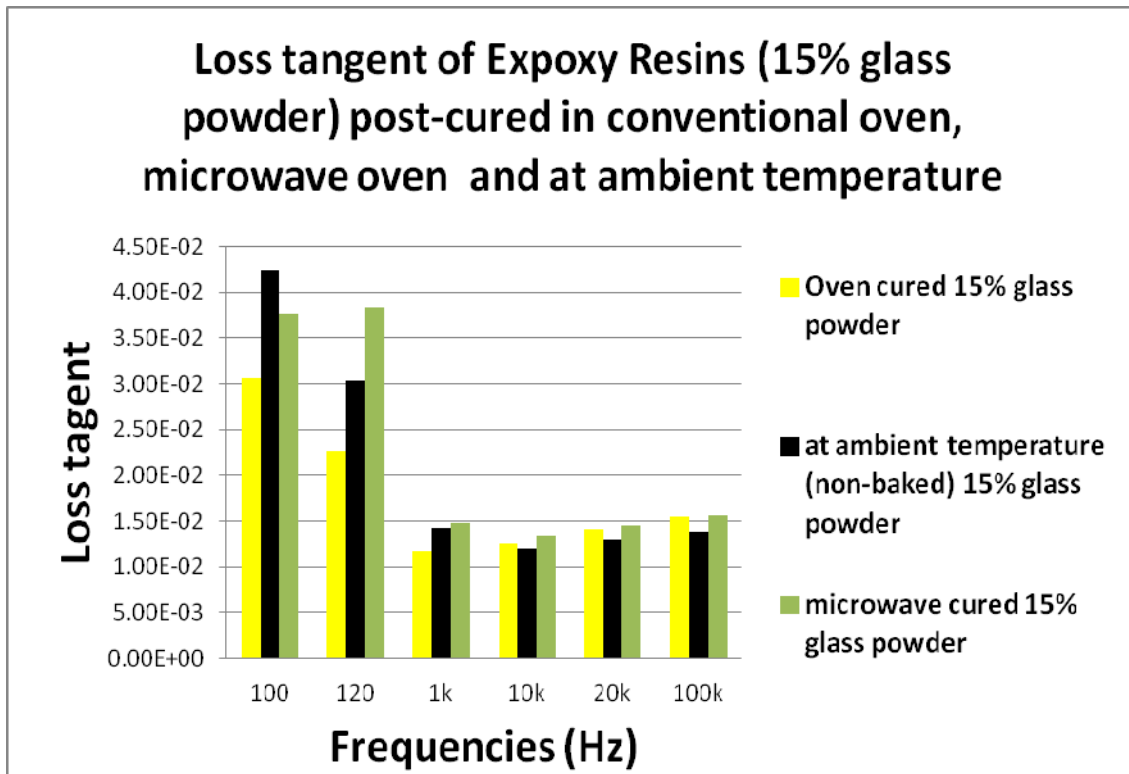


Figure 4. 4: Comparison of loss tangent of 15 % weight of glass powder filled epoxy resins from different curing method

4.3 Dynamic Mechanical Analysis (DMA) Test Results

Figure 4.5 shows the change in storage modulus, loss modulus and loss tangent with increase in temperature for sample with 5 % weight of glass powder cured in microwave oven. At the starting of test, storage modulus has maximum value. As the temperature rises, material turns from elastic solid to viscous fluid state. Accordingly, storage modulus which represents elastic property of material drops down and loss modulus rises and reaches to maximum. The temperature at which it reaches to maximum is called glass transition temperature (T_g).

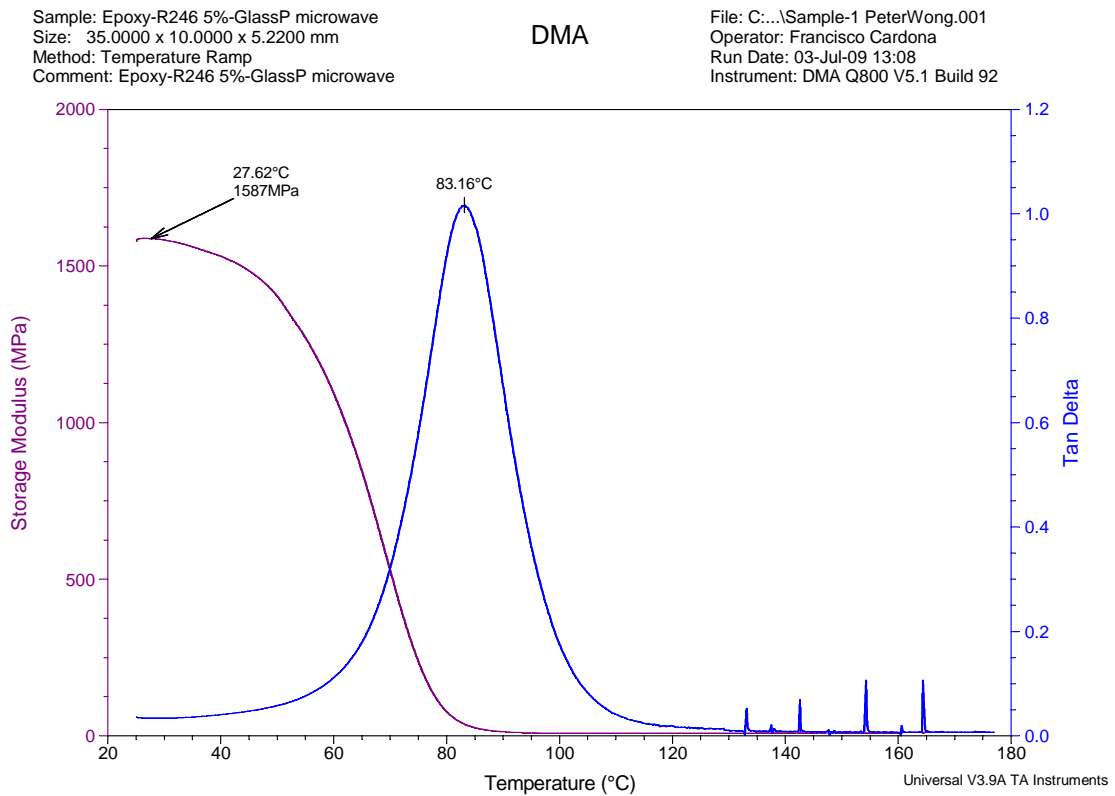


Figure 4. 5: DMA test results for samples cured in microwaves with 5 % weight of glass powder

As shown in Figure 4.5, sample with 5 % weight glass powder has storage modulus of 1587 MPa, glass transition temperature (T_g) of 83.16°C and loss tangent of 1.025. From the values of storage modulus and loss tangent, loss modulus (E'') can be calculated using equation 2.8. Loss modulus, $E'' = 1.025 \times 1587 = 1626.68$ MPa.

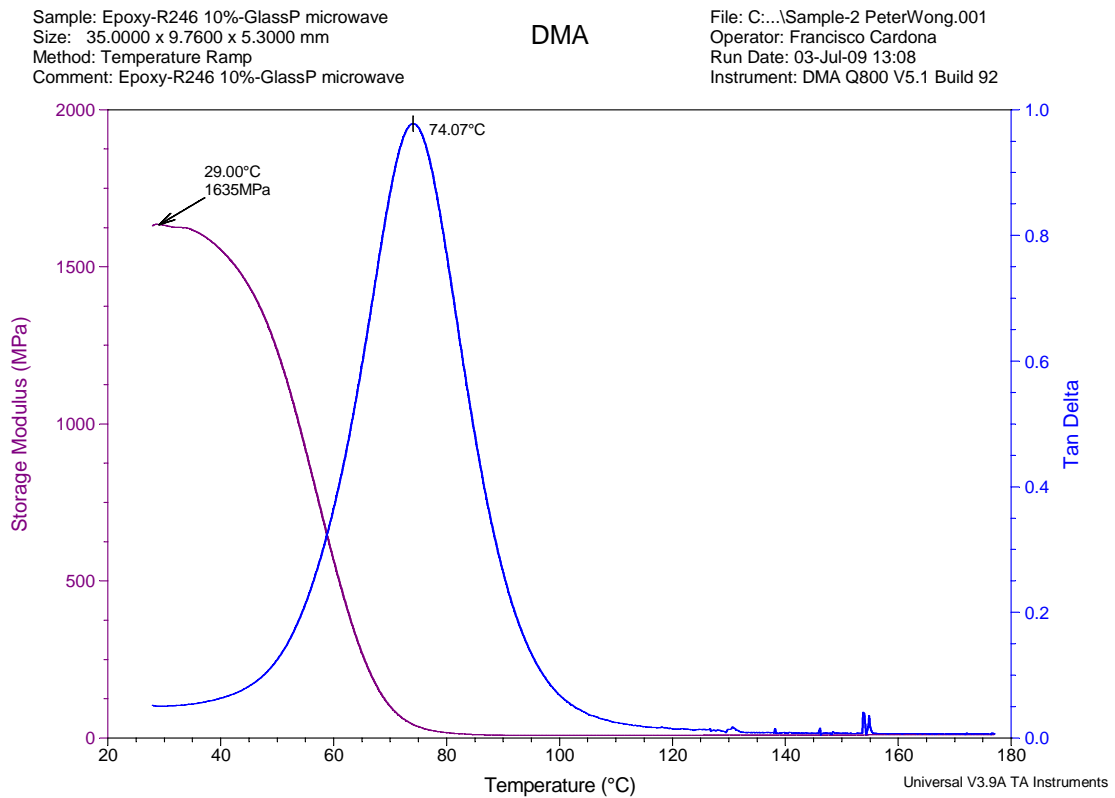


Figure 4. 6: DMA test results for samples cured in microwaves with 10 % weight of glass powder

As shown in Figure 4.6, sample with 10 % weight glass powder has storage modulus of 1635 MPa, glass transition temperature (T_g) of 74.07°C and loss tangent of 0.975. From the values of storage modulus and loss tangent, loss modulus (E'') can be calculated using equation 2.8. Loss modulus, $E'' = 0.975 \times 1635 = 1594.13$ MPa

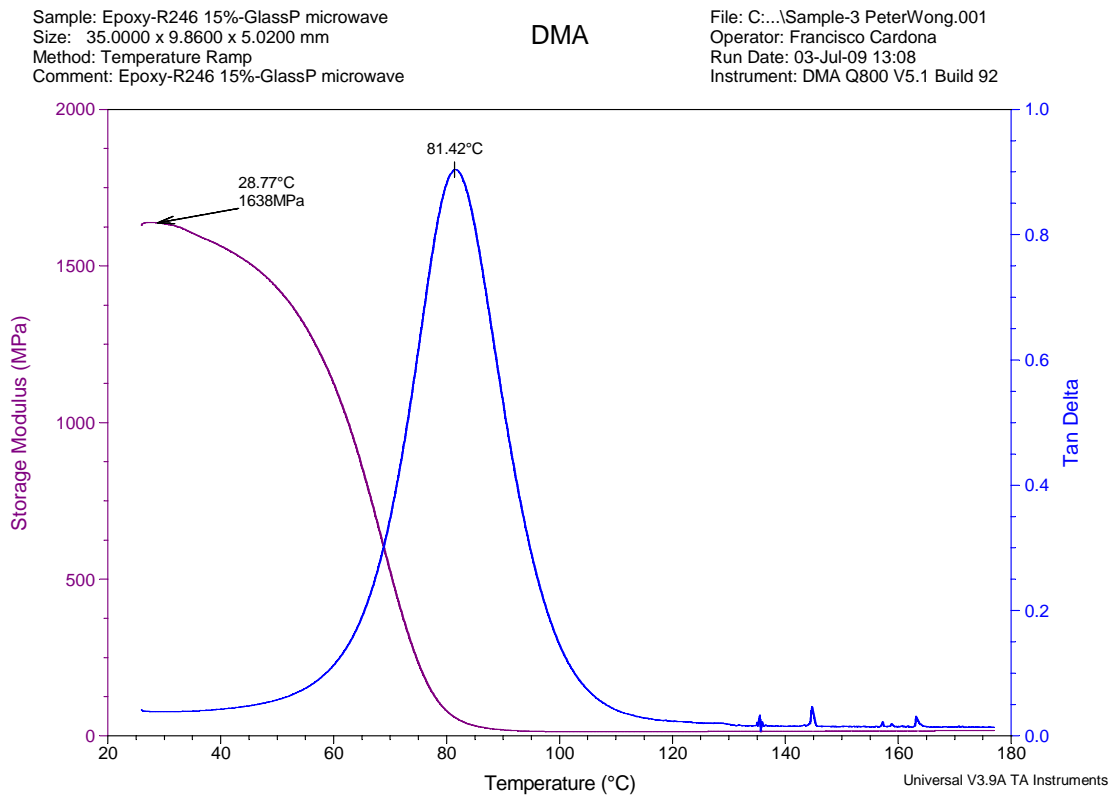


Figure 4. 7: DMA test results for samples cured in microwaves with 15 % weight of glass powder

As shown in Figure 4.7, sample with 15 % weight glass powder has storage modulus of 1638 MPa, glass transition temperature (T_g) of 81.42°C and loss tangent of 0.90. From the values of storage modulus and loss tangent, loss modulus (E'') can be calculated using equation 2.8. Loss modulus, $E'' = 0.9 \times 1638 = 1474.20$ MPa

Table 4. 1: DMA test results for samples cured in microwaves

% weight of glass powder	T_g (°C)	E' (MPa)	Tan δ	E'' (MPa)
5	83.16	1587	1.025	1626.68
10	74.07	1635	0.975	1594.13
15	81.42	1638	0.90	1474.20

4.3.1 Relationship Between Glass Transition Temperature And Percentage Of Glass Powder

As shown in the Table 4.1, glass transition temperature, T_g varies with varying percentage of glass powder. Therefore it can be concluded that the strength of the epoxy cross linking is affected with increase in the amount of glass powder. Difference between the values of T_g for samples post cured in microwaves with difference % weight glass powder is 9.09 °C which shows that cross linking in epoxy composites varies with varying percentage of glass powder. The drop of glass transition temperature at 10 % weight glass powder was not yet clear.

4.3.2 Relationship Between Storage Modulus (E') And Percentage Of Glass Powder

As shown in Table 4.1, microwave cured samples have consistent trend in storage modulus, E' value with varying percentage of glass powder. The value of storage modulus increases with % weight of glass powder.

4.3.3 Relationship Between Loss Modulus (E'') And Percentage Of Glass Powder

As shown in Table 4.1, microwave cured samples have consistent trend in Loss modulus, E'' value with varying percentage of glass powder. The value of storage modulus decreases with % weight of glass powder.

4.4 Tensile Test Results

4.4.1 Yield strength

Figure 4.8 illustrates the yield strengths of varying percentage by weight of glass hollow spheres reinforced epoxy matrix composites. The yield strength of the neat resin was 17.95 MPa, which was higher than those of the composites with any percentage by weight of glass powder other than 5 w/t % (18.24 MPa) of glass powder. After dropping to 14.64 MPa at 10% by weight of filler, it remained stable up to 20 % percent by weight of glass powder. After this, it dropped further to 13.62 MPa at 25 % by weight of filler and remained so up to 35 % percent by weight of glass powder. In general, the higher the percentage by weight of glass powder, the lower was the yield strength.

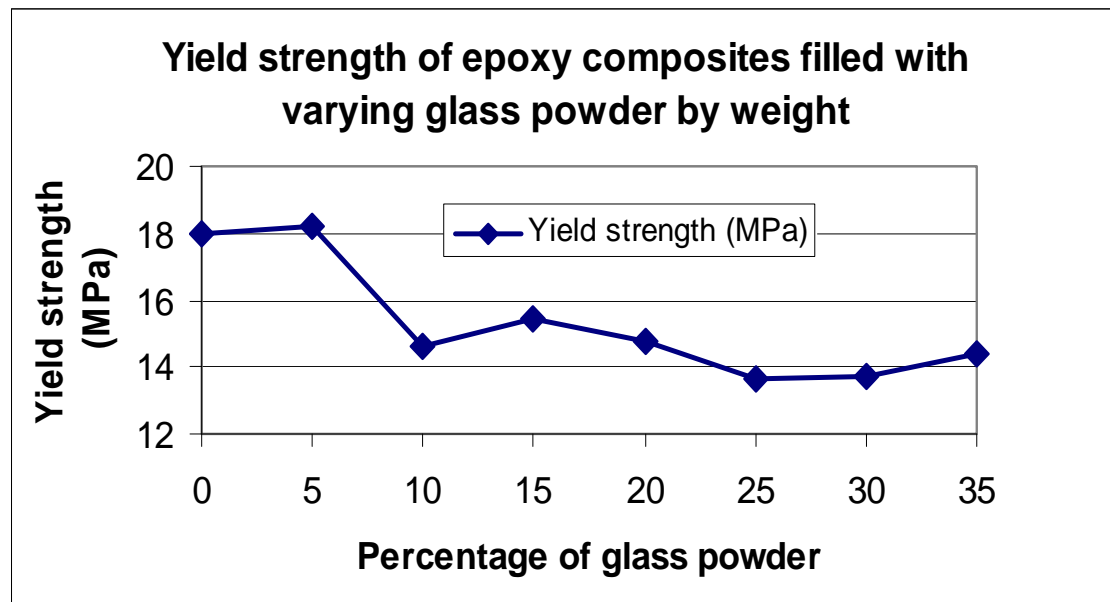


Figure 4. 8: Yield strength of epoxy composite reinforced with varying glass powder by weight post-cured in an oven

4.4.2 Tensile Strength

Figure 4.9 shows the tensile strengths of epoxy composites with varying percentage of glass powder by weight. The tensile strength of the neat resin was 24.80 MPa, which was only lower than that (25.14 MPa) of composite with 5 % by weight of filler, but higher than those of the composites with any percentage by weight of glass powder. At 10 percent by weight of filler, the tensile strength dropped to 17.79 MPa; it then remained up to 20 % percent by weight of glass powder; after this glass powder reinforcement dragged the values of tensile strength further down; it dropped to 14.72 MPa when the percentage by weight of filler was 25% remained so up to 35 % percent by weight of glass powder. The variation of tensile strength with respect to percentage by weight of glass powder is the same as that of yield strength. If cost and tensile strength were considered at the same time, composite with 5 % by weight of filler is the best. It can be found that the trend for the graphs of yield and tensile strengths are the same and it can be argued that the results were correct in trend.

The tensile strength of neat resin used in the study (24.8 MPa) is much lower than that used by the studies of Nakamura et al. (77.3 MPa) and Radford (75.9 MPa). The former did not mention the epoxy resin used and the latter used anhydride-cured epoxy resin. In this study, the pot life of the hardener is 120 minutes; therefore, the epoxy resin used must be amine-cured as well. Effects of particle size on the tensile properties of cured epoxy resins, filled with spherical silica particles prepared by hydrolysis of silicon tetrachloride, were studied by Nakamura et al.. Particles were sorted into five kinds of different mean sizes in the range from 6-42 microns. Static tensile tests were carried out. Tensile strengths were found to increase with a decrease in the particle size but with increase particle contents. This trend is supported by the tensile strength results of epoxy/alumina trihydrate particulate composites in Table 2. In this study, the tensile strengths were found to decrease with increase particulate loading and it can be argued that this happened because the glass powder particles had not been treated by hydrolysis of silicon tetrachloride.

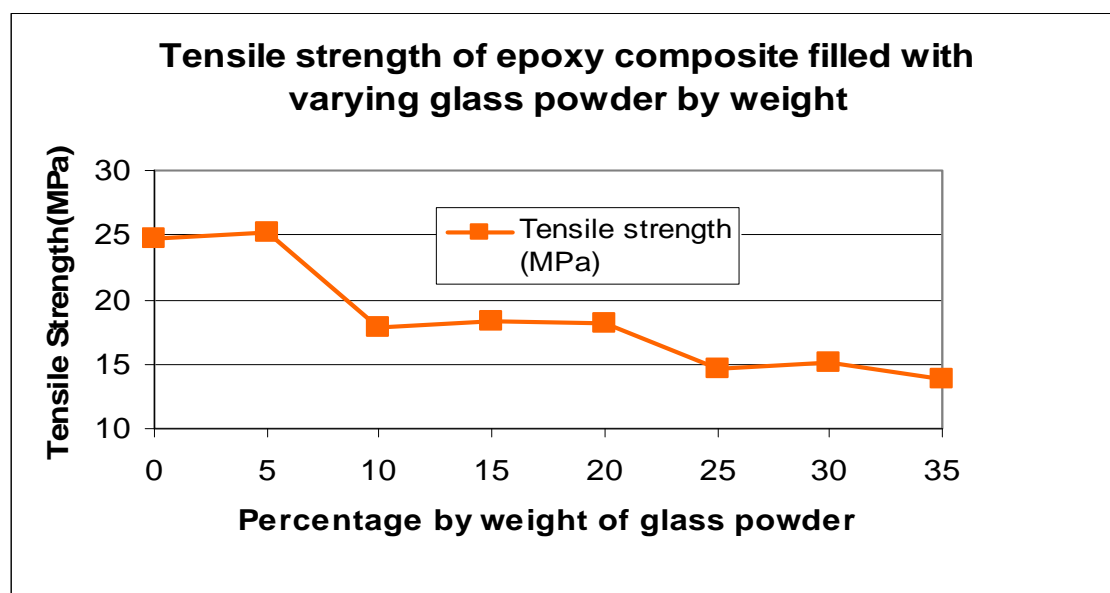


Figure 4. 9: Tensile strength of epoxy composite reinforced with varying glass powder by weight post-cured in an oven

4.4.3 Young's Modulus

Figure 4.10 shows the Young's modulus of varying by weight of glass hollow spheres reinforced phenol formaldehyde matrix composite. The Young's modulus of the neat resin

was 2.91 GPa and it dropped to 2.63 GPa when the percentage by weight of glass powder was 15%. It remained stable up until 25 % by weight of glass powder. It then bounced back to 3.02 GPa at 35 % by weight of filler. From neat resin to 20 % by weight of glass powder, the yield strength, tensile strength and Young's modulus behaviors of the composites were more or less the same. From 20+ % to 35 % by weight of the filler, values of yield and tensile strength decreased further with increasing particulate loading, while those of Young's modulus moved in the opposite direction.

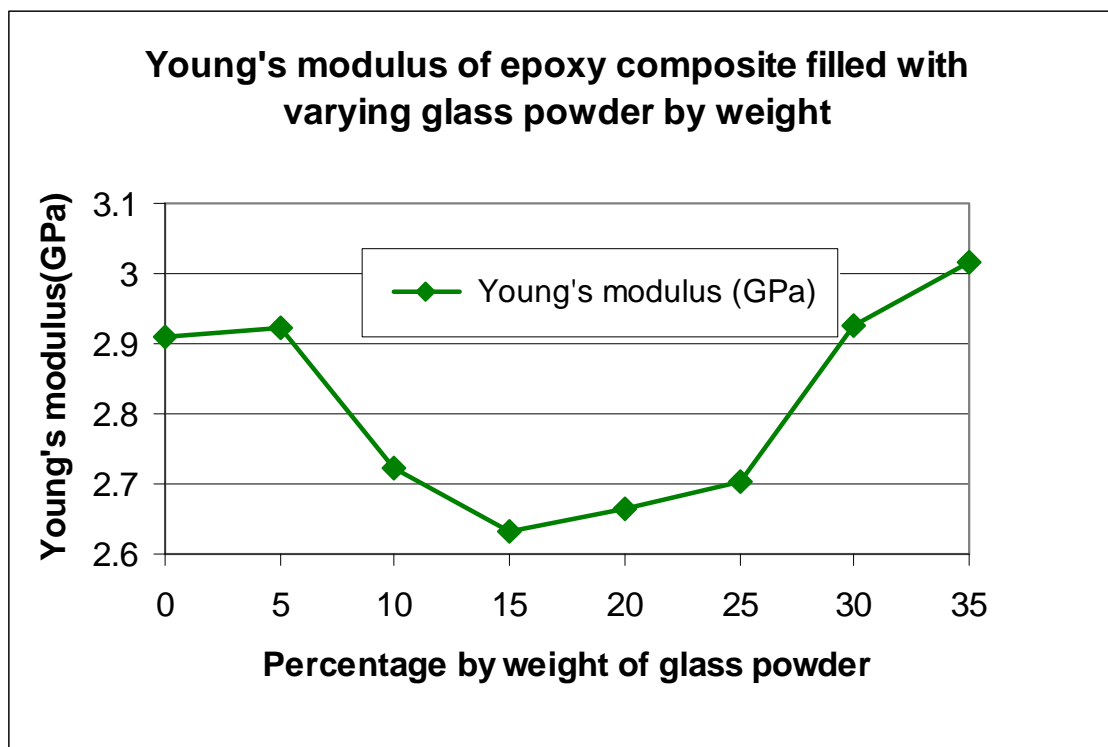


Figure 4. 10: Young's modulus of epoxy composite reinforced with varying glass powder by weight post-cured in an oven

It was found that a reduction in cost by one percent is followed by 1.5 % increase in tensile strength. For other percentages by weight of filler, the loss in tensile strength will not be compensated by the reduction in cost. It can be argued that 5 % by weight of filler is the best.

4.5 Scanning Electron Microscope (SEM) Results

Figure 4.11 shows the scanning electron microscope image of neat epoxy resin post-cured for a total of 40 hours at 40 °C, 50 °C and 60 °C respectively at a magnification of 200 times. Faint striations followed by a ‘turbulent flow’ can be found in the fractured surface of the neat resin. This shows that plastic deformation had taken place in the resin.

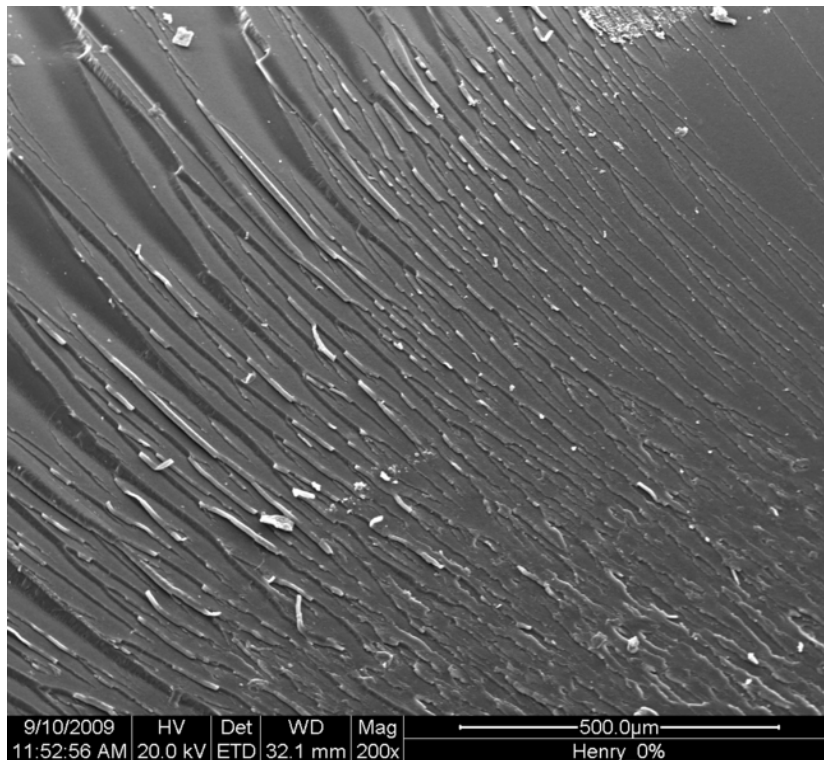


Figure 4. 11: SEM image of fractured neat epoxy resin, 200X

Figure 4.12 illustrates the scanning electron microscope image of epoxy reinforced by 25 % by weight of glass powder and post-cured for the same number of hours and temperatures at a magnification of 200 times. Holes were spotted and this explained why the tensile strength (24.80 MPa) of neat epoxy resin was stronger than that (14.72 MPa) of epoxy composite with 25 % by weight of glass powder. The holes were formed during the mixing process and the higher the percentage by weight of glass powder, the more holes would be expected.

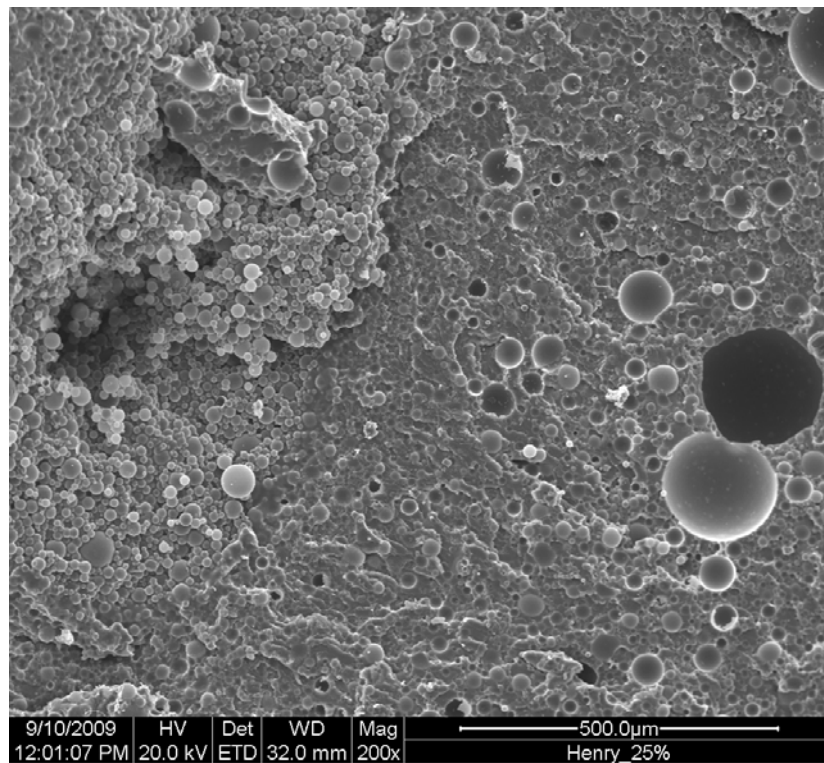


Figure 4. 12: SEM image of fractured 25 % glass powder filled epoxy composite, 200X

4.6 Modelling

Various models are available to predict the mechanical properties of particulate composites. Models are available to predict yield and tensile strength as well as the elastic modulus and elongation at breakage of composite materials. In general these properties are determined by developing a relationship between the different constituents of the composites, in this case the matrix, epoxy resin, and the filler, glass powder.

Studies have shown that when the aspect ratio, which is determined by dividing the length of the particle by its diameter, is at unity, the particles can be considered spherical. The Young's modulus of the composite is governed by a number of factors including the particulate loading and particle size. Fu et al. (2008) conducted this study and in doing so found that adhesion at the interface between the matrix and the filler has negligible effect on the modulus of particulate composites. It must be noted that small differences in particle size tend to have little to no effect on the mechanical properties of the composite and only when the particle size is reduced into the nano scale will there be a major difference.

In this study, the density of the glass powder used is 0.6 g/cc. The density of epoxy resin used is 2 g/cc. The elastic modulus of the epoxy resin is 2.71 GPa. For composites with 10 W/t % of glass powder, the mass of glass powder in 100 g of the composite is 10 g and that of the epoxy resin is 90g.

$$\text{The volume of the glass powder in 100g of the composite} = \frac{\text{mass}}{\text{density}} = \frac{10}{0.6} = 16.67 \text{ cc.}$$

$$\text{The volume of the epoxy resin in 100g of the composite} = \frac{\text{mass}}{\text{density}} = \frac{90}{2} = 45 \text{ cc.}$$

$$\text{The volume fraction of the glass powder} = \frac{16.67}{16.67 + 45} = 0.27.$$

$$\text{The volume fraction of the resin} = 1 - 0.27 = 0.73.$$

The volume fractions of other W/t % of glass powder and epoxy resin considered are shown in Table 4.2 below.

Table 4. 2: Volume fractions of other W/t % of glass powder and epoxy resin

W/t % of glass powder	V_f of glass powder	V_m of epoxy resin
0	0	0
5	0.15	0.85
10	0.27	0.73
15	0.37	0.63
20	0.45	0.55
25	0.53	0.47
30	0.59	0.41
35	0.64	0.36

4.6.1 Yield Strengths

According to Nicolais and Narkis' prediction,

$$\sigma_{yc} = \sigma_{ym} \left[1 - \left(\frac{V_f}{V_m} \right)^{2/3} \right] \quad (4.1)$$

where σ_{yc} is the yield strength of the composite

σ_{ym} is the yield strength of the matrix

v_f is the volume fraction of the filler

v_m is the volume fraction of the matrix

Values of yield strength of the composites obtained from Nicolais and Narkis' prediction and experiments are shown in Table 4.3.

Table 4. 3: Yield strengths from Nicolais and Narkis' prediction

W/t % of glass powder	Nicolais & Narkis' prediction	Post-cured in an oven	Post-cured in microwaves
0	17.95	17.95	20.34
5	15.84	18.24	20.68
10	13.52	14.64	19.31
15	10.92	15.47	19.64
20	7.76	14.73	17.98
25	4.46	13.62	13.88
30	0.73	13.73	13.08
35	0.00	14.41	14.07

Figure 4.13 shows the values of yield strength of the composites obtained from Nicolais and Narkis' prediction and experiments. It can be found that the values of yield strength of the samples post-cured in microwaves were higher than their counterparts post-cured in an oven. The values of yield strength obtained from Nicolais and Narkis' prediction were much lower than those from experiments, particularly at higher particulate loading.

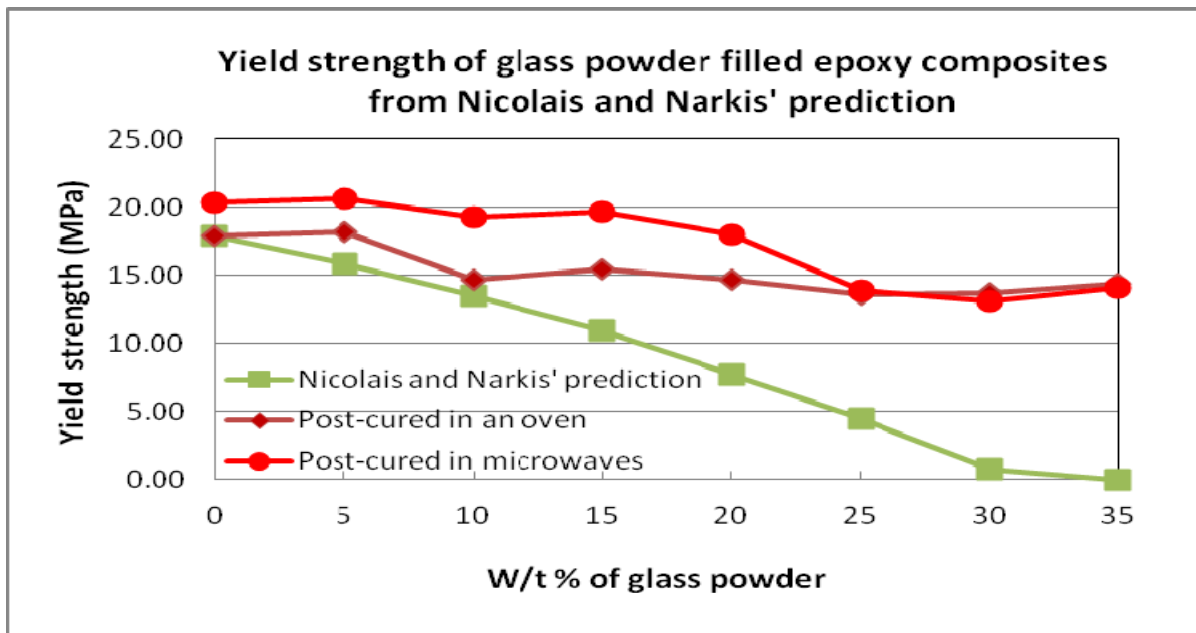


Figure 4. 13: Values of yield strength of the composites obtained from Nicolais and Narkis' prediction and experiments

Ku and Wong's model was therefore developed to suit these types of particulates, e.g. glass powder. In Ku and Wong's model, $\sigma_{yc} = \sigma_{ym} [1 - 0.15 (\frac{V_f}{V_m})]$ (4.2)

Figure 4.14 illustrates the yield strengths of glass powder filled epoxy composites post-cured in an oven and from Ku and Wong's model. The yield strength of neat resin, σ_{ym} used is that of neat resin post-cured in an oven. It can be found that the model predicted the values of yield strength of the composites very accurately and was within the 5 % markers.

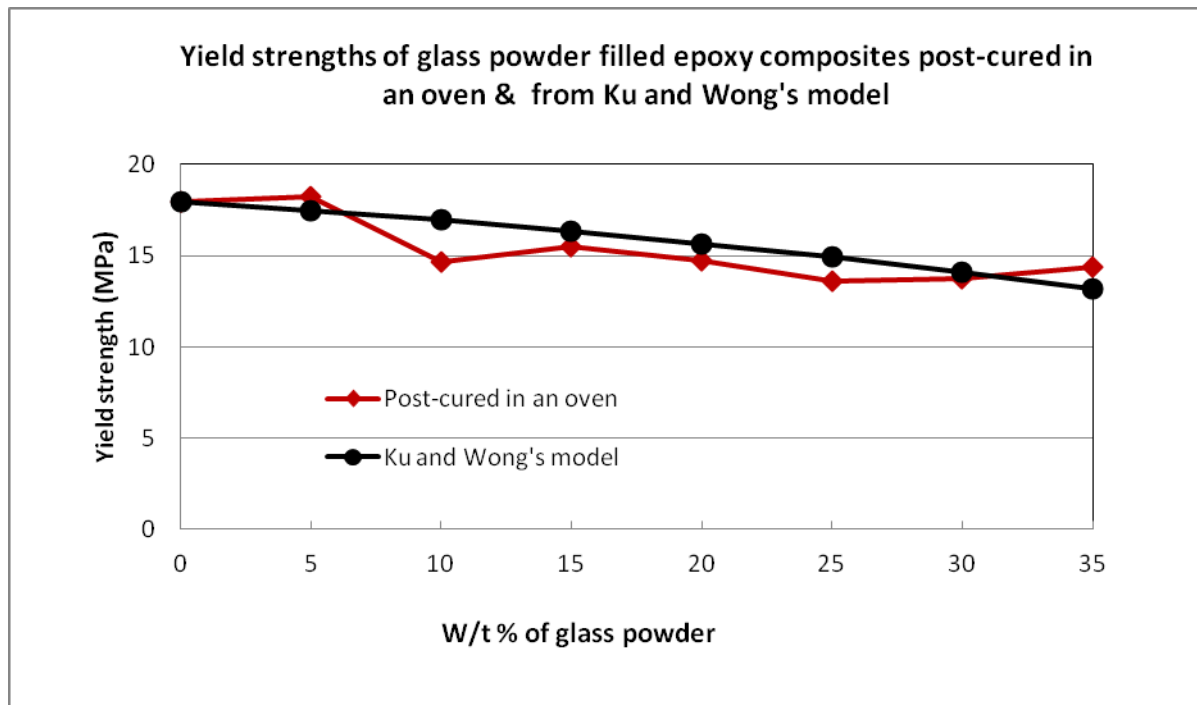


Figure 4. 14: The yield strengths of glass powder filled epoxy composites post-cured in an oven and from Ku and Wong's model

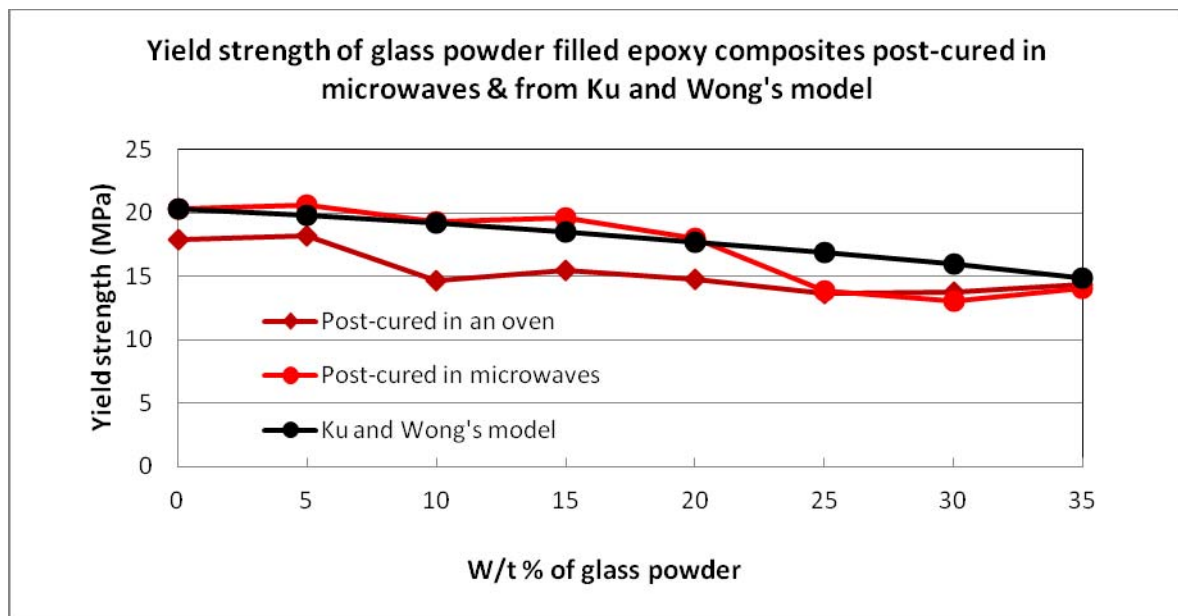


Figure 4. 15: yield strengths of glass powder filled epoxy composites post-cured in microwaves and from Ku and Wong's model

The yield strengths of glass powder filled epoxy composites post-cured in microwaves and from Ku and Wong's model are depicted in Figure 4.15. The yield strength of neat resin, σ_{ym} used is that of neat resin post-cured in microwaves. It can be found that the model predicted the values of yield strength of the composites very accurately and was within the 5 % markers.

4.6.2 Tensile Strengths

According to Tavman's model, $\sigma_c = \sigma_m (1-b.v_f^{2/3})$ (4.3)

where σ_c is the tensile strength of the composite

σ_m is the tensile strength of the matrix

$b = 1.1$ for densely packed hexagonal packing in the plane of highest density

$b = 1.21$ for poor adhesion and spherical particles

The values of tensile strength of the composites obtained from Tavman's prediction and experiments are depicted in Figure 4.16. The value of b used is 1.21. The tensile strength of the matrix, σ_m used is that of tensile strength of neat resin post-cured in an oven. It was found that the prediction for this model was not satisfactory as the values dropped significantly with particulate loading. Figure 4.17 shows the values of tensile strengths of glass powder filled epoxy composites post-cured in microwaves and from Tavman's model. The value of b used is 1.21. The tensile strength of the matrix, σ_m used is that of tensile strength of neat resin post-cured in microwaves. It was found that the prediction for this model was not satisfactory as the values dropped significantly with particulate loading; the case was similar to composited post-cured in an oven.

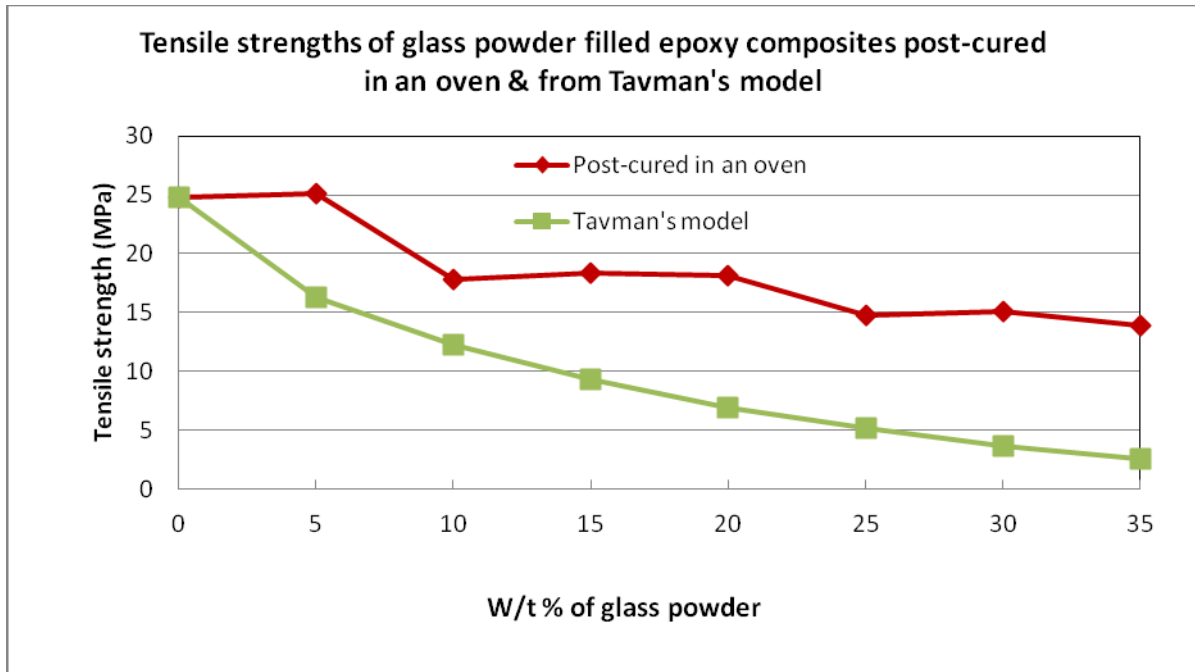


Figure 4. 16: Tensile strengths of glass powder filled epoxy composites post-cured in an oven and from Tavman's model

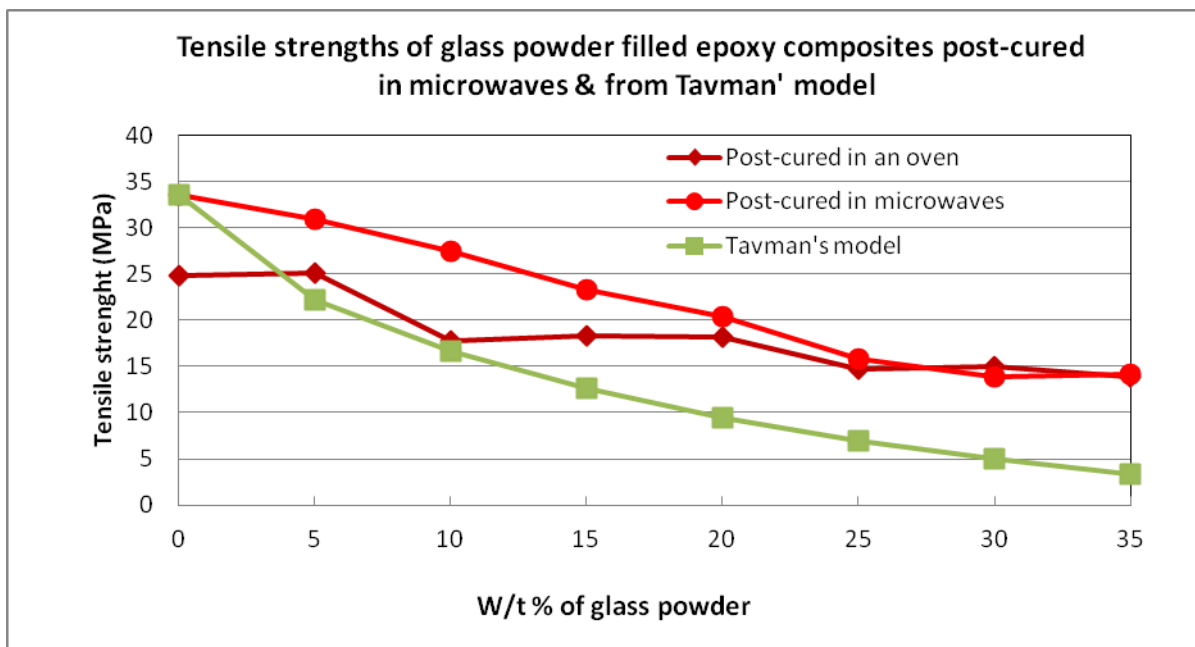


Figure 4. 17: Tensile strengths of glass powder filled epoxy composites post-cured in microwaves and from Tavman's model

Ku and Wong's model was therefore developed to suit these types of particulates, e.g. glass powder, in which adhesion between the filler and the matrix was not too bad, particularly at lower particulate loading. In Ku and Wong's model,

$$\sigma_c = \sigma_m (1 - b \cdot v_f^{2/3}) \quad (4.4)$$

but $b = 0.5$ for samples post-cured in an oven. For samples post-cured in microwaves, the value of $b = 0.5$ for lower concentration of filler (lower bound) and in this case it was 15 W/t %; after this the value of b has to be increased to 0.7 (upper bound). Figure 4.18 illustrates tensile strengths of glass powder filled epoxy composites post-cured in an oven and from Ku and Wong's model. It was found that the model predicted the results of the experiments quite well.

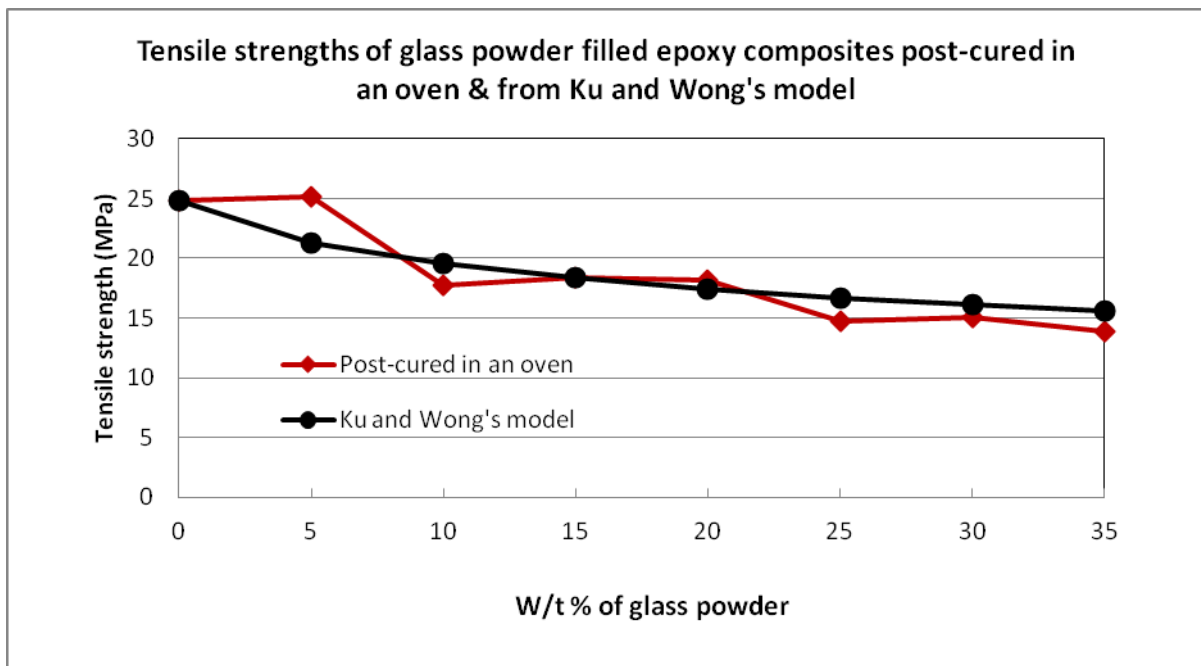


Figure 4. 18: Tensile strengths of glass powder filled epoxy composites post-cured in an oven and from Ku and Wong's model

The tensile strengths of glass powder filled epoxy composites post-cured in microwaves and from Ku and Wong's model were depicted in Figure 4.19. It was found that the model predicted the experimental data accurately.

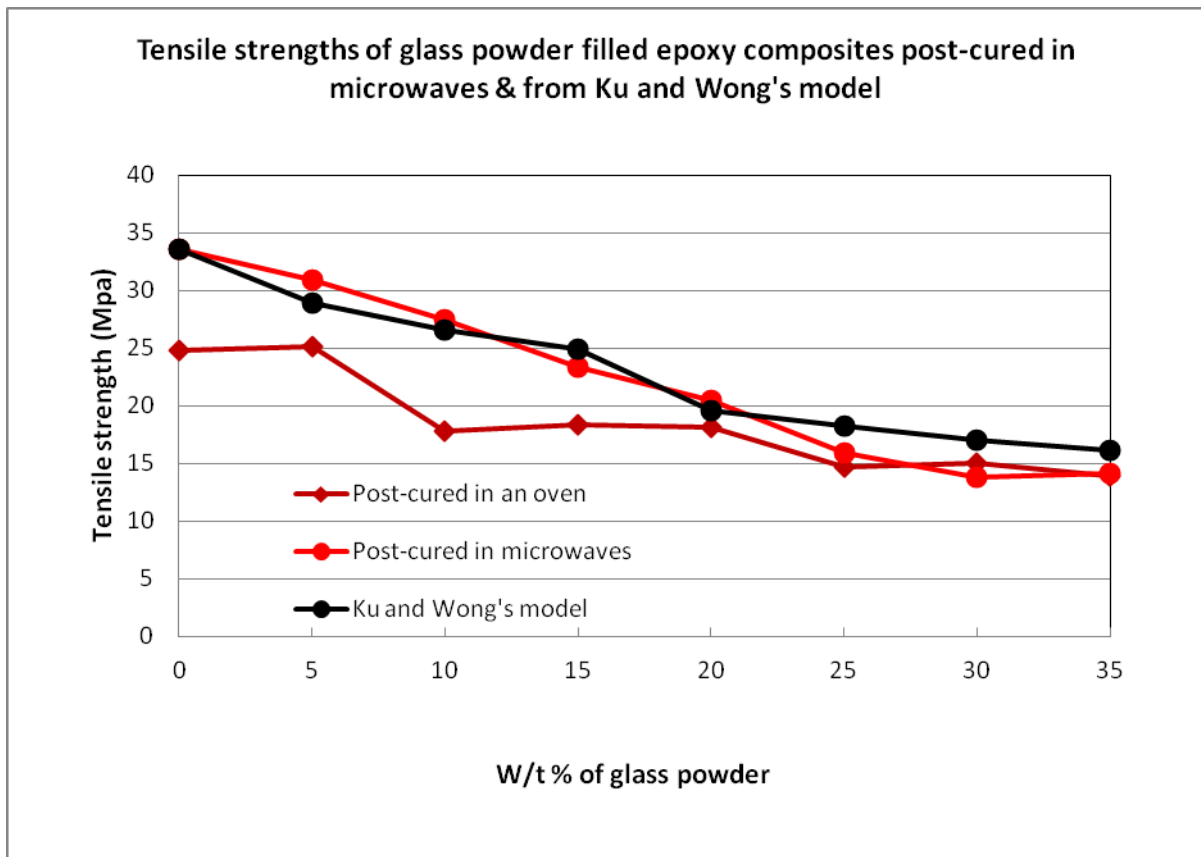


Figure 4. 19: Tensile strengths of glass powder filled epoxy composites post-cured in microwaves and from Ku and Wong's model

4.6.3 Young's Modulus

Using Neilsen's model, $E_c = E_m (1 + 2.5 V_f)$ (4.5)

the Young's modulus of the composites were calculated. Figure 4.20 shows the values of Young's moduli obtained from Neilsen's model and experiments, post-cured in an oven and in microwaves, respectively. It was found that the values of Young's modulus post-cured in microwaves were more reasonable and realistic when compared to those post-cured in an oven. The Young's modulus of resins reinforced with particulate fillers will usually increase slowly to a maximum at a particular filler loading depending on the attributes of the filler, but usually at low concentration of filler. Up to this particular weight content of filler, the adhesion between the particle and the matrix is ideal; after this, the amount of resin can no longer encapsulate the particles completely, leading to the generation of a large number of voids, thus lowering the Young's modulus of the composites. The values from Neilsen's

model rose steadily and conclusion may be drawn that Neilsen's model significantly overestimates the Young's modulus of the types of composites concerned in these study.

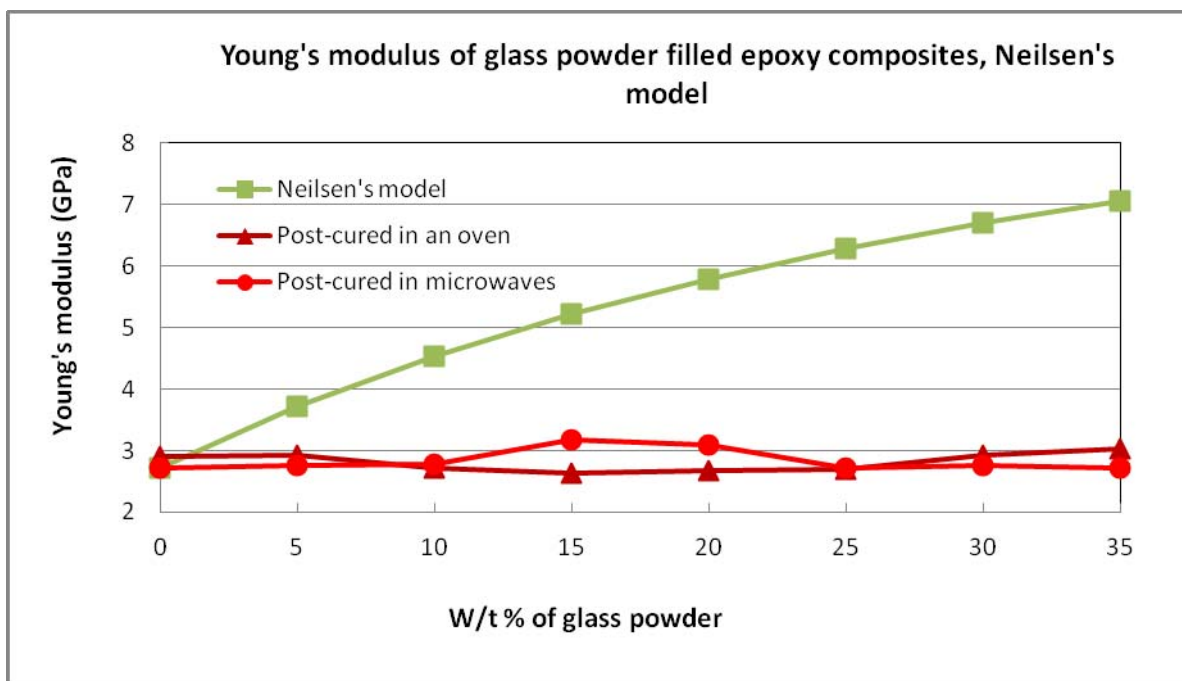


Figure 4. 20: Young's moduli of glass powder filled composites of Neilsen's model, post-cured in an oven and post-cured in microwaves

Using the equation developed from Einstein's theory,

$$E_c = E_m (1 + V_f) \quad (4.6)$$

the Young's modulus of the composites were calculated. Figure 4.21 shows the values of Young's moduli obtained from Neilsen's model, Einstein's theory and experiments, post-cured in microwaves. It can be found that the Einstein's theory graph predicted the Young's modulus of the composites quite accurately at lower particulate loading (up to 15 W/t % of glass powder) but it was incorrect at higher concentration of fillers. The adhesion between the particle and the matrix was no longer ideal; after this W/t % of filler, the amount of resin

can no longer encapsulate the particles completely, leading to the generation of a large number of voids, thus lowering the Young's modulus of the composites (Ray, 2006).

Ku and Wong's model was therefore proposed for these types of fillers. It consisted of two equations, one was for lower particulate loading (lower bound) and the other was for higher filler (upper bound) content.

$$E_c^l = E_m (1 + 0.5V_f) \quad (4.7)$$

$$E_c^u = E_{m(\text{highest})} (1 - V_f^4) \quad (4.8)$$

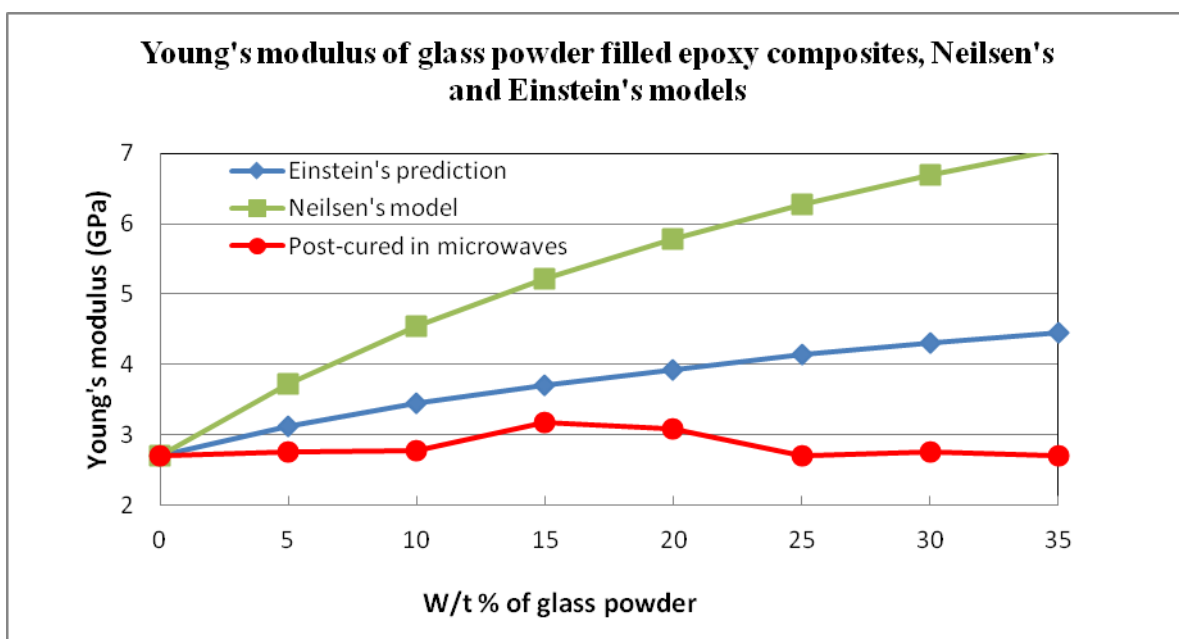


Figure 4. 21: Young's moduli of glass powder filled composites of Neilsen's model, Einstein's prediction and post-cured in microwaves

The first Ku and Wong's equation, $E_c^l = E_m (1 + 0.5V_f)$, was developed from Einstein's prediction and it was for lower particulate loading (lower bound), W/t % of filler up to 15. The second equation, $E_c^u = E_{m(\text{highest})} (1 - V_f^4)$, had the elastic modulus of the matrix changed so that it was the highest value obtained from the first equation.

Figure 4.22 illustrates that the values of Young's moduli obtained from Ku and Wong's model, Einstein's prediction and experiments, post-cured in microwaves. It was found that Ku and Wong's model predicted the results of the experiments quite closely to its lower and upper bounds, hence Ku and Wong's model was suitable for particulate, like glass powder, that would render the adhesion between the particle and the matrix no longer ideal at higher particulate loading, and the amount of resin can no longer encapsulate the particles completely.

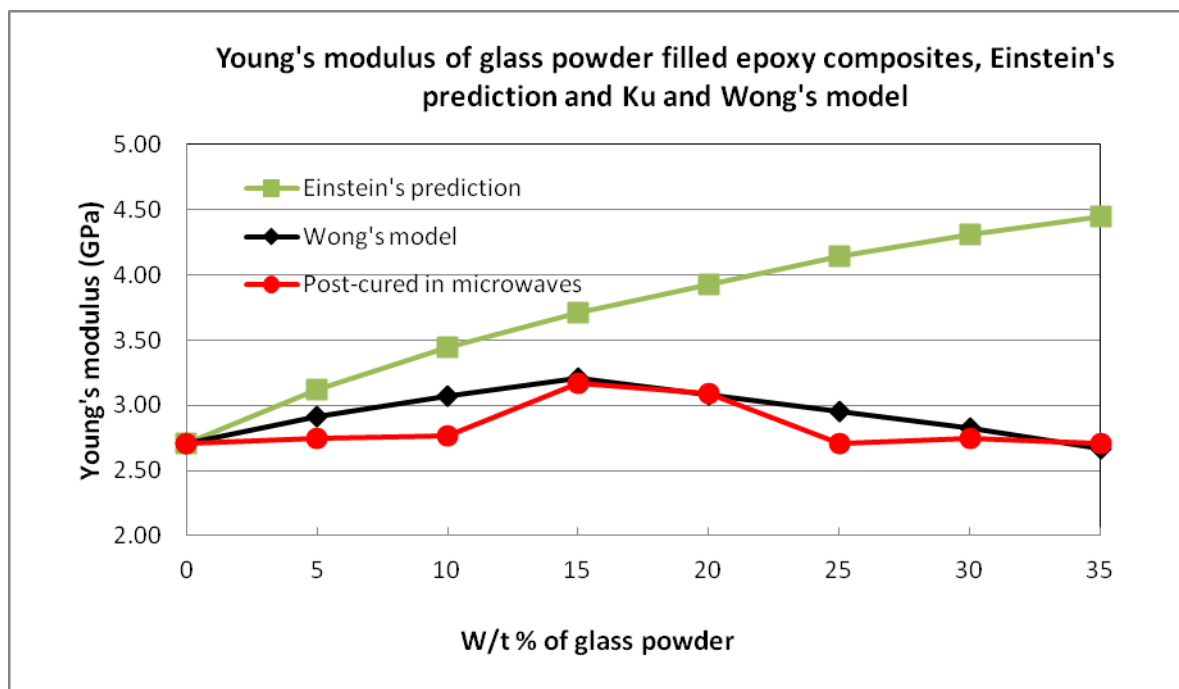


Figure 4. 22: Young's moduli of glass powder filled composites of Ku and Wong's model, Einstein's prediction and post-cured in microwaves

4.6.4 Other Models

Ishai and Cohen presented a model that depend on an upper and a lower bound. Hsieh et al. performed similar experiments on a particulate filled metal matrix. They used a method of determining upper and lower bounds that used equations established by Voigt and Reuss (Voigt's

model, $E_c = E_m V_m + E_f V_f$; Reuss' model, $E_c = \frac{E_m E_f}{E_m V_f + E_f V_m}$). The Voigt and Reuss bounds

were relatively wide apart, and modifications had accordingly been proposed by many researchers. Among these modifications, the Hashin and Shtrikman model (H-S model) had

received wide attention. Hashin and Shtrikman treated the system containing one particulate phase and one continuous matrix phase. They employed the “minimum energy” principle and introduced bounds on the bulk modulus, K and shear modulus, G as

$$K_c^l = K_m + \frac{V_p}{(1/K_p - K_m) + (3V_m/3K_m + 4G_m)} \quad (4.9)$$

$$K_c^u = K_p + \frac{V_m}{(1/K_m - K_p) + (3V_p/3K_p + 4G_m)} \quad (4.10)$$

$$G_c^l = G_m + \frac{V_p}{(1/G_p - G_m) + (6(K_m + 2G_m)V_m/5G_m(3K_m + 4G_m))} \quad (4.11)$$

$$G_c^u = G_p + \frac{V_m}{(1/G_m - G_p) + (6(K_p + 2G_p)V_p/5G_p(3K_p + 4G_p))} \quad (4.12)$$

where V_p is V_f , volume fraction of the particle or filler. The subscripts m and p denote, matrix and particle, respectively.

The lower and upper bounds on the elastic modulus can be estimated by using the following equations as

$$E_c^l = \frac{9K_c^l G_c^l}{3K_c^l + G_c^l} \quad (4.13)$$

$$E_c^u = \frac{9K_c^u G_c^u}{3K_c^u + G_c^u} \quad (4.14)$$

The upper and lower bounds proposed by the H–S model were relatively closer to each other. Therefore, the H–S model provided a more precise expression for the elastic and shear moduli of a two-phase material.

A prediction on the elongation of a composite specimen could be made using a model developed by Nielsen. Tavman mentioned that this model assumed that perfect adhesion was present between the particles and the matrix. Due to the random sizes and surface finishes present this assumption was not entirely accurate, however for the purpose of this study might be used to form a comparison. The equation was $\varepsilon_c = \varepsilon_p (1 - V_f^{1/3})$ (4.15)

4.6.5 New Models

According to G. Bourkas, B. Paul, O. Ishai and R. Ogorckiewicz, the models shown in Figures 4.23(a) and (b), named model 1 and 2 respectively, were three-part composites. From Figure 4.23 the filler volume fraction was given by

$$V_f = \frac{a^3}{c^3} \quad (4.16)$$

For uniaxial load in the figures direction, their elastic moduli are given, respectively, by [10–13]

$$E_c^{(1)} = E_m \left(\frac{1 + (m-1)v_f^{2/3}}{1 + (m-1)(v_f^{2/3} - v_f)} \right) \quad (4.17)$$

$$E_c^{(2)} = E_m \left(1 + \frac{v_f}{m/(m-1) - v_f^{1/3}} \right) \quad (4.18)$$

where $m = \frac{E_f}{E_m}$ and E_f , E_m , and E_c are the elastic moduli of the filler, matrix and composite, respectively. The indices (1) and (2) of E_c refer to model 1 and 2, respectively.

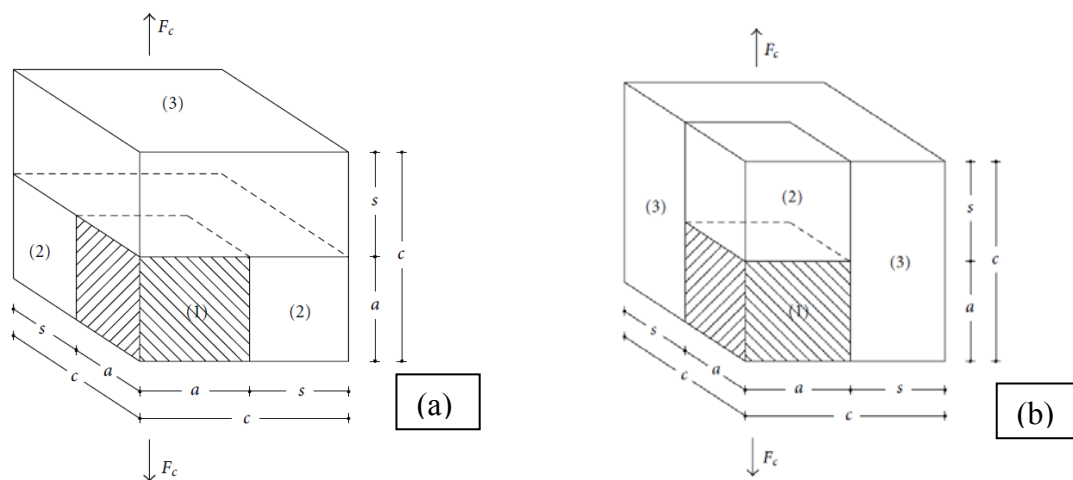


Figure 4. 23: The three-part models: (a) Paul model, model 1, (b) Ishai-Cohen model, model 2

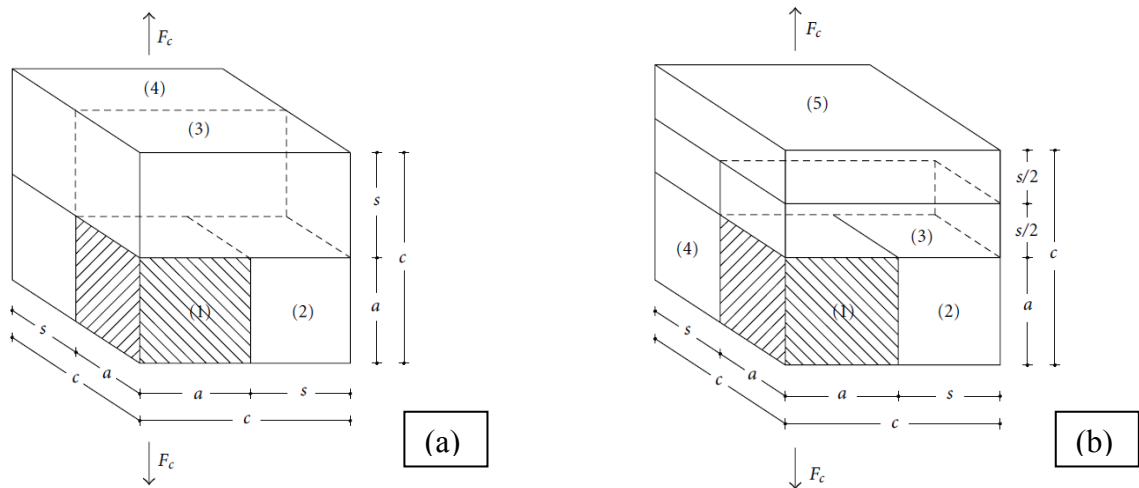


Figure 4. 24: proposed models: (a) Four-part model, model 3, (b) Five-part model, model 4

The model presented in Figure 4.24(a) according to [10–13] named model 3, for uniaxial loading in the figure direction, had four components. The components (1) and (2) were in parallel, and both were in series with component (3). The above components were in parallel with component (4). For uniaxial loading in Figure 4.24(a) direction, from forces equilibrium and elongations equality, one could write the following equations [10]:

$$E_c^{(3)} = E_m \left(1 + \frac{v_f}{1/(m-1) + v_f^{1/3} - v_f^{2/3}} \right) \quad (4.19)$$

where $m = \frac{E_f}{E_m}$

$$E_c^{(4)} = E_m \cdot \left(1 + \frac{2v_f^{2/3}}{(mv_f^{1/3} + 1)/(m-1) - v_f^{2/3}} \right) \quad (4.20)$$

$$E_c^{(4)} = E_m \left(1 + \frac{v_f^{1/3} + v_f^{2/3}}{2/(n-1) + v_f^{1/3} - v_f^{2/3}} \right) \quad (4.21)$$

where the indices 1, 2, 3, 4, and c correspond to the parts (1), (2), (3), and (4) and the composite, respectively,

and $m = \frac{E_f}{E_m}$, $n = \frac{E_a}{E_m}$

5 CONCLUSIONS

5.1 Introduction

This chapter will discuss the mechanical, thermal and electrical properties of epoxy composite for varying percentages of glass powder obtained through permittivity, DMA and tensile tests. It will summarize the important findings throughout the project.

5.2 Discussion Of Results

It can be concluded from the obtained results that microwave post-curing method is more effective when the glass powder percentage in the epoxy composite is low. Samples having higher percentage of glass powder irrespective of post curing method exhibit similar results. Composite with 5 % weight of glass powder post-cured in microwaves has shown comparatively good electrical, mechanical and thermal properties. Although, the tensile strength and yield strength of the composite are low compare to pure epoxy resin, it can reduce the overall cost of material without much affecting desirable properties of the material.

5.2.1 Permittivity Test

Samples have higher value of loss tangent at lower frequency; but lower values at higher frequency. Samples with 5 % weight of glass powder composites have the low values of loss tangent, while higher values of loss tangent have been noted for higher percentage of glass powder mixture. Samples with 5 % weight glass powder have lowest values of loss tangent at all frequency, while 15 % weight of glass powder microwave cured composite has higher values of loss tangent. Therefore, it can be concluded that value of lost tangent increases with addition of glass powder.

Sample post cured in microwave is more effective to convert incoming microwave energy in to heat compare to conventional oven. Loss tangent is inversely proportional to skin depth. It means that samples cured in conventional oven can penetrate to more depth compare to samples cured in microwave. Depth of penetration increases with increase in the glass powder percentage and frequency. Samples with 5 % weight and 15 % weight of glass powder have shown similar behaviour. However, values of loss tangent increases with increase in the percentage of glass powder.

Unlike samples with lower percentage of glass powder, samples with 15 % weight of glass powder have higher values of loss tangent cured in conventional oven compare to samples cured in microwave. Therefore, it can be concluded that conventional oven curing is more preferable over microwave curing for the samples with higher percentage of glass powder.

5.2.2 DMA Tests

At the starting of test, storage modulus has maximum value. As the temperature rises, material turns from elastic solid to viscous fluid state. Accordingly, storage modulus which represents elastic property of material drops down and loss modulus rises and reaches to maximum.

Glass transition temperature, T_g varies with varying percentage of glass powder. Therefore it can be concluded that the strength of the epoxy cross linking is affected with increase in the amount of glass powder. Difference between the values of T_g for samples post cured in microwaves with difference % weight glass powder is 9.09 °C shows that cross linking in epoxy composites varies with varying percentage of glass powder.

Microwave cured samples have consistent trend in loss modulus, E'' value with varying percentage of glass powder. The value of storage modulus increases with % weight of glass powder.

Microwave cured samples have consistent trend in Loss modulus, E'' value with varying percentage of glass powder. The value of storage modulus decreases with % weight of glass powder.

5.2.3 Tensile Tests

In general, the higher the percentage by weight of glass powder, the lower was the yield strength. The variation of tensile strength with respect to percentage by weight of glass powder is the same as that of yield strength. If cost and tensile strength were considered at the same time, composite with 5 % by weight of filler is the best. It can be found that the trend for the graphs of yield and tensile strengths are the same and it can be argued that the results were correct in trend. Tensile strengths were found to increase with a decrease in the particle

size but with increase particle contents. This trend is supported by the tensile strength results of epoxy/alumina trihydrate particulate composites. In this study, the tensile strengths were found to decrease with increase particulate loading and it can be argued that this happened because the glass powder particles had not been treated by hydrolysis of silicon tetrachloride. From neat resin to 20 % by weight of glass powder, the yield strength, tensile strength and Young's modulus behaviours of the composites were more or less the same. From 20+ % to 35 % by weight of the filler, values of yield and tensile strength decreased further with increasing particulate loading, while those of Young's modulus moved in the opposite direction. It was found that a reduction in cost by one percent is followed by 1.5 % increase in tensile strength. For other percentages by weight of filler, the loss in tensile strength will not be compensated by the reduction in cost. It can be argued that 5 % by weight of filler is the best. Addition of the glass powder reduces the yield strength and tensile strength of the epoxy resin composites. However, the Young's modulus was improved with the increase in the percentage of glass powder. It can be concluded that microwave post curing is more effective for epoxy composites with low percentage by weight of glass powder. As the standard deviation in the values of tensile strength, yield strength and Young's modulus was low for all specimens, it can be argued that results are reliable.

5.2.4 Microscopic Inspection

Faint striations followed by a 'turbulent flow' can be found in the fractured surface of the neat resin. This shows that plastic deformation had taken place in the resin. Holes were spotted and this explained why the tensile strength (24.80 MPa) of neat epoxy resin was stronger than that (14.72 MPa) of epoxy composite with 25 % by weight of glass powder. The holes were formed during the mixing process and the higher the percentage by weight of glass powder, the more holes would be expected.

5.2.5 Modelling

By using curve fits, Ku and Wong's model has been developed and proposed in this research project.

In Ku and Wong's model, Yield strength:

$$\sigma_{yc} = \sigma_{ym} \left[1 - 0.15 \left(\frac{V_f}{V_m} \right) \right] \quad (5.1)$$

where σ_{yc} is the yield strength of the composite

σ_{ym} is the yield strength of the matrix

It can be found that the model predicted the values of yield strength of the composites accurately and was within the 5 % markers.

In Ku and Wong's model, Tensile strength:

$$\sigma_c = \sigma_m (1 - b \cdot V_f^{2/3}) \quad (5.2)$$

where σ_c is the tensile strength of the composite

σ_m is the tensile strength of the matrix

Figure 4.18 illustrates tensile strengths of glass powder filled epoxy composites post-cured in an oven and from Ku and Wong's model. It was found that the model predicted the results of the experiments quite well. The tensile strengths of glass powder filled epoxy composites post-cured in microwaves and from Ku and Wong's model were depicted in Figure 4.19. It was found that the model predicted the experimental data accurately.

In Ku and Wong's model, Young's modulus:

$$E_c^l = E_m (1 + 0.5V_f) \quad (5.3)$$

$$E_c^u = E_{m(\text{highest})} (1 - V_f^4) \quad (5.4)$$

where E_c is the Young's modulus of the composite

E_m is the Young's modulus of the matrix

It consisted of two equations, one was for lower particulate loading (lower bound) W/t % of filler up to 15 and the other had the elastic modulus of the matrix changed was for higher filler (upper bound) content. It was found that Ku and Wong's model predicted the results of the experiments quite closely, hence Ku and Wong's model was suitable for particulate, like glass powder, that would render the adhesion between the particle and the matrix no longer ideal at higher particulate loading, and the amount of resin can no longer encapsulate the particles completely.

5.3 Recommendation And Future Research Scope

In order to have more accurate electrical properties of the material in microwave, the suitable method should be resonant cavity method. Therefore, it is necessary to measure the loss tangent and dielectric constant with resonant cavity method to provide more reliable results for further research work and practical applications. Ways and means should be further investigated and developed to reduce holes during the mixing process. The surface treatment of glass powder can improve the mechanical properties of epoxy composites (Wang et al. 2004). This project can be further investigated by doing surface treatment of glass powder before mixing it to epoxy resin. The Ku and Wong's model developed using curve fit and proposed in this research project could further be argued and generalized to become more accurate and hence more applicable and practical if more experiments can be done on other resin-based particulate composites.

LIST OF REFERENCES

References

Al-Hajjaj, A Tahseen and Saki, A, Improving the design stresses of high density polyethylene pipes and vessels used in reverse osmosis desalination plants, Journal of Saudi Chemical Society, 2010, Vol. 14, pp. 251–256.

Agilent Technologies, undated, Basics of measuring the dielectric properties of materials, Viewed 15 September 2011, <<http://www3.imperial.ac.uk/pls/portallive/docs/1/11949698.PDF>>.

Amdouni, N, Sautereau, H and Gerard, J, Epoxy composite based on glass beads: II mechanical properties, Journal of Applied Polymer science, 1992, Vol. 46, pp. 1723-1735.

ASTM (American society for testing and materials), undated, Test Method for Measuring Relative Complex Permittivity and Relative Magnetic Permeability of Solid Materials at Microwave Frequencies, Standard D556 – 08, viewed 25 October 2011, (Online USQ databases).

Åström, B, Manufacturing of Polymer Composites, Chapman and Hall, 1997, pp. 80-84.

ATL composites Pty Ltd, Kinetix Thixotropic Laminating Resin, undated, Australia, pp. 1-3.

ATL composites Pty Ltd, Kinetix Thixotropic Laminating Resin, undated, Australia, pp. 1-3.

Australian Standard 1145.2 (2001), Determination of tensile properties of plastic materials – Test conditions for moulding and extrusion plastics.

Ball, J and Hancock, N, Fields and Waves, USQ studybook, 2007, pp.3.1 – 3.3.

Bhatnagar, M 1996, ‘Epoxy resin’, The Polymeric Materials Encyclopaedia, CRC Press, Richmond.

Bows, JR 1999, ‘Variable Frequency Microwave Heating of Food’, Journal of Microwave Power and Electromagnetic Energy, vol. 34, no. 4, pp.227-38, (Online ProQuest).

Bourkas, G, Prassianakis, I, Kytopoulos, V, Sideridis, E and Younis, C, Estimation of Elastic Moduli of Particulate Composites by New Models and Comparison with Moduli Measured by Tension, Dynamic, and Ultrasonic Tests, Advances in Materials Science and Engineering, 2010, Volume 2010, Article ID 891824, pp. 1-13.

Budinski, K, Engineering Materials, Properties and Selection, 4th edition, Prentice Hall International Editions, pp. 142-145.

Callister, W, *Materials Science and Engineering: An Introduction*, Wiley, 2003, pp. 505, 550.

Epaarachchi, J, Ku, H, and Gohel, K, A simplified empirical model for prediction of mechanical properties of random short fibre / vinylester composites, *Journal of Composite Materials*, 44(6), (2010), 779-788

Epaarachchi, J, and Reushle, M, Performance of Aluminium / Vinylester Particulate Composite, *Materials Science Forum Vols. 654-656 (2010) pp 2656-2659 (2010) Trans Tech Publications, Switzerland*, doi:10.4028/www.scientific.net/MSF.654-656.2656

Ferry, J 1980, *Viscoelastic Properties of Polymers*, 3rd ed, John Wiley and Sons, New York.

Fu, S Feng, X Lauke, B & Mai, Y Effects of particle size, particle/matrix interface adhesion and particle loading on mechanical properties of particulate-polymer composites", *Composites: Part B*, 2008, Issue 39, pp. 933-961.

Harper, C 1992, *Handbook of plastics, elastomers, and composites*, 2nd edn, McGraw-Hill, Inc , New York, United States.

Kraus, J, *Electromagnetics*, 4th edition, McGraw-Hill, 1992, pp.95-98, 186-189.

Hsieh, C, Tuan, W and Wu, T, Elastic behaviour of a model two-phase material, *Journal of the European Ceramic Society*, 2004, Vol. 24, pp. 3789–3793.

Ishai, O and Cohen, L, Elastic properties of filled and porous epoxy composites, *International Journal of Mechanical Sciences*, 1967, Vol. 9, No. 8, pp. 539–546.

Ishai, O and Cohen, L, Effect of Fillers and Voids on Compressive Yield of Epoxy Composites, *Journal of Composite Materials* July 1968, Vol. 2, pp. 302-315.

Ku, H, Cardona, F, Ball, J, Jacobsen, W and Trada, M, *Journal of Composite Materials*, Vol. 42, No. 19, pp. 2083-2095.

Ku, H, Ball, J, Siores, E & Chan, P 1999, Complex permittivity of low loss thermoplastic composites using a resonant cavity method. ICCM-12: 12th International Conference on Composite Materials, Paris, France.

Ku, H, Siores, E, Ball, J and Horsfield, B 1998, An Important Step in Microwave Processing of Materials: Permittivity Measurements of thermoplastic Composites at Elevated Temperatures, *Proceedings of 1998 Pacific Conference on Manufacturing*, Brisbane, Australia, August 18 - 21, (1998) pp. 68-73.

Ku, H Wong, P Maxwell, A Huang, J Fung, H & Mohan, T 2010, A pilot study on the Relationship between Mechanical and Electrical Loss Tangents of Glass Powder Reinforced Epoxy Composites Post-cured in Microwaves, *Journal of Applied Polymer Science*, Volume 119, no. 5, pp. 2495–3116.

Ku, H, Wong, P, Huang, J, Fung, H and Trada, M, Tensile Tests of Glass Powder Reinforced Epoxy Composites: Pilot Study, *Advanced Materials Research*, 2011, Vol. 214, pp. 1-5.

Ku, H, Wong, P, Maxwell, A, Huang, J, Fung, H and Trada, M, A pilot study on the Relationship between Mechanical and Electrical Loss Tangents of Glass Powder Reinforced Epoxy Composites Post-cured in Microwaves, *Advanced Materials Research*, 2011, Vol. 214, pp 26-30.

Ku, H, Cardona, F, Ball, J, Jacobsen, W and Trada, M, *Journal of Composite Materials*, Vol. 42, No. 19, pp. 2083-2095.

Lee, S and Delomonte, J 1990, 'Historical Perspectives of Composites', *International Encyclopaedia of Composites*, VCH Publishers, New York.

Lubin, G 1982, *Handbook of Composites*, Van Nostrand Reinhold Company, New York.

Marrett, C, Moulart, A, Colton, J and Tcharkhtchi, A Flexible polymer composite electromagnetic crystals, *Polymer Engineering Science*, 2003, Vol. 43, No. 4, pp. 822–830.

Menard, K 1999, *Dynamic Mechanical Analysis: A Practical Introduction*, 2nd ed, CRC Press, Boca Raton.

Meredith, R 1998, *Engineers' handbook of industrial microwave heating*, The Institution of Electrical Engineers, London, United Kingdom.

Metaxas, A and Meredith, R, *Industrial Microwave Heating*, Peter Peregrinus Ltd., 1983, 5-6, 28-31, 43, 211, 217, 278, 284-5.

Nakamura, Y, Yamaguchi, M, Okubo, M, and Matsumoto, T, *Journal of Applied Polymer Science*, Vol. 45, Issue 7, pp. 1281-1289.

National Research Council (U.S.) 1994, *Microwave processing of materials*, National Academy Press, Washington DC, U.S.

Nicolais, L and Narkis, M, Stress–strain behaviour of styrene–acrylonitrile bead composites in the glassy region, *Polymer Engineering Science*, 1971, Vol.11, No. 3, pp. 194–203.

Ogorckiewicz, R and Weidman, G, Tensile stiffness of a thermoplastic reinforced with glass fibres or spheres, *Journal of Mechanical Engineering Science*, 1974, Vol. 16-1, pp. 10–17.

Paul, B, Prediction of Elastic Constants of Multiphase Materials, *Transactions of The Metallurgical Society of AIME*, 1960, Vol. 218, pp. 36–41.

Peters, S 1998, Epoxy resins, *Handbook of Composites*, Chapman & Hall, London.

Potters Industries, undated, <http://www.pottersbeads.com/markets/polySpherice1.asp> <viewed on 14 August 2009>

Potters Industries, undated, <http://www.pottersbeads.com/markets/polycomposites.asp> viewed on 14 August 2009>

Qi, S, Li, C, and Huang, Y, AIAA 57th International Astronautical Congress, IAC 2006, v 8, pp. 5237-5240

Ray, D, Bhattacharya, D, Mohanty, A, Drzal, L and Misra, M, Static and Dynamic Mechanical Properties of Vinylester Resin Matrix Composites Filled with Fly Ash, *Journal of Applied Polymer Science*. 2006, Vol. 291, pp. 784-792.

Sadiku, M, 2001, *Elements of electromagnetics*, 3rd ed, Oxford University Press, New York.

Schwartz, M, *Joining of Composite-matrix materials*, ASM International, 1995, p. 64.
Mallick, P, Editor and Chapter Writer, *Composite Engineering Handbook*, Marcel Dekker, Inc., 1997, pp. 1, 4, 9, 11-2.

Schwartz, M, *Composite Materials, Volume 1: Properties, Nondestructive Testing and Repair*, Prentice Hall, 1997, pp.1-3, 10.

Schwikart, J 1998, *Dynamic mechanical analysis: A practical introduction*, *Journal of chemical engineering*, vol. 106, no. 8, pp. 10-16 (online ProQuest).

Silva, V 2006, *Mechanics and strength of materials*, 3rd ed., Springer, Berlin.

Strong, A, *Fundamentals of Composite Manufacturing: Materials, Methods and Applications*, Society of Manufacturing Engineers, 1989, pp.70-5, 143.

Strong, B 2000, *Plastics, Materials and Processing*, 2nd ed., Prentice Hall, New Jersey.

Tavman, H, *Thermal and Mechanical Properties of Aluminium Powder-Filled High-Density Polymer Composites*, *Journal of Applied Polymer Science*, 1996, Vol 62, pp. 2161-2167.

Tereshchenko, O Buesink, J Leferink, K, 2011, *An overview of the techniques for measuring the dielectric properties of materials*, University of Twente Enschede, viewed on 22 October 2011, <<http://ursigass2011.org/abstracts/ursi/A04-1.pdf>>.

Wang, H Wenjue, H Tian, H Wang, Y 2005, 'The preparation and properties of glass powder reinforced epoxy resin', *Journal of Materials Letters*, vol. 59, no. 1, pp. 94– 99, (online Science direct).

Appendix A

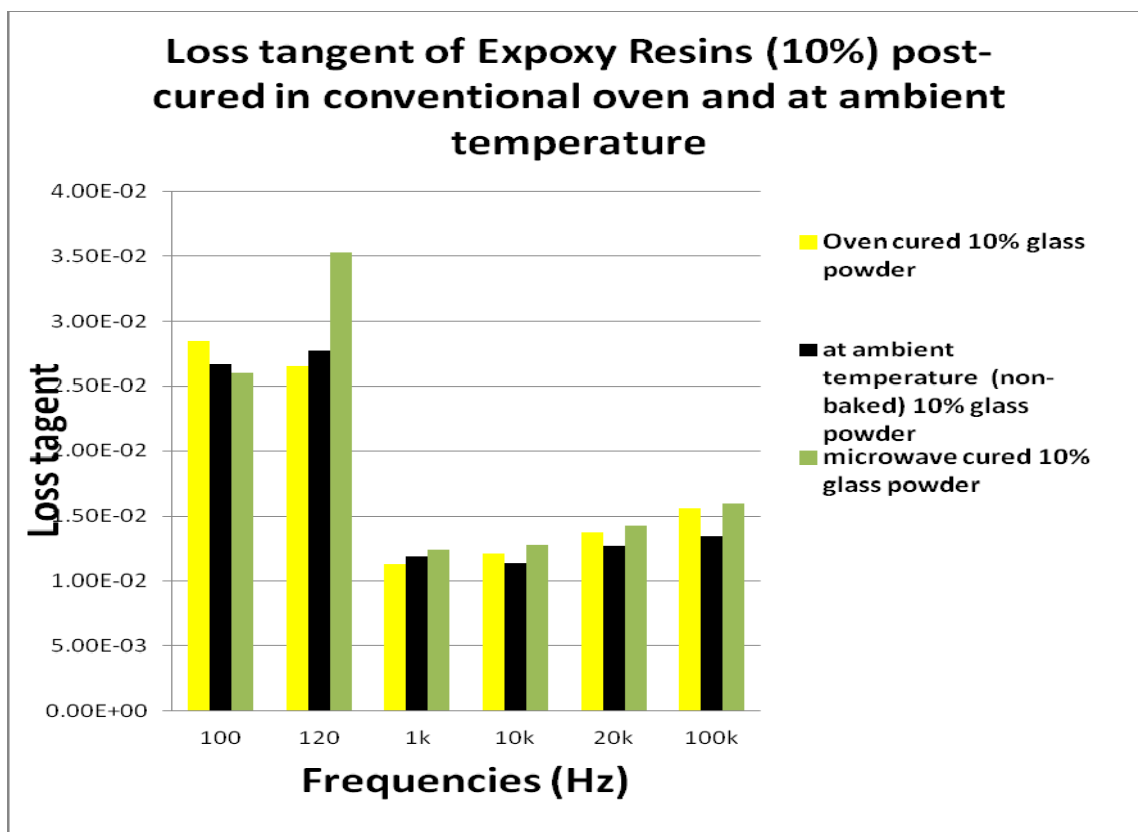
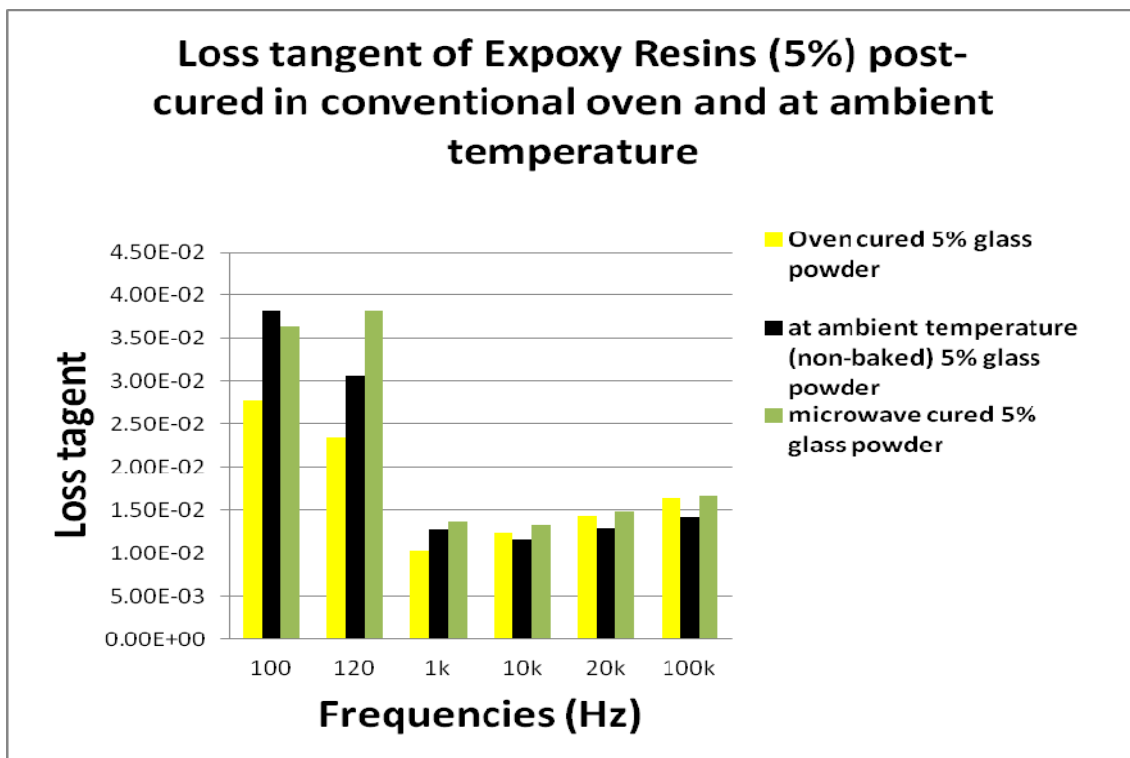
A.1. Permittivity Test Results

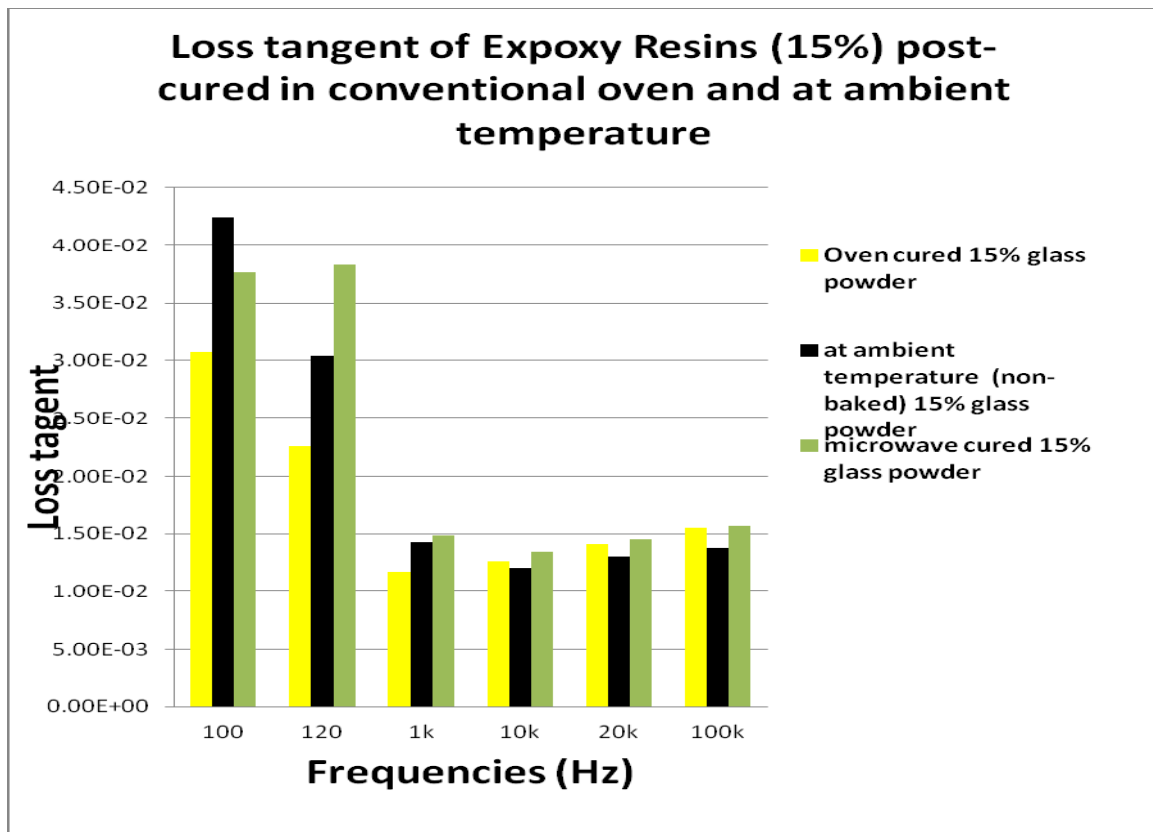
Loss tangent measurement

Table A.1.1: Loss tangent of epoxy composite samples with varying weight percent of glass powder post cured in microwave			
f(Hz)	5% weight of glass powder	10% weight of glass powder	15% weight of glass powder
100	3.64E-02	2.60E-02	3.77E-02
120	3.82E-02	3.53E-02	3.83E-02
1000	1.37E-02	1.24E-02	1.48E-02
10000	1.34E-02	1.28E-02	1.34E-02
20000	1.48E-02	1.42E-02	1.45E-02
100000	1.67E-02	1.59E-02	1.57E-02

Table A.1.2: Loss tangent of epoxy composite samples with varying weight percent of glass powder post cured in conventional oven			
f(Hz)	5% weight of glass powder	10% weight of glass powder	15% weight of glass powder
100	2.77E-02	2.85E-02	3.07E-02
120	2.35E-02	2.66E-02	2.26E-02
1000	1.03E-02	1.13E-02	1.17E-02
10000	1.24E-02	1.21E-02	1.26E-02
20000	1.43E-02	1.38E-02	1.41E-02
100000	1.65E-02	1.56E-02	1.55E-02

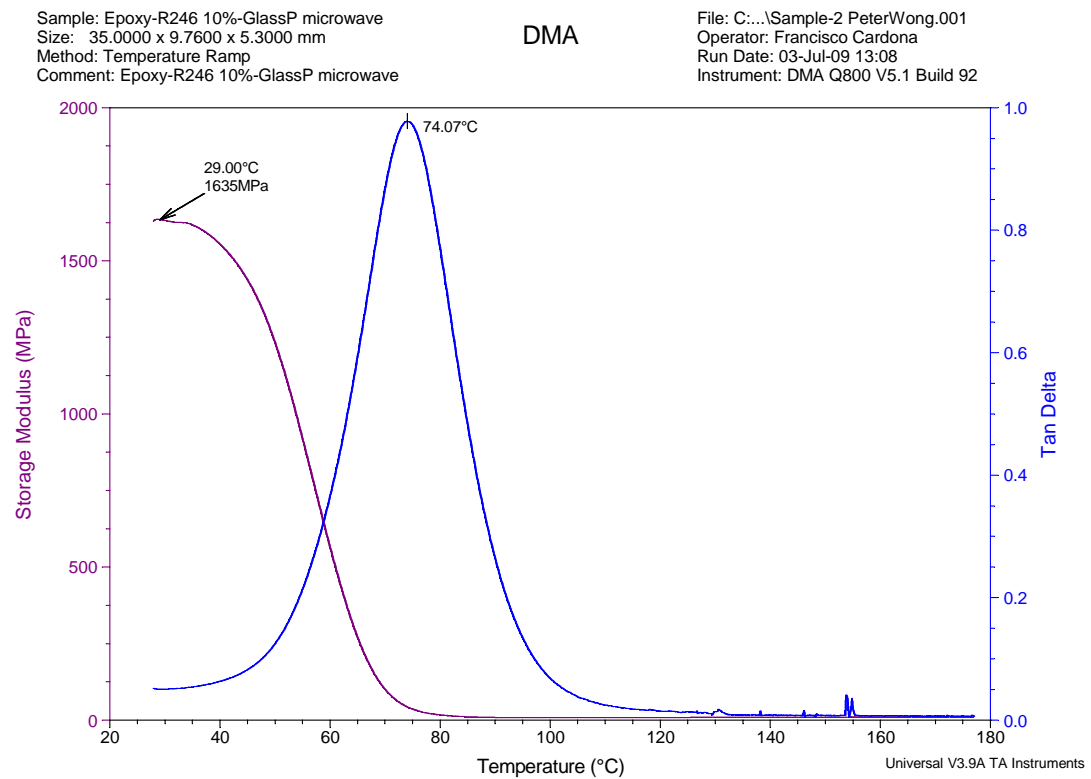
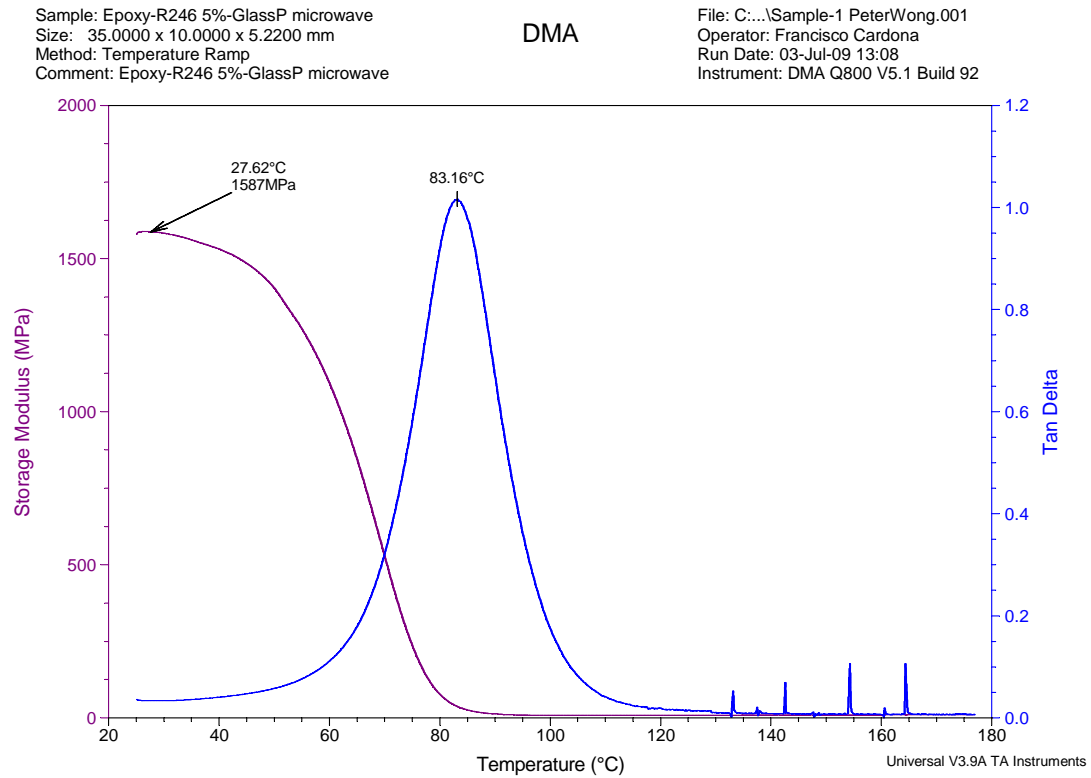
Figure A.1.1: Loss tangents vs Frequency graph for epoxy composite samples with varying weight percent of glass powder in different curing conditions





A.2. DMA Test Graphs

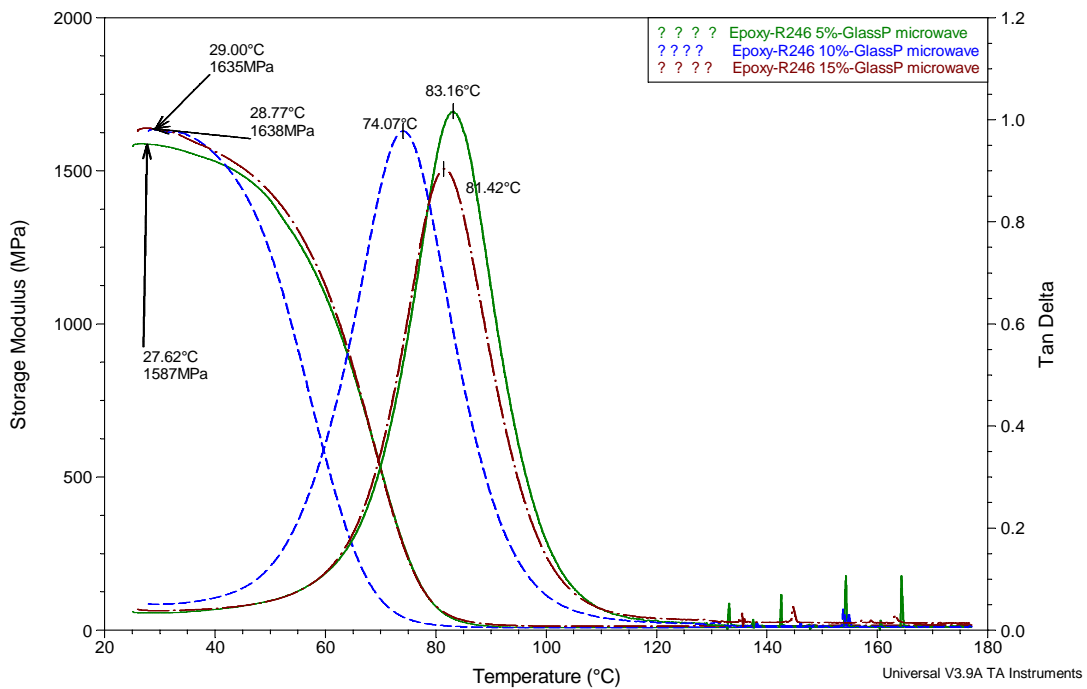
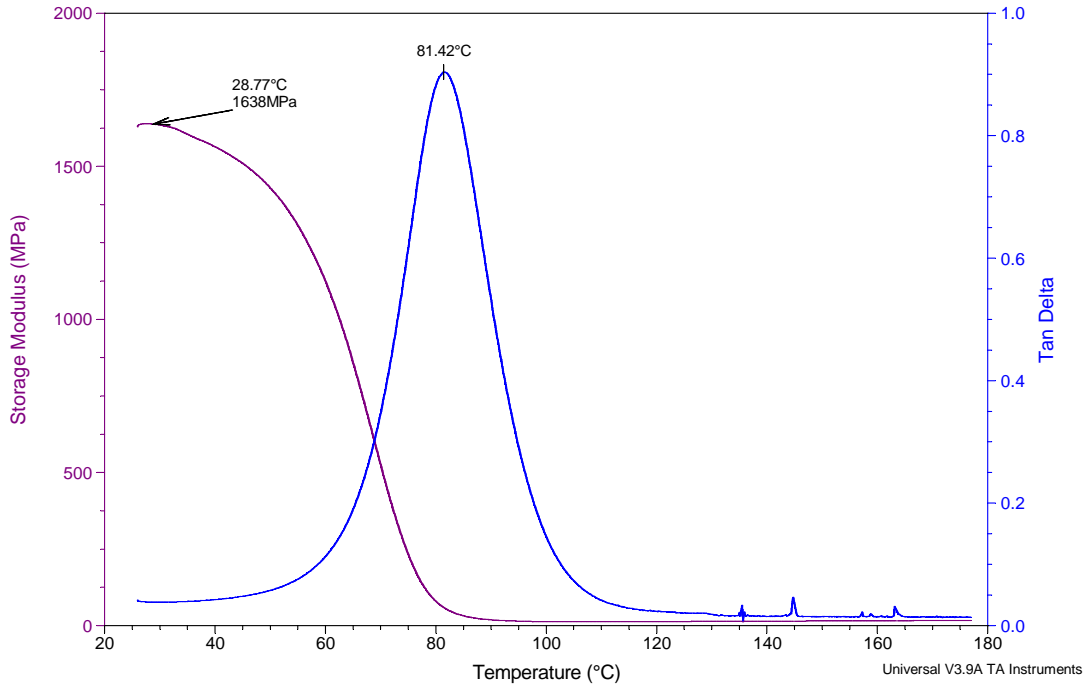
Graphs for samples cured in microwave



Sample: Epoxy-R246 15%-GlassP microwave
 Size: 35.0000 x 9.8600 x 5.0200 mm
 Method: Temperature Ramp
 Comment: Epoxy-R246 15%-GlassP microwave

DMA

File: C:\...\Sample-3 PeterWong.001
 Operator: Francisco Cardona
 Run Date: 03-Jul-09 13:08
 Instrument: DMA Q800 V5.1 Build 92



A.3. Tensile Test (Microwave cured sample)

Microwave cured sample results

0% weight of glass powder post cured in microwave

Test Date : 18/08/2009

Method : MMT Tensile Test with return.msm

Specimen Results:

Specimen #	Thickness mm	Width mm	Area mm ²	Peak Load N	Peak Stress MPa	Break Load N	Break Stress MPa
1	14.900	5.500	82	2786	34.00	2786	34.00
2	14.890	5.570	83	2273	27.41	2273	27.41
3	14.820	5.540	82	3315	40.38	3315	40.38
4	15.110	5.430	82	3074	37.46	3074	37.46
5	14.780	5.630	83	2273	27.31	2273	27.31
6	15.050	5.450	82	2878	35.08	2878	35.08
Mean	14.925	5.520	82	2767	33.61	2767	33.61
Std Dev	0.129	0.075	1	423	5.31	423	5.31

Specimen #	Elongation At Break mm	Stress At Offset Yield MPa	Load At Offset Yield N				
1	1.944	18.680	1530.808				
2	1.370	15.098	1252.174				
3	2.650	20.231	1661.061				
4	1.852	19.558	1604.663				
5	1.162	17.106	1423.383				
6	1.596	18.909	1550.951				
Mean	1.762	18.264	1503.840				
Std Dev	0.524	1.871	146.724				

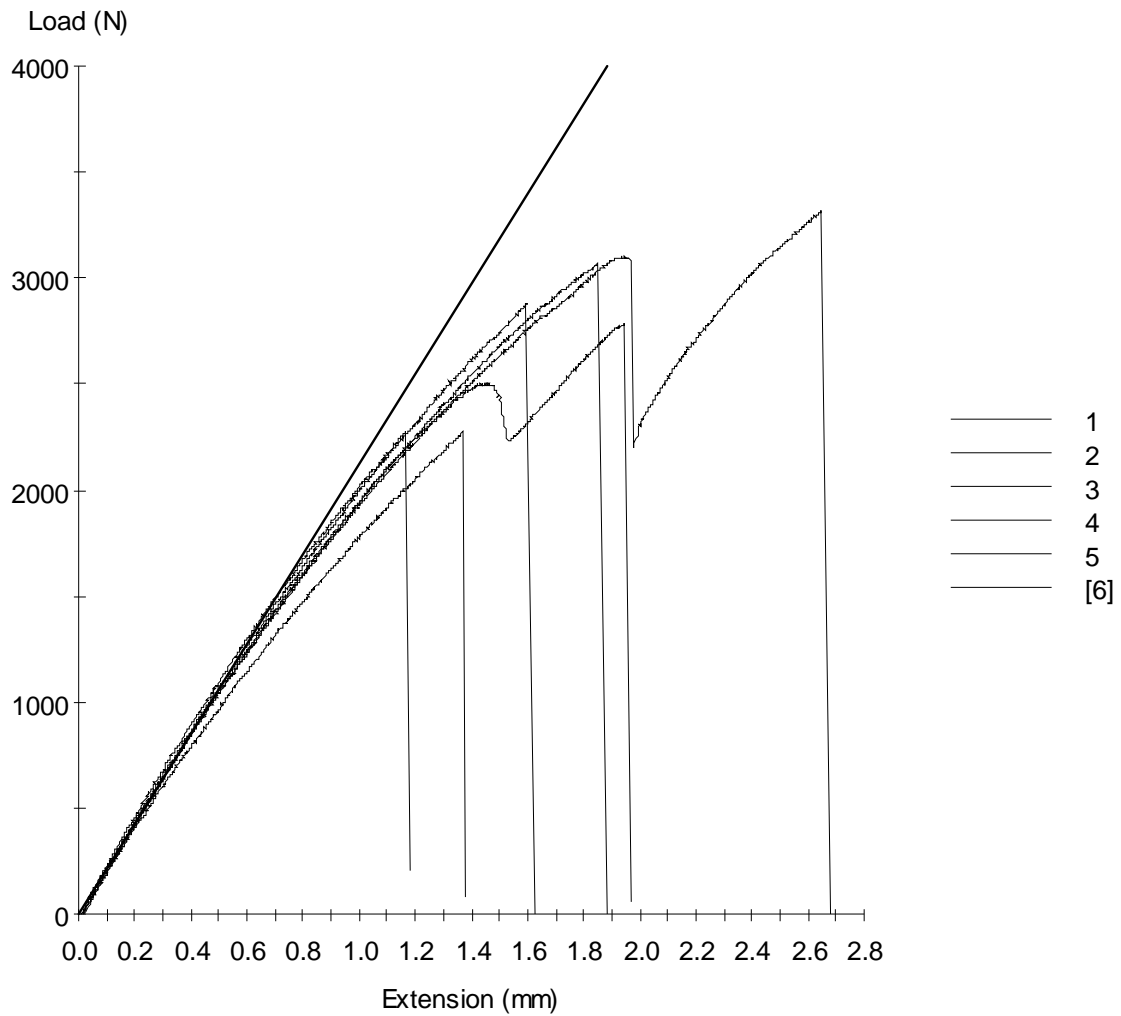


Fig A.3.1: Load vs Extension of 0% weight of glass powder post cured in microwave

Microwave cured sample results**5% weight of glass powder post cured in microwave**

Test Date : 18/08/2009

Method : MMT Tensile Test with return.msm

Specimen Results:

Specimen #	Thickness mm	Width mm	Area mm ²	Peak Load N	Peak Stress MPa	Break Load N	Break Stress MPa
1	15.190	5.600	85	2449	28.79	2449	28.79
2	15.030	5.600	84	1893	22.50	1893	22.50
3	15.160	5.340	81	2788	34.44	2788	34.44
4	15.050	5.340	80	2691	33.48	2690	33.48
5	15.200	5.440	83	2815	34.04	2815	34.04
6	15.100	5.400	82	2623	32.16	2623	32.16
Mean	15.122	5.453	82	2543	30.90	2543	30.90
Std Dev	0.073	0.120	2	344	4.60	344	4.60

Specimen #	Elongation At Break mm	Stress At Offset Yield MPa	Load At Offset Yield N				
1	1.292	16.260	1383.099				
2	0.969	14.287	1202.490				
3	1.646	18.810	1522.751				
4	1.584	17.861	1435.469				
5	1.651	18.805	1554.979				
6	1.389	18.518	1509.995				
Mean	1.422	17.424	1434.79 7				
Std Dev	0.265	1.812	129.980				

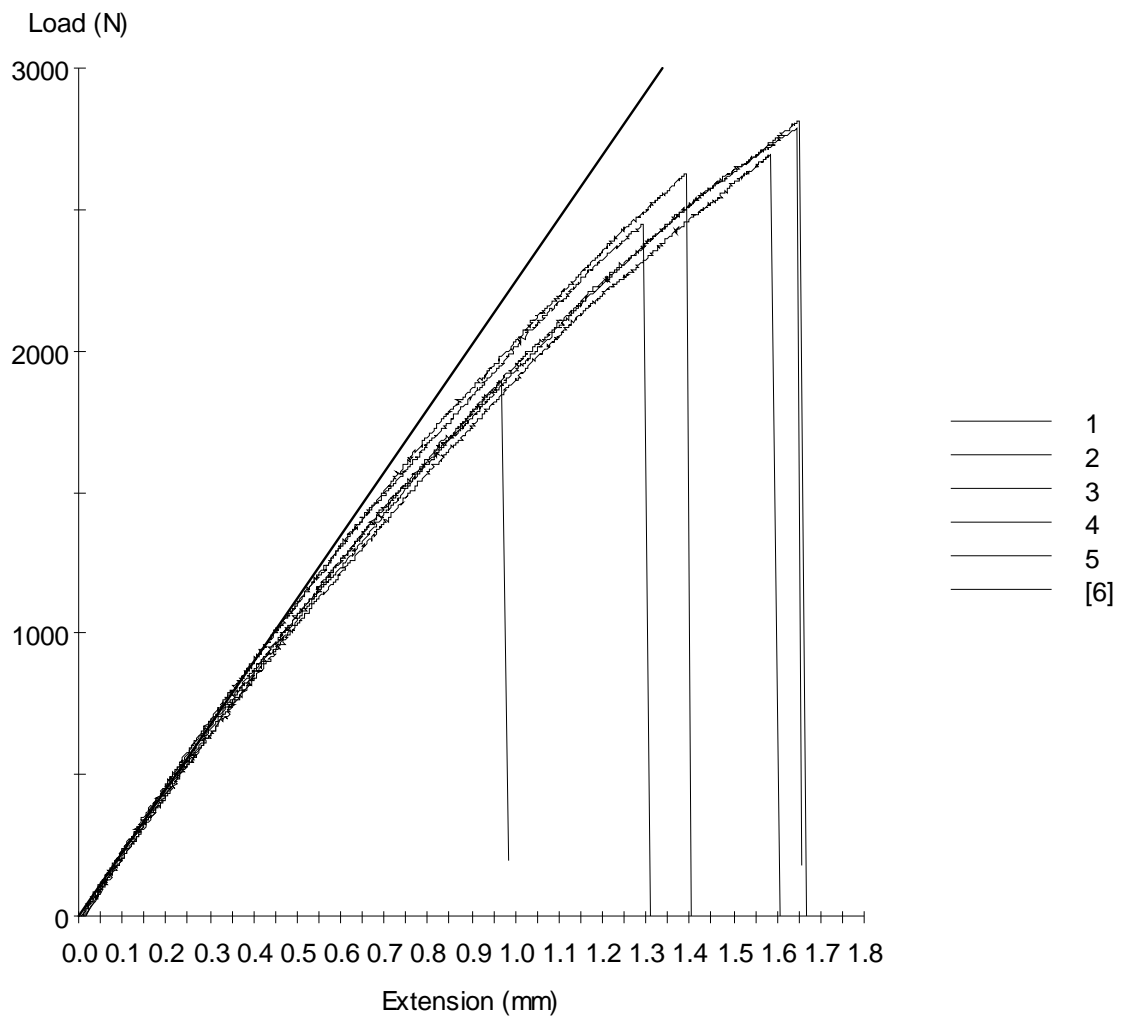


Fig A.3.2: Load vs Extension of 5% weight of glass powder post cured in microwave

Microwave cured sample results**10% weight of glass powder post cured in microwave**

Test Date : 18/08/2009

Method : MMT Tensile Test with return.msm

Specimen Results:

Specimen #	Thickness mm	Width mm	Area mm ²	Peak Load N	Peak Stress MPa	Break Load N	Break Stress MPa
1	15.460	5.490	85	2241	26.41	2239	26.38
2	15.110	5.670	86	2766	32.28	2766	32.28
3	14.910	5.560	83	2179	26.28	2179	26.28
4	14.870	5.520	82	2078	25.32	2078	25.32
5	15.400	5.510	85	2410	28.41	2410	28.41
6	15.200	5.520	84	2163	25.77	2163	25.77
Mean	15.158	5.545	84	2306	27.41	2306	27.41
Std Dev	0.244	0.065	1	251	2.61	251	2.61

Specimen #	Elongation At Break mm	Stress At Offset Yield MPa	Load At Offset Yield N				
1	1.164	14.682	1246.132				
2	1.511	16.779	1437.483				
3	1.098	15.712	1302.530				
4	1.026	16.320	1339.625				
5	1.282	15.311	1299.173				
6	1.108	14.892	1249.489				
Mean	1.198	15.616	1312.40				
Std Dev	0.176	0.818	70.723				

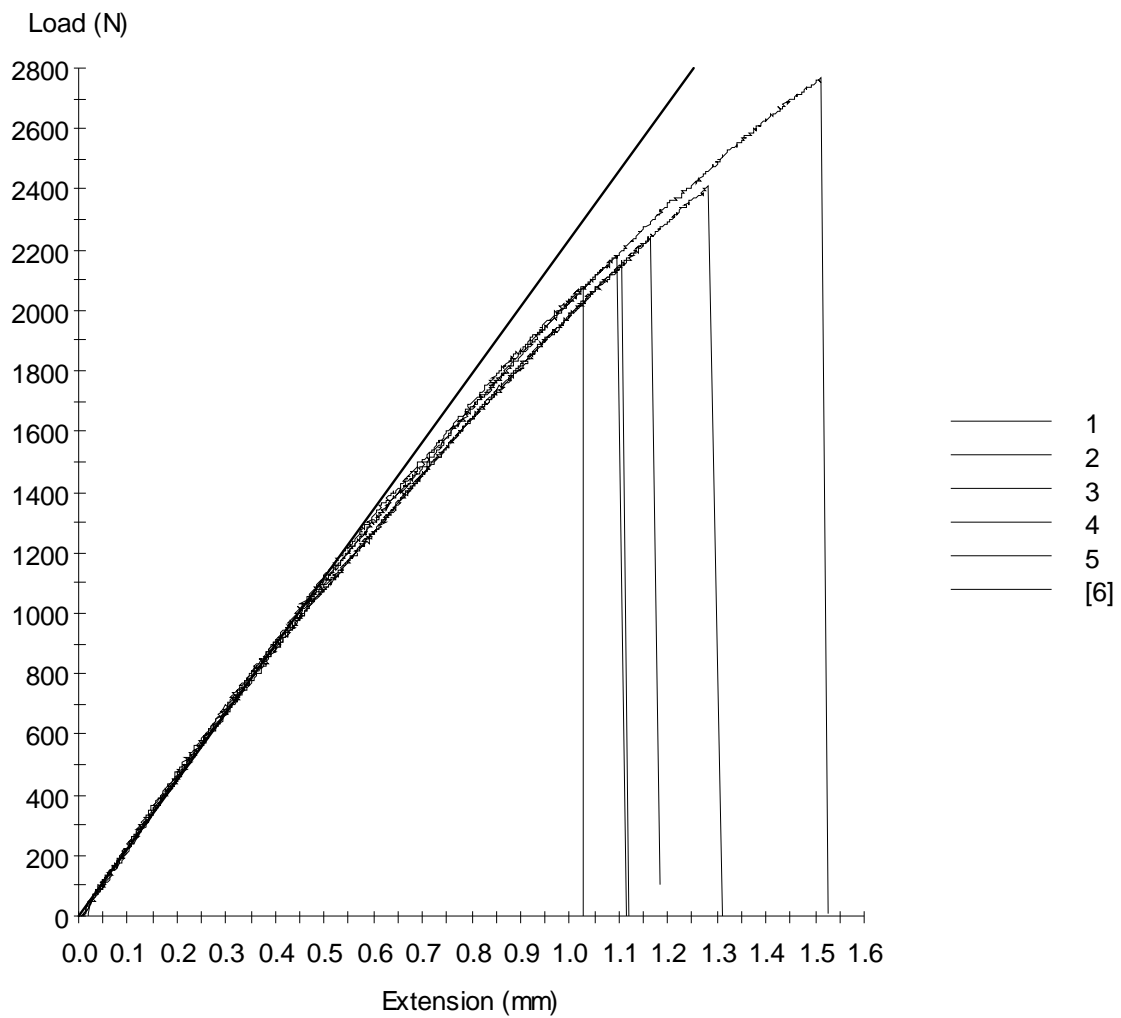


Fig A.3.3: Load vs Extension of 10% weight of glass powder post cured in microwave

Microwave cured sample results**15% weight of glass powder post cured in microwave**

Test Date : 18/08/2009

Method : MMT Tensile Test with return.msm

Specimen Results:

Specimen #	Thickness mm	Width mm	Area mm ²	Peak Load N	Peak Stress MPa	Break Load N	Break Stress MPa
1	14.640	5.990	88	2117	24.14	2003	22.84
2	14.960	6.110	91	2228	24.38	2228	24.38
3	14.660	5.820	85	1779	20.85	1779	20.85
4	14.880	5.890	88	2366	27.00	2365	26.98
5	14.830	5.670	84	2271	27.01	2271	27.01
6	14.890	5.690	85	1393	16.44	1393	16.44
Mean	14.810	5.862	87	2026	23.30	2007	23.09
Std Dev	0.131	0.171	3	371	4.06	368	4.04

Specimen #	Elongation At Break mm	Stress At Offset Yield MPa	Load At Offset Yield N				
1	1.135	17.108	1500.259				
2	0.916	15.866	1450.240				
3	0.768	14.023	1196.448				
4	1.012	18.156	1591.235				
5	0.989	17.191	1445.540				
6	0.572	14.542	1232.032				
Mean	0.899	16.148	1402.626				
Std Dev	0.200	1.626	155.452				

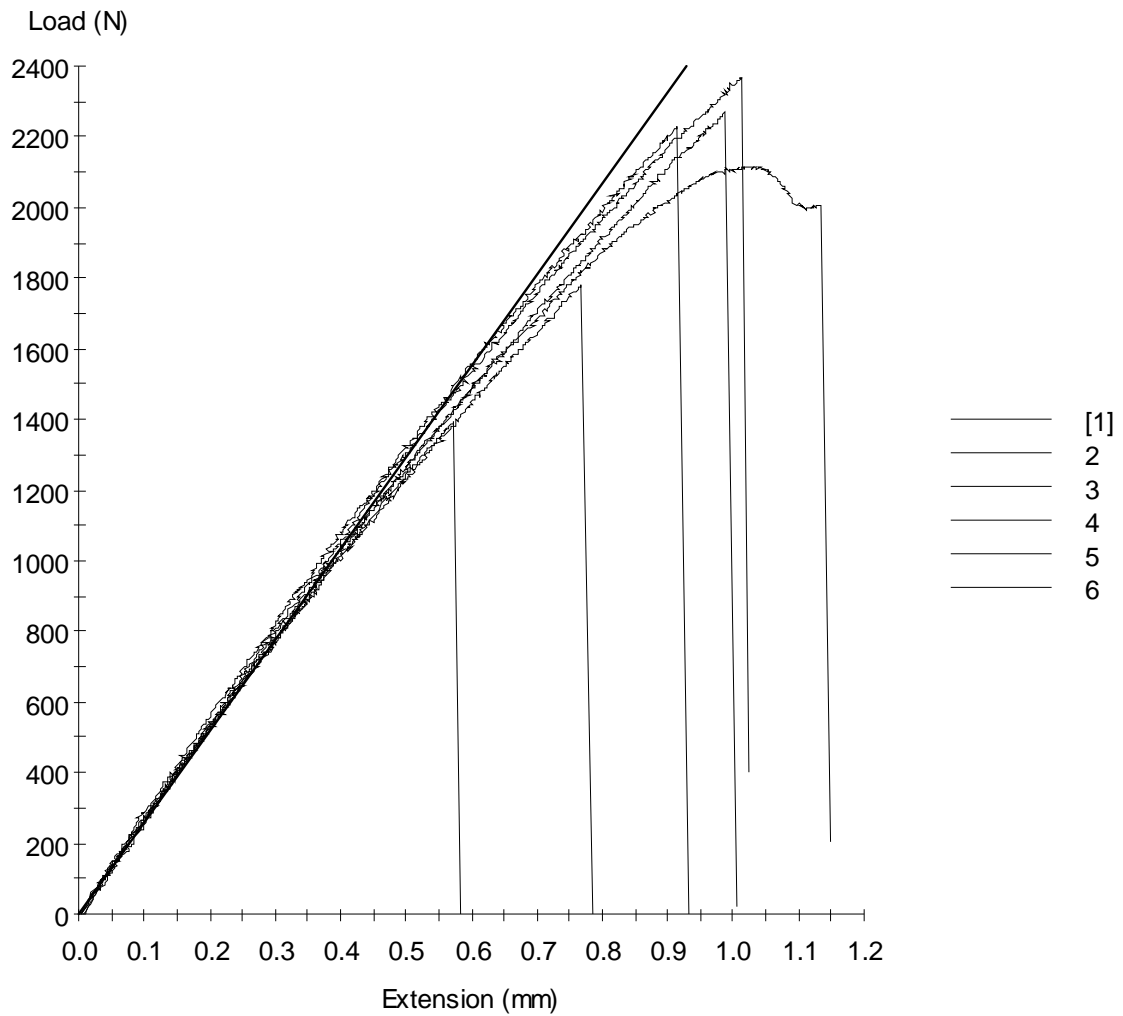


Fig A.3.4: Load vs Extension of 15% weight of glass powder post cured in microwave

Microwave cured sample results**20% weight of glass powder post cured in microwave**

Test Date : 18/08/2009

Method : MMT Tensile Test with return.msm

Specimen Results:

Specimen #	Thickness mm	Width mm	Area mm ²	Peak Load N	Peak Stress MPa	Break Load N	Break Stress MPa
1	14.800	5.780	86	1595	18.64	1593	18.62
2	14.900	5.860	87	1783	20.42	1783	20.42
3	14.890	5.790	86	2024	23.48	2024	23.48
4	14.930	6.250	93	1452	15.56	1444	15.47
5	15.020	5.690	85	1752	20.50	1752	20.50
6	14.930	6.050	90	2165	23.97	2165	23.97
Mean	14.912	5.903	88	1795	20.43	1794	20.41
Std Dev	0.071	0.208	3	264	3.12	267	3.15

Specimen #	Elongation At Break mm	Stress At Offset Yield MPa	Load At Offset Yield N				
1	0.685	14.481	1238.746				
2	0.777	14.572	1272.317				
3	0.912	15.124	1303.873				
4	0.614	10.541	983.612				
5	0.724	15.634	1336.100				
6	0.923	15.461	1396.527				
Mean	0.773	14.302	1255.196				
Std Dev	0.124	1.900	143.674				

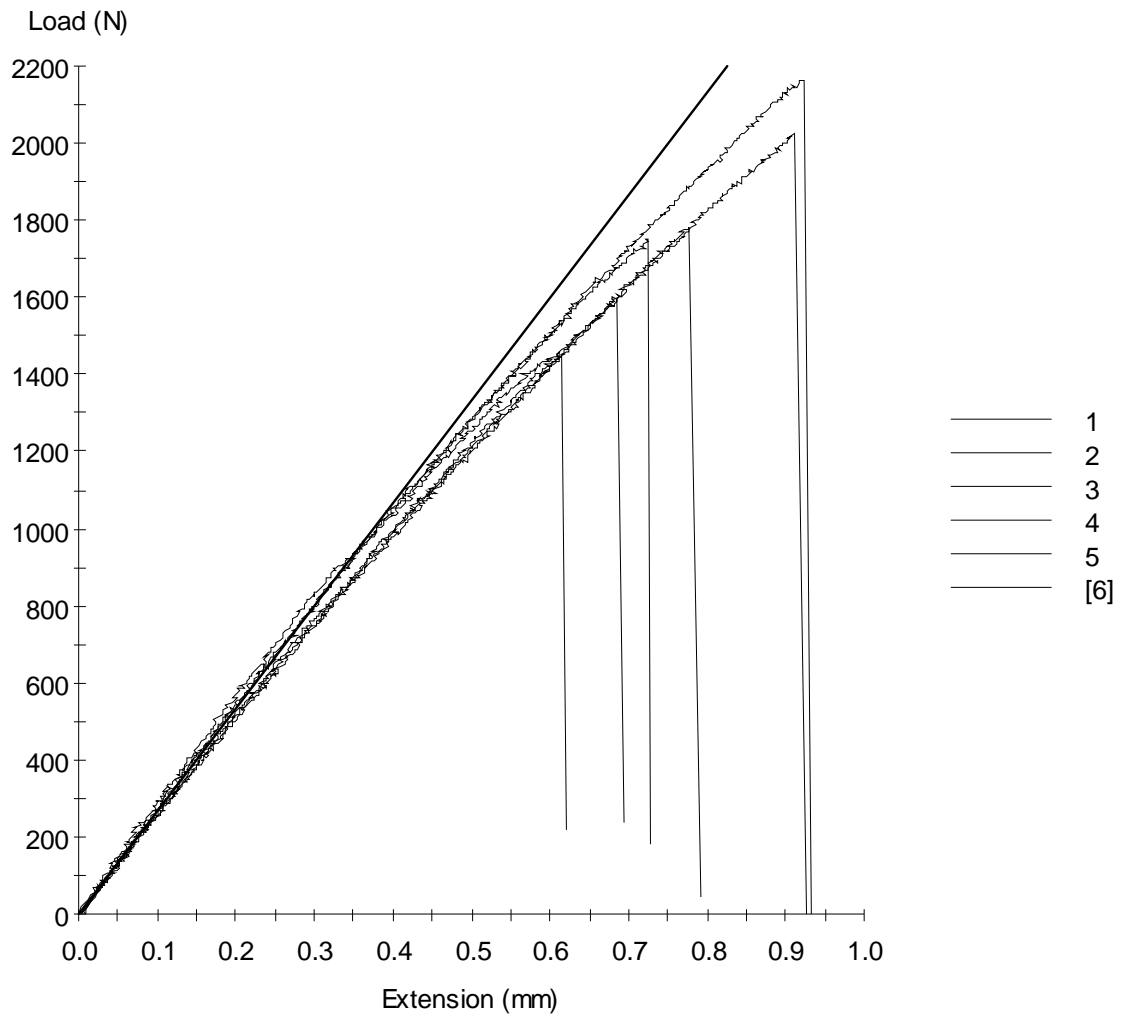


Fig A.3.5: Load vs Extension of 20% weight of glass powder post cured in microwave

Microwave cured sample results**25% weight of glass powder post cured in microwave**

Test Date : 18/08/2009

Method : MMT Tensile Test with return.msm

Specimen Results:

Specimen #	Thickness mm	Width mm	Area mm ²	Peak Load N	Peak Stress MPa	Break Load N	Break Stress MPa
1	14.970	5.630	84	1480	17.57	1480	17.57
2	15.230	5.830	89	1524	17.16	1524	17.16
3	14.930	5.790	86	1291	14.94	1282	14.83
4	15.080	5.660	85	1418	16.61	1418	16.61
5	15.260	5.650	86	1286	14.91	1285	14.90
6	15.220	5.810	88	1241	14.03	1241	14.03
Mean	15.115	5.728	87	1373	15.87	1372	15.85
Std Dev	0.143	0.091	2	117	1.43	118	1.45

Specimen #	Elongation At Break mm	Stress At Offset Yield MPa	Load At Offset Yield N				
1	0.719	12.467	1050.752				
2	0.748	12.167	1080.294				
3	0.696	11.767	1017.182				
4	0.719	10.619	906.400				
5	0.674	12.023	1036.653				
6	0.626	10.151	897.671				
Mean	0.697	11.533	998.159				
Std Dev	0.043	0.929	77.296				

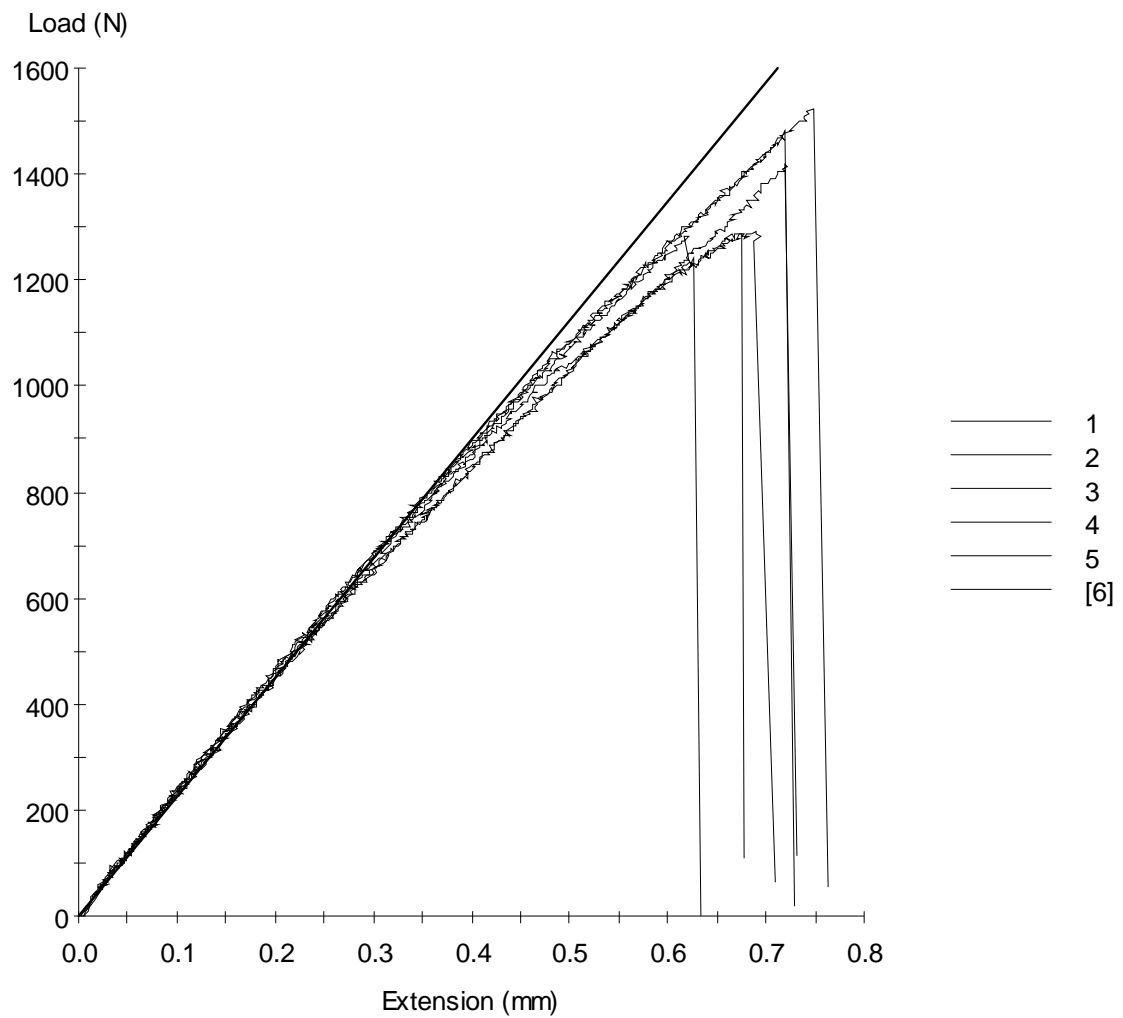


Fig A.3.6: Load vs Extension of 25% weight of glass powder post cured in microwave

Microwave cured sample results**30% weight of glass powder post cured in microwave**

Test Date : 18/08/2009

Method : MMT Tensile Test with return.msm

Specimen Results:

Specimen #	Thickness mm	Width mm	Area mm ²	Peak Load N	Peak Stress MPa	Break Load N	Break Stress MPa
1	14.960	5.440	81	929	11.42	929	11.42
2	14.910	5.160	77	849	11.04	849	11.04
3	14.890	5.330	79	1151	14.51	1151	14.51
4	14.820	5.400	80	1345	16.81	1345	16.81
5	14.790	5.510	81	1243	15.26	1243	15.26
Mean	14.874	5.368	80	1104	13.81	1104	13.81
Std Dev	0.069	0.133	2	209	2.50	209	2.50

Specimen #	Elongation At Break mm	Stress At Offset Yield MPa	Load At Offset Yield N				
1	0.471	9.570	778.832				
2	0.434	8.116	624.409				
3	0.593	12.216	969.512				
4	0.655	14.430	1154.820				
5	0.648	12.490	1017.853				
Mean	0.560	11.364	909.085				
Std Dev	0.102	2.508	208.491				

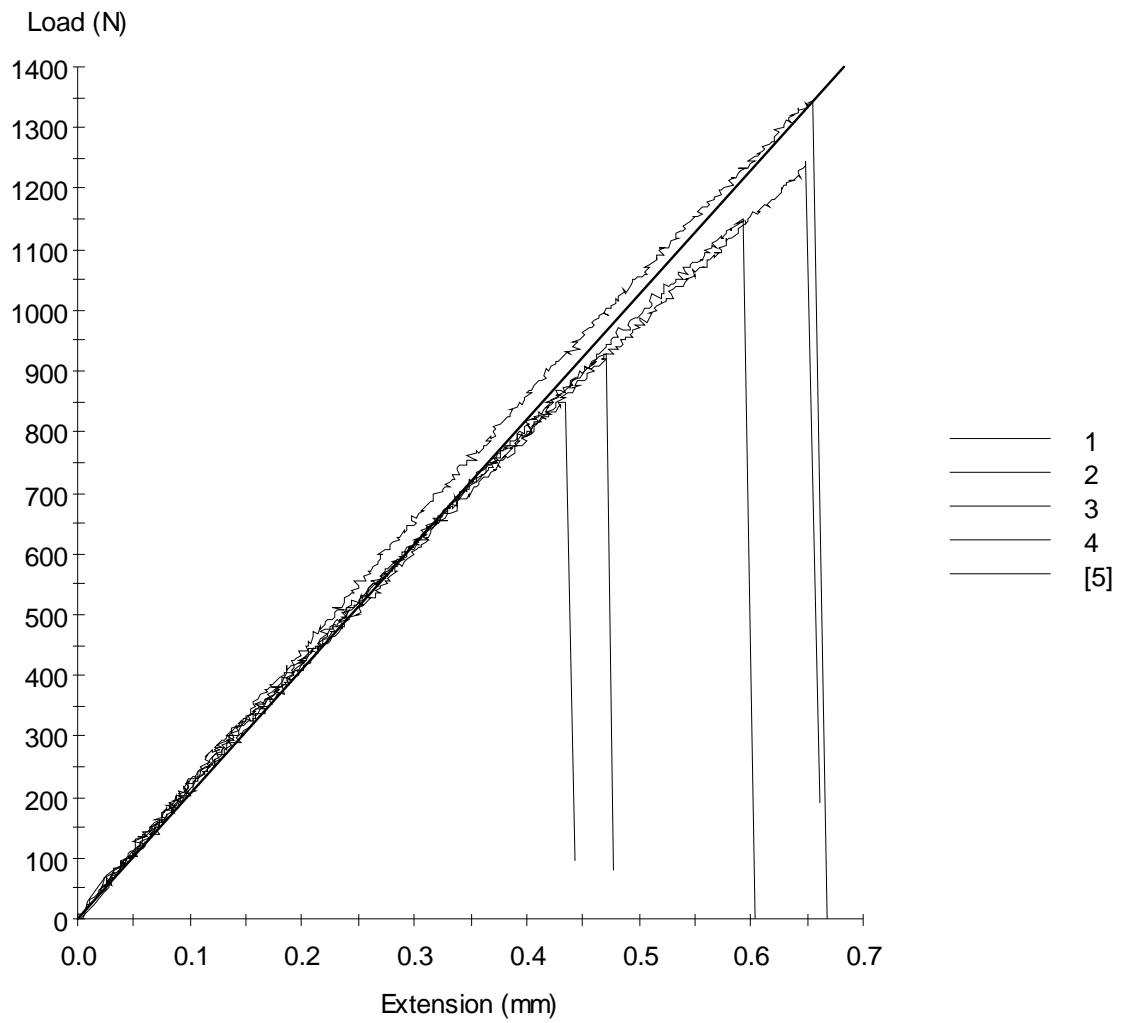


Fig A.3.7: Load vs Extension of 30% weight of glass powder post cured in microwave

Microwave cured sample results**35% weight of glass powder post cured in microwave**

Test Date : 18/08/2009

Method : MMT Tensile Test with return.msm

Specimen Results:

Specimen #	Thickness mm	Width mm	Area mm ²	Peak Load N	Peak Stress MPa	Break Load N	Break Stress MPa
1	14.980	5.450	82	1246	15.26	1246	15.26
2	15.250	5.660	86	906	10.50	906	10.49
3	15.010	5.760	86	1219	14.10	1219	14.10
4	15.110	5.620	85	957	11.27	957	11.27
5	15.020	5.470	82	1112	13.54	1112	13.54
6	14.660	6.510	95	1291	13.53	1286	13.48
Mean	15.005	5.745	86	1122	13.03	1121	13.02
Std Dev	0.195	0.393	5	159	1.80	159	1.80

Specimen #	Elongation At Break mm	Stress At Offset Yield MPa	Load At Offset Yield N				
1	0.585	12.747	1040.681				
2	0.394	1.282	110.614				
3	0.538	12.549	1084.994				
4	0.401	1.686	143.144				
5	0.523	13.320	1094.394				
6	0.483	11.678	1114.536				
Mean	0.487	8.877	764.727				
Std Dev	0.077	5.753	494.772				

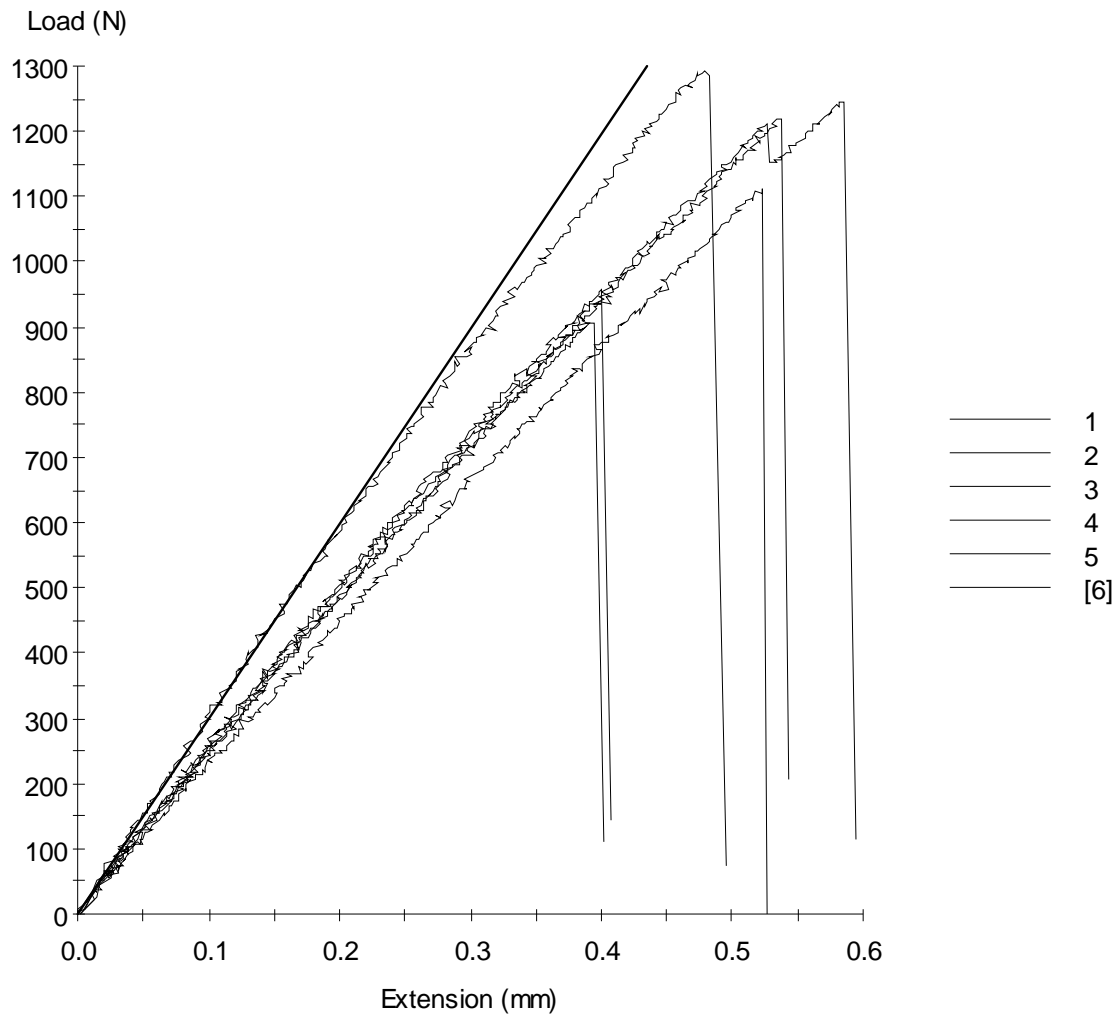


Fig A.3.8: Load vs Extension of 35% weight of glass powder post cured in microwave

A.4. Tensile Test (Sample Cured Conventionally)

Sample cured conventionally

0% weight of glass powder post cured in conventional oven

Test Date : 7/08/2009

Method : MMT Tensile Test with return.msm

Specimen Results:

Specimen #	Thickness mm	Width mm	Area mm ²	Peak Load N	Peak Stress MPa	Break Load N	Break Stress MPa
1	5.610	15.380	86	2551	29.57	2551	29.57
2	5.460	14.960	82	3378	41.35	3370	41.26
Mean	5.535	15.170	84	2964	35.46	2961	35.42
Std Dev	0.106	0.297	3	584	8.33	579	8.27

Specimen #	Elongation At Break mm	Stress At Offset Yield MPa	Load At Offset Yield N				
1	1.403	14.162	1221.961				
2	3.085	20.085	1640.583				
Mean	2.244	17.124	1431.27				
Std Dev	1.189	4.188	296.011				

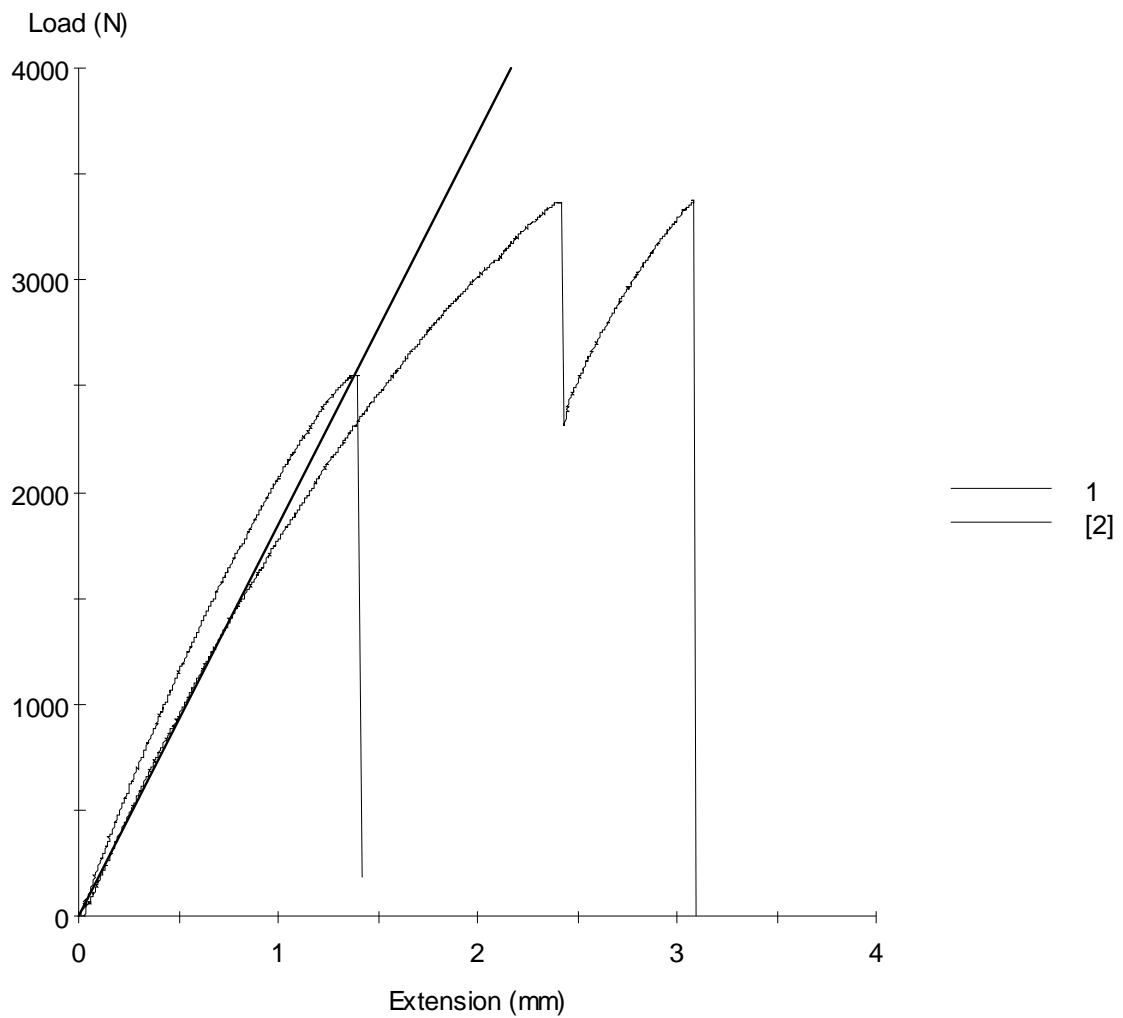


Fig A.4.1: Load vs Extension of 0% weight of glass powder post cured in conventional oven

Sample cured conventionally**5% weight of glass powder post cured in conventional oven**

Test Date : 28/07/2009

Method : MMT Tensile Test with return.msm

Specimen Results:

Specimen #	Thickness mm	Width mm	Area mm ²	Peak Load N	Peak Stress MPa	Break Load N	Break Stress MPa
1	5.470	14.970	82	2554	31.18	2554	31.18
2	5.530	15.200	84	2187	26.02	2187	26.02
3	5.830	15.210	89	2055	23.17	2055	23.17
4	5.640	15.120	85	1559	18.29	1418	16.63
5	5.650	14.910	84	1914	22.71	1914	22.71
6	5.560	15.280	85	2503	29.46	2503	29.46
Mean	5.613	15.115	85	2129	25.14	2105	24.86
Std Dev	0.126	0.146	2	374	4.75	419	5.25

Specimen #	Elongation At Break mm	Stress At Offset Yield MPa	Load At Offset Yield N				
1	1.338	14.759	1208.533				
2	1.141	12.243	1029.099				
3	0.962	11.259	998.382				
4	0.743	8.424	718.406				
5	0.910	10.839	913.114				
6	1.402	13.710	1164.724				
Mean	1.082	11.872	1005.376				
Std Dev	0.257	2.244	177.843				

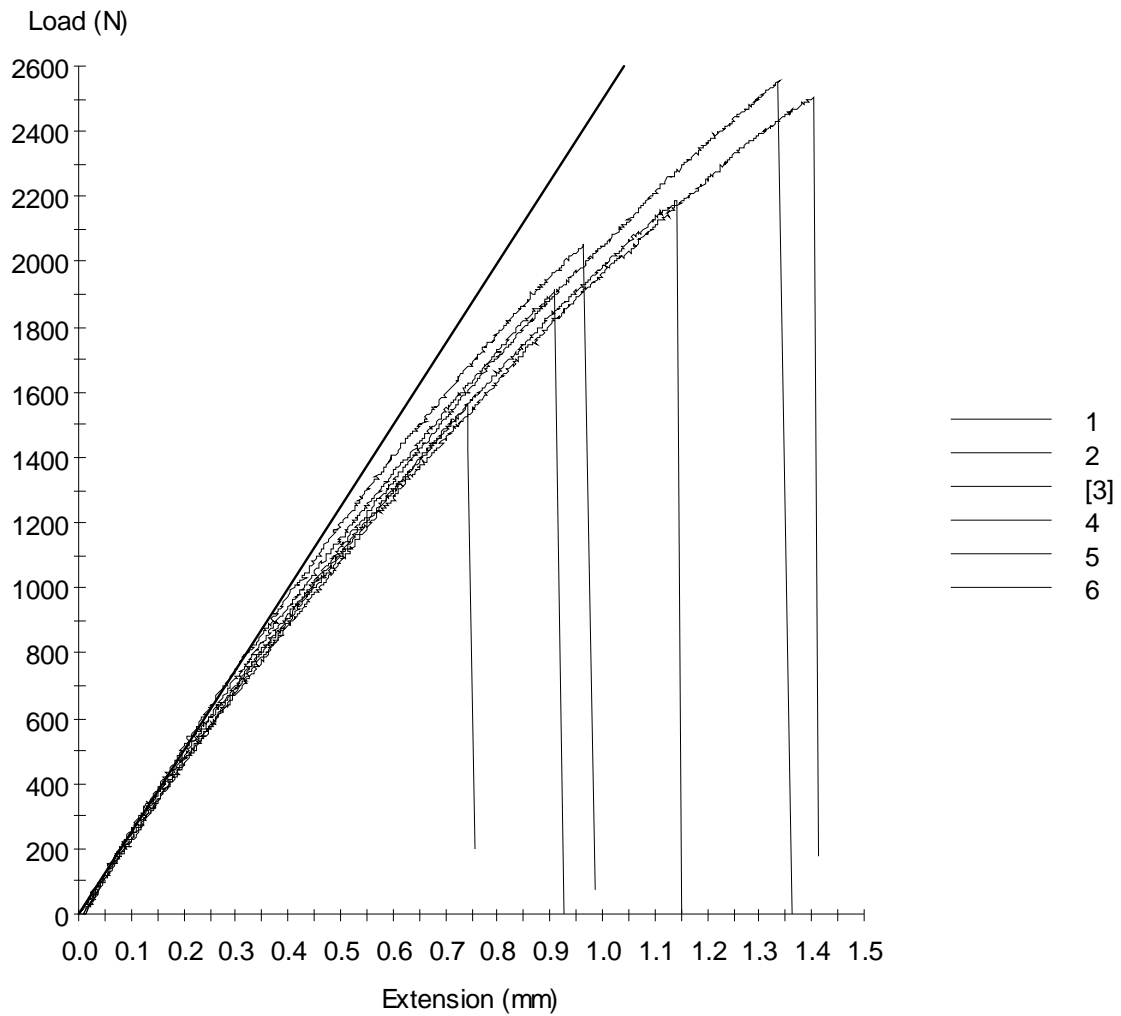


Fig A.4.2: Load vs Extension of 5% weight of glass powder post cured in conventional oven

Sample cured conventionally**10% weight of glass powder post cured in conventional oven**

Test Date : 13/07/2009

Method : MMT Tensile Test with return.msm

Specimen Results:

Specimen #	Thickness mm	Width mm	Area mm ²	Peak Load N	Peak Stress MPa	Break Load N	Break Stress MPa
1	6.000	15.000	90	1571	17.46	1571	17.46
2	5.620	15.180	85	1258	14.75	1258	14.75
3	5.130	15.050	77	1911	24.76	1911	24.76
4	5.780	14.930	86	1239	14.35	1239	14.35
5	5.790	15.280	88	1561	17.64	1561	17.64
Mean	5.664	15.088	85	1508	17.79	1508	17.79
Std Dev	0.328	0.141	5	276	4.18	276	4.18

Specimen #	Elongation At Break mm	Stress At Offset Yield MPa	Load At Offset Yield N				
1	0.863	8.922	803.003				
2	0.654	7.398	631.123				
3	1.098	11.653	899.686				
4	0.612	7.275	627.766				
5	0.834	8.917	788.903				
Mean	0.812	8.833	750.096				
Std Dev	0.194	1.765	118.112				

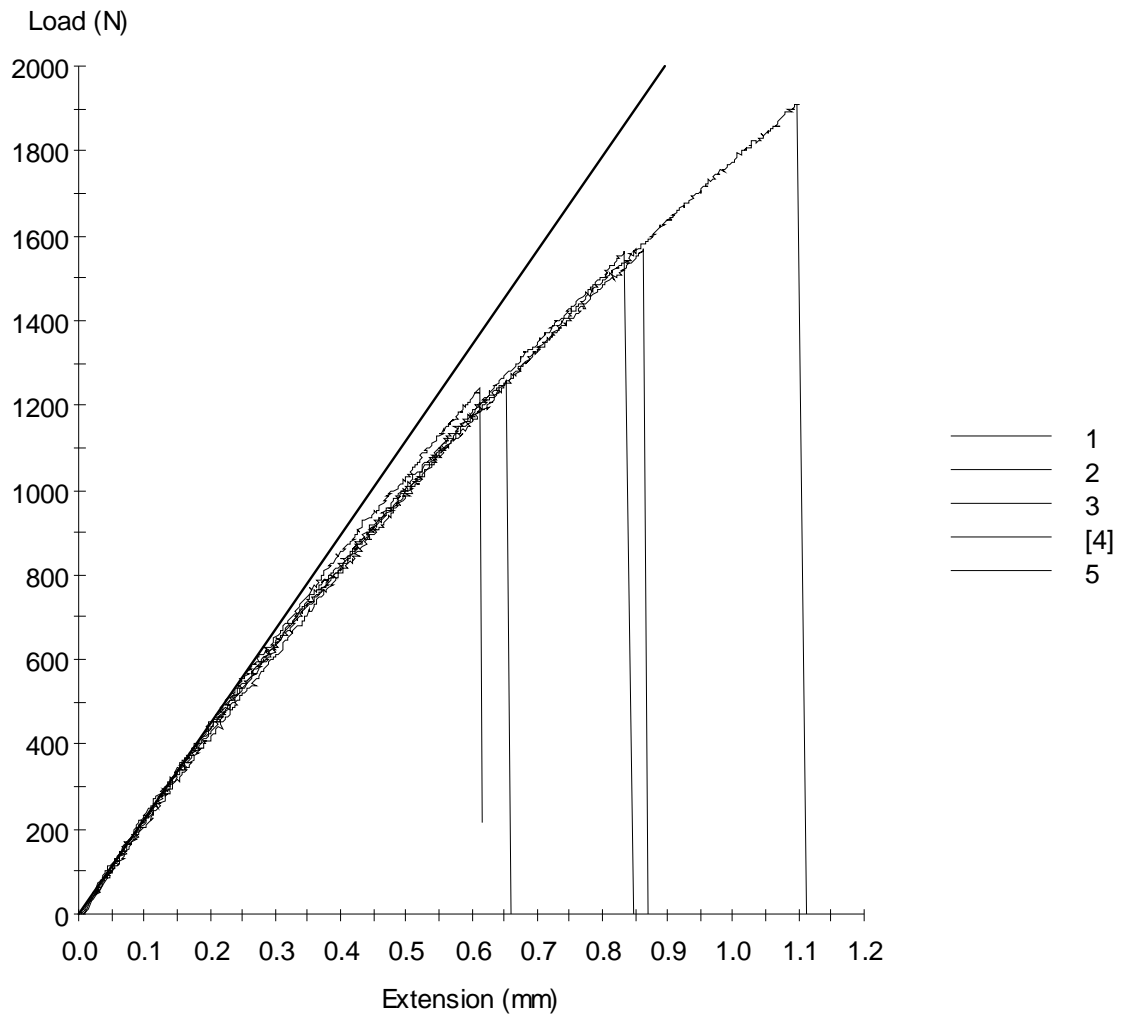


Fig A.4.3: Load vs Extension of 10% weight of glass powder post cured in conventional oven

Sample cured conventionally**15% weight of glass powder post cured in conventional oven**

Test Date : 28/07/2009

Method : MMT Tensile Test with return.msm

Specimen Results:

Specimen #	Thickness mm	Width mm	Area mm ²	Peak Load N	Peak Stress MPa	Break Load N	Break Stress MPa
1	5.720	15.180	87	1683	19.38	1683	19.38
2	5.480	15.080	83	1416	17.14	1415	17.13
3	5.370	15.270	82	1504	18.35	1504	18.35
4	5.200	14.940	78	1195	15.38	1195	15.38
5	5.920	15.260	90	2034	22.52	2034	22.52
6	5.630	15.130	85	1478	17.35	1478	17.35
Mean	5.553	15.143	84	1552	18.35	1552	18.35
Std Dev	0.258	0.124	4	284	2.44	284	2.44

Specimen #	Elongation At Break mm	Stress At Offset Yield MPa	Load At Offset Yield N				
1	0.861	8.974	779.168				
2	0.740	8.708	719.581				
3	0.879	8.608	705.817				
4	0.691	6.609	513.459				
5	1.098	10.182	919.828				
6	0.779	8.749	745.262				
Mean	0.841	8.638	730.519				
Std Dev	0.144	1.152	131.352				

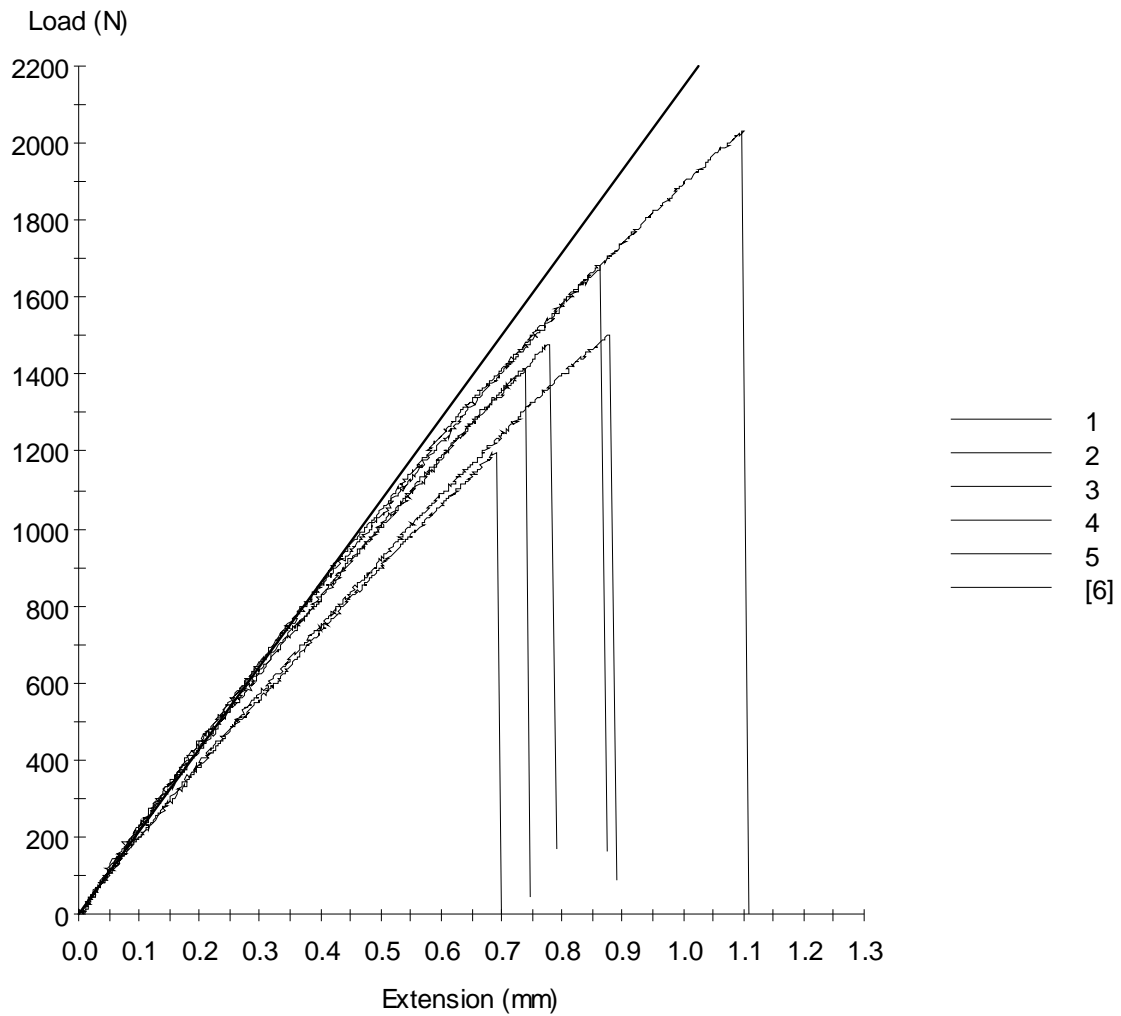


Fig A.4.4: Load vs Extension of 15% weight of glass powder post cured in conventional oven

Sample cured conventionally**20% weight of glass powder post cured in conventional oven**

Test Date : 7/08/2009

Method : MMT Tensile Test with return.msm

Specimen Results:

Specimen #	Thickness mm	Width mm	Area mm ²	Peak Load N	Peak Stress MPa	Break Load N	Break Stress MPa
1	5.030	15.060	76	1527	20.16	1523	20.11
2	5.440	15.160	82	1433	17.38	1433	17.38
3	5.030	15.100	76	1574	20.73	1574	20.73
4	5.060	15.070	76	1217	15.96	1217	15.96
5	5.340	15.350	82	1307	15.95	1307	15.95
6	5.200	15.210	79	1473	18.62	1473	18.62
Mean	5.183	15.158	79	1422	18.14	1421	18.13
Std Dev	0.175	0.110	3	136	2.06	135	2.05

Specimen #	Elongation At Break mm	Stress At Offset Yield MPa	Load At Offset Yield N				
1	0.791	9.304	704.810				
2	0.757	9.175	756.676				
3	0.946	9.326	708.335				
4	0.741	7.176	547.197				
5	0.733	7.038	576.907				
6	0.780	8.701	688.192				
Mean	0.791	8.453	663.686				
Std Dev	0.079	1.068	82.502				

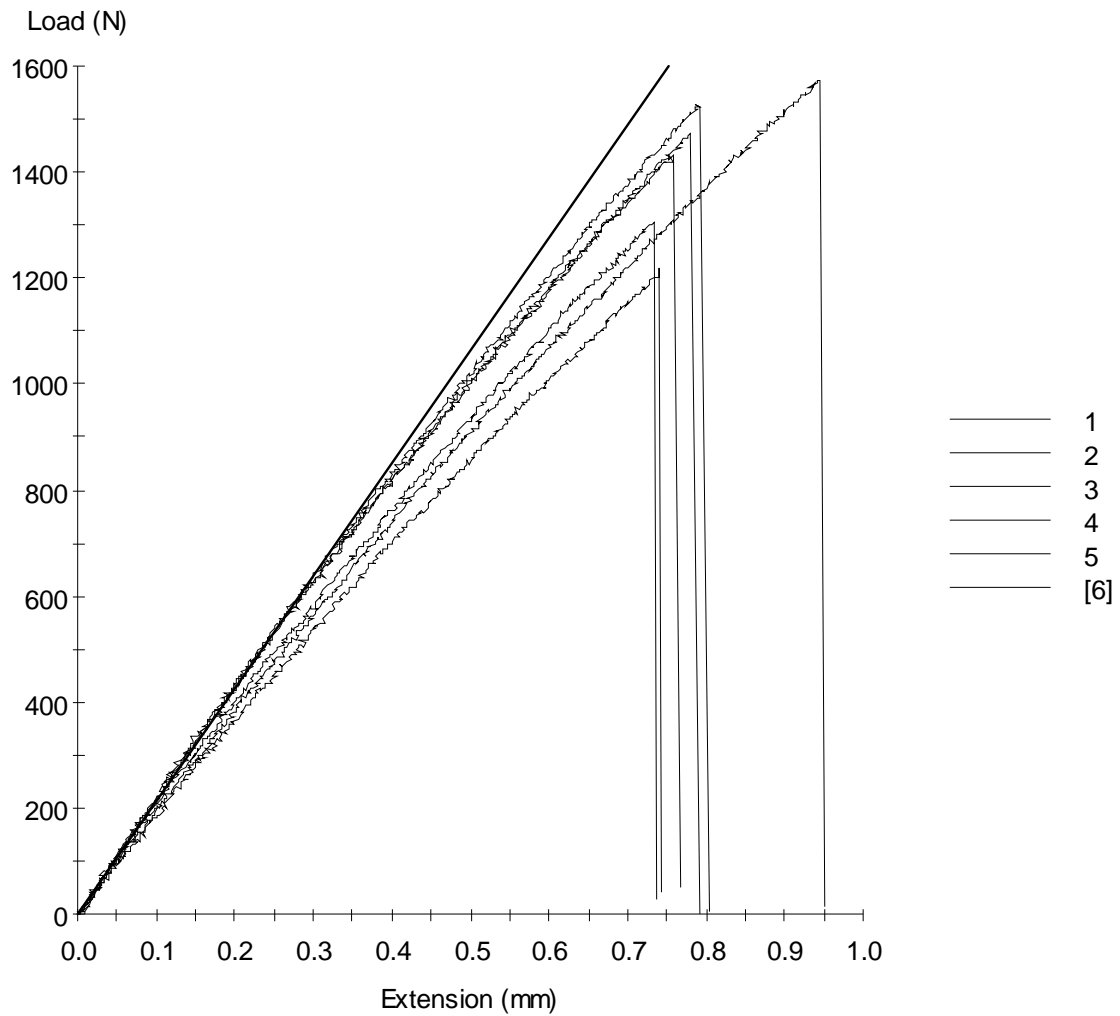


Fig A.4.5: Load vs Extension of 20% weight of glass powder post cured in conventional oven

Sample cured conventionally**25% weight of glass powder post cured in conventional oven**

Test Date : 7/08/2009

Method : MMT Tensile Test with return.msm

Specimen Results:

Specimen #	Thickness mm	Width mm	Area mm ²	Peak Load N	Peak Stress MPa	Break Load N	Break Stress MPa
1	5.110	15.490	79	1188	15.01	1188	15.01
2	5.150	15.410	79	1253	15.79	1252	15.78
3	5.110	15.620	80	1021	12.79	1021	12.79
4	5.070	15.480	78	1098	13.99	1098	13.99
5	4.850	15.020	73	1162	15.94	1162	15.94
6	5.090	15.450	79	1162	14.77	1162	14.77
Mean	5.063	15.412	78	1147	14.72	1147	14.71
Std Dev	0.108	0.204	3	80	1.18	79	1.18

Specimen #	Elongation At Break mm	Stress At Offset Yield MPa	Load At Offset Yield N				
1	0.594	8.557	677.282				
2	0.701	7.542	598.560				
3	0.625	6.771	540.483				
4	0.637	7.143	560.625				
5	0.607	7.466	543.840				
6	0.680	7.618	599.063				
Mean	0.641	7.516	586.642				
Std Dev	0.042	0.598	51.286				

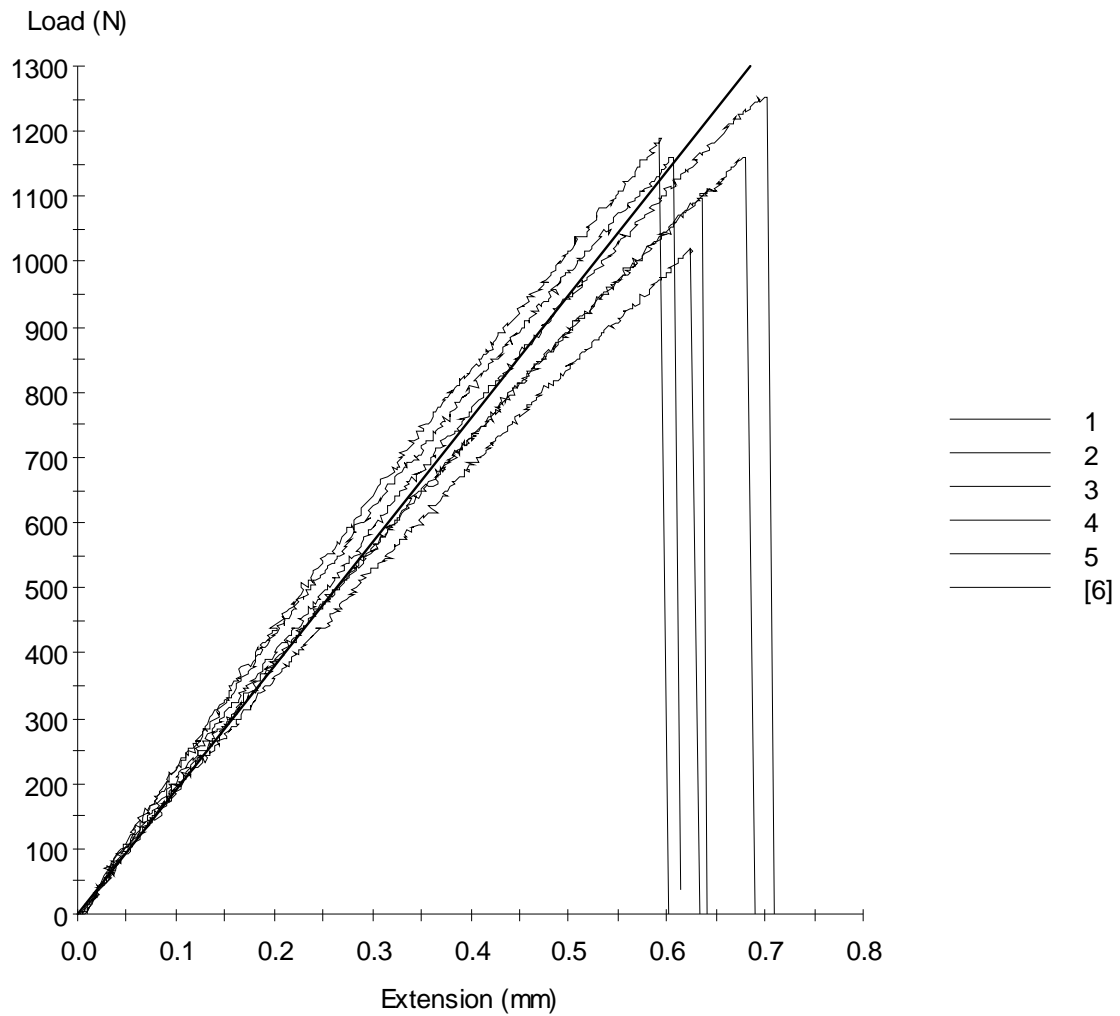


Fig A.4.6: Load vs Extension of 25% weight of glass powder post cured in conventional oven

Sample cured conventionally**30% weight of glass powder post cured in conventional oven**

Test Date : 7/08/2009

Method : MMT Tensile Test with return.msm

Specimen Results:

Specimen #	Thickness mm	Width mm	Area mm ²	Peak Load N	Peak Stress MPa	Break Load N	Break Stress MPa
1	5.010	15.340	77	963	12.54	963	12.54
2	4.600	15.310	70	775	11.01	775	11.01
3	5.370	15.560	84	1249	14.95	1249	14.95
4	5.400	15.370	83	1386	16.70	1386	16.70
5	5.840	15.080	88	1916	21.75	1916	21.75
6	5.030	15.680	79	1049	13.30	1049	13.30
Mean	5.208	15.390	80	1223	15.04	1223	15.04
Std Dev	0.425	0.209	6	401	3.83	401	3.83

Specimen #	Elongation At Break mm	Stress At Offset Yield MPa	Load At Offset Yield N				
1	0.509	5.591	429.701				
2	0.451	5.911	416.272				
3	0.617	6.750	563.982				
4	0.655	9.748	809.046				
5	0.801	12.084	1064.180				
6	0.537	7.321	577.410				
Mean	0.595	7.901	643.432				
Std Dev	0.125	2.524	249.964				

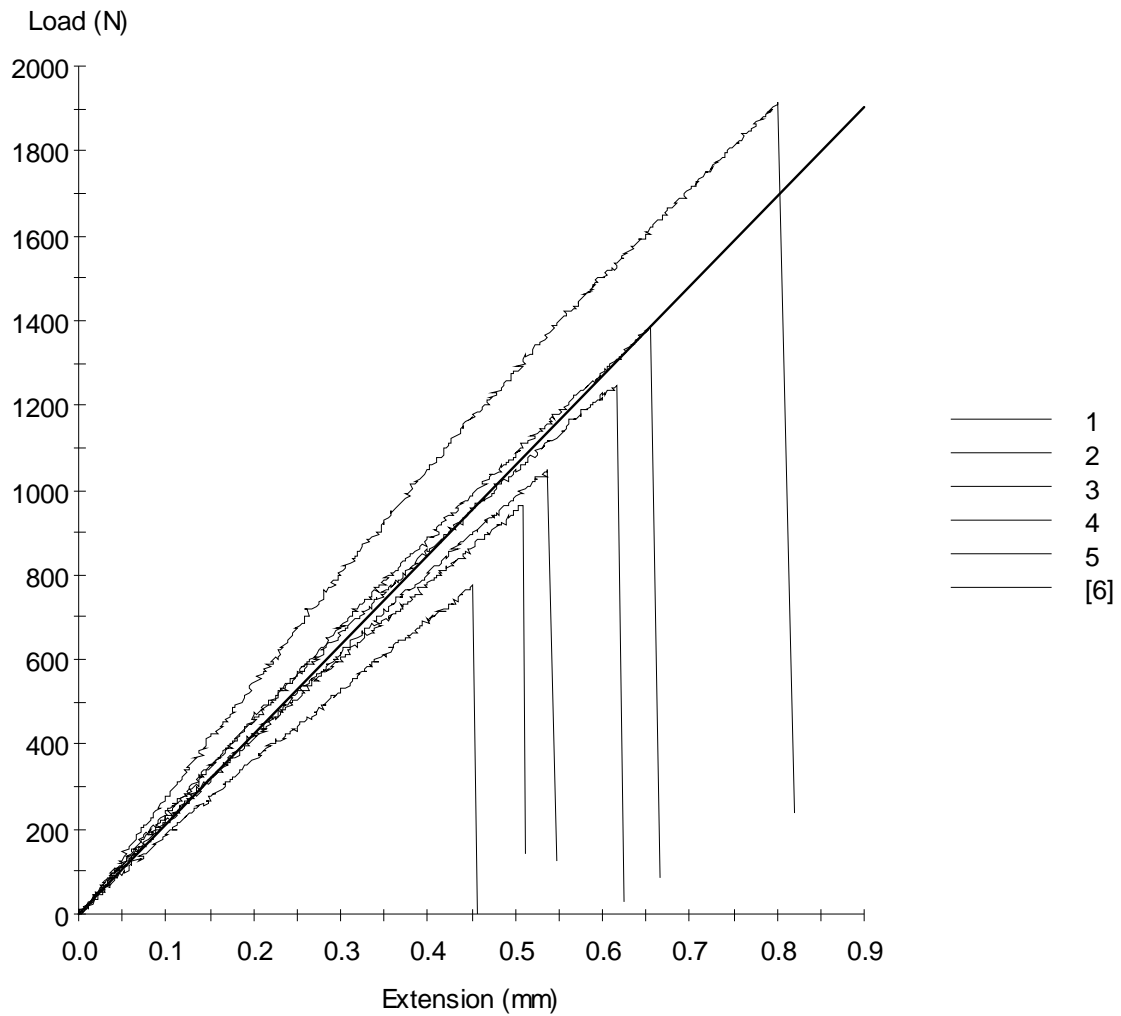


Fig A.4.7: Load vs Extension of 30% weight of glass powder post cured in conventional oven

Sample cured conventionally**35% weight of glass powder post cured in conventional oven**

Test Date : 6/08/2009

Method : MMT Tensile Test with return.msm

Specimen Results:

Specimen #	Thickness mm	Width mm	Area mm ²	Peak Load N	Peak Stress MPa	Break Load N	Break Stress MPa
1	5.710	14.820	85	1242	14.68	1242	14.68
2	5.550	15.080	84	1212	14.48	1212	14.48
3	5.650	15.290	86	700	8.10	700	8.10
4	5.350	14.800	79	1036	13.09	1036	13.08
5	5.400	15.010	81	994	12.26	994	12.26
6	5.340	15.020	80	1202	14.98	1202	14.98
Mean	5.500	15.003	83	1064	12.93	1064	12.93
Std Dev	0.159	0.181	3	205	2.59	205	2.59

Specimen #	Elongation At Break mm	Stress At Offset Yield MPa	Load At Offset Yield N				Specimen 3 is deleted
1	0.534	9.005	762.047				
2	0.511	6.739	563.982				
3	0.272	-0.225	-19.437				
4	0.429	9.323	738.212				
5	0.419	7.704	624.409				
6	0.526	7.952	637.837				
Mean	0.449	6.750	551.175				
Std Dev	0.100	3.542	289.166				

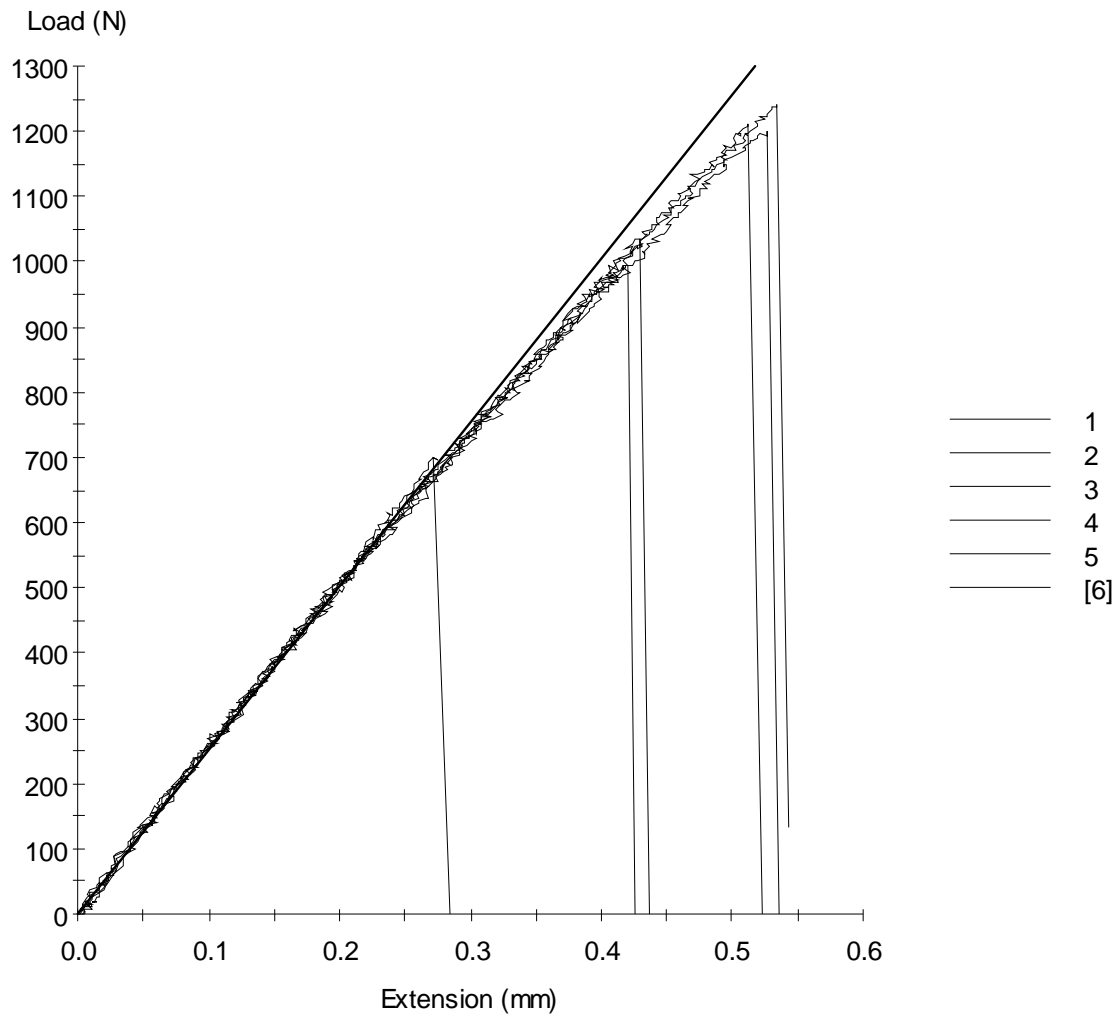


Fig A.4.8: Load vs Extension of 35% weight of glass powder post cured in conventional oven